CHEMICAL REVIEWS

pubs.acs.org/CR

Review

Light in Gold Catalysis

Sina Witzel, A. Stephen K. Hashmi, and Jin Xie*

Cite This: https://dx.doi.org/10.1021/acs.chemrev.0c00841

Read Online

ACCESS | Metrics & More | Article Recommendations

ABSTRACT: Within the wide family of gold-catalyzed reactions, gold photocatalysis intrinsically features unique elementary steps. When gold catalysis meets photocatalysis, a valence change of the gold center can easily be achieved via electron transfer and radical addition, avoiding the use of stoichiometric sacrificial external oxidants. The excellent compatibility of radicals with gold catalysts opens the door to a series of important organic transformations, including redox-neutral C−C and C−X coupling, C−H activation, and formal radical−radical cross-coupling. The photocatalysis with gold complexes nicely complements the existing photoredox catalysis strategies and also opens a new avenue for gold chemistry. This review covers the achieved transformations for both mononuclear gold(I) catalysts (with and without a photosensitizer) and dinuclear gold(I) photocatalysts. Various fascinating methodologies, their value for organic chemists, and the current mechanistic understanding are discussed. The most recent examples also demonstrate the feasibility of both, mononuclear and dinuclear gold(I) complexes to participate in excited state energy transfer (EnT), rather than electron transfer. The rare applications of gold(III) photocatalysts, both homogeneous and heterogeneous, are also summarized.

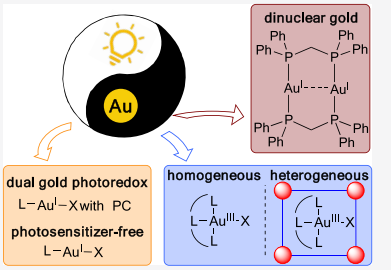

CONTENTS

1. INTRODUCTION

1.1. Redox Au(I)/Au(III) Catalysis

Gold was historically known as a "catalytically dead metal", but during the last two decades homogeneous gold catalysis has evolved to an important field of research, a field dominated by the π-activation of unsaturated C−C bonds.[1−10] This property results from an excellent carbophilic π-acidity, both gold(I) or gold(III) complexes serve as powerful tools to increase the electrophilicity of C−C multiple bonds and thus enabling a nucleophilic attack (Scheme 1). This process takes place without a change in oxidation state of the gold center in the whole catalytic cycle.[11−20]

The reason why gold catalysts have for a long time only been considered as an activator for multiple bonds was the relatively high redox potential of the Au(I)/Au(III)couple (E^0 = +1.41

Special Issue: Gold Chemistry

Received: August 9, 2020

Scheme 1. Typical Gold-Catalyzed Activation of Unsaturated C−C Bonds

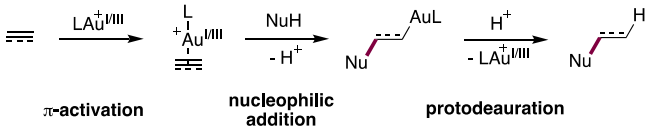

V) (compare Pd(0)/Pd(II): E^0 = 0.92 V).[21] The application of strong external oxidants, such as hypervalent iodine reagents or electrophilic fluorinating reagents, e.g., 1-(chloromethyl)-4-fluoro-1,4-diazabicyclo[2.2.2]octane bis(tetrafluoroborate) (Selectfluor) or *N*-fluorobenzenesulfonimide (NFSI), led to the success of overcoming this potential (Scheme 2).[22−28] Although this finding represented a huge success and a number of oxidative gold-catalyzed cross-coupling reactions were developed, they came along with some intrinsic limitations. The application of stoichiometric amounts of strong external oxidants, hardly tolerated highly oxidant-sensitive functional groups, thus restricting the synthetic value of these methodologies. Moreover, these external oxidants functioned as stoichiometric sacrificial oxidants, lacking an efficient atom economy.[29−31] Two attractive features classical gold catalysis usually exhibited were diminished: mild reaction conditions and excellent functional group tolerance. Therefore, the development of mild redox coupling reactions represents the state-of-the-art of gold chemistry and remains highly desirable. In general, a major challenge that comes along with the development of methodologies, including the redox couple Au(I)/Au(III), is that the competing protodeauration to the classical hydrofunctionalized products has to be suppressed in order to obtain the desired cross-coupled product.

1.2. Gold Photoredox Catalysis

The study of photochemical reactions goes back to the 18th century.[32] The exploration to harness solar energy to drive organic reactions can be attributed back to the 19th century to Giacomo Ciamician.[33−35] However, the use of sunlight in photochemical transformations is fundamentally challenging owing to the insufficient absorption of the visible area of the spectrum by the majority of organic molecules.[36,37] To address this obstacle, suitable photosensitizers were introduced. Those can be transition metal complexes or organic dyes. Figure 1A illustrates the photocatalysts (PC) (with their respective redox potentials and excitation wavelengths) that take on a role in this review.[34,38−42] Irradiation of a PC with visible light leads to an excited photocatalysts (PC*), which can now either accept an electron from a donor molecule (D) in a reductive quenching process or donate an electron to an acceptor molecule (A) in an oxidative quenching process (Figure 1B).[36,43] In contrast to its ground state (PC), the photoexcited state (PC*) can be oxidized or reduced more easily.

In the case of transition metal-based photocatalysts, mostly polypyridyl complexes are employed (compare Figure 1A) which enables an efficient metal-to-ligand charge transfer (MLCT) upon visible light irradiation.[44−46] This scenario is exemplified by the common photocatalyst $Ru(bpy)_3^{2+}$ (Figure 1C). Owing to the MLCT and the intersystem crossing (ISC), the excited $Ru(bpy)_3^{2+*}$ earns the capability to more easily donate (to, e.g., Ar-NO_2, Ar-N_2BF_4, Fe^{3+}, $S_2O_8^{2-}$) or accept (from, e.g., tertiary amines, xanthate, ascorbate) an electron than its corresponding ground state.

Photochemical conversions involving gold catalysis have added a synthetically new reactivity pattern in this research area.[49−55] The approach of combining gold catalysis with photoredox catalysis addressed the barrier of the Au(I)/Au(III) cycle by circumventing the previously described harsh reaction conditions. As will be thoroughly discussed in this review, the initial and majority of applications of mononuclear gold(I) complexes in photoredox catalysis applied a photosensitizer (such as $Ru(bpy)_3Cl_2$) and aryldiazonium salts (or aryl iodonium salts) to achieve the oxidation of the gold catalyst.[50,55] Subsequently, Hashmi and co-workers revealed that the presence of a photosensitizer is redundant. The sole use of a gold catalyst was capable of undergoing the redox cycle for a series of coupling reactions, complementing the classical Pd-catalyzed transformations. In this review, the incredible achievements are discussed as well as their respective proposed mechanisms outlined.

While the application of mononuclear gold(I) complexes in photoinduced transformations using other photoredox catalysts was initiated in 2013 and is based on preceding work with stoichiometric chemical oxidants in a kind of continuous development, the employment of the dinuclear gold(I) catalyst resulted from the seminal work by C.-M. Che in 1989.[56,57] He was the first to prepare the dinuclear gold(I) catalyst $[Au_2(\mu\text{-dppm})_2]^{2+}$ (dppm = bis(diphenylphosphino)methane) (the first synthesis of a dinuclear gold(I) complex with an aurophilic interaction in general was conducted by Schmidbauer)[58] and investigated these with respect to their photophysical properties. He showed that upon irradiation of the dinuclear gold(I) catalyst with UV-light, unactivated alkyl halides, benzyl chloride (**1**), and pentyl bromide (**3**) can undergo dimerization in the presence of triethylamine, albeit in low yields (Scheme 3).[57] First mechanistic insights showed that this novel photoredox reaction proceeded via a radical pathway

Scheme 2. General Oxidative Procedure of Gold(I) to Gold(III) with External Oxidants

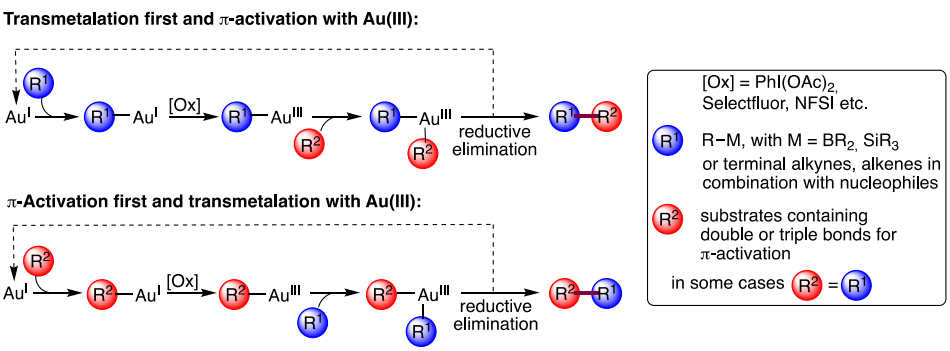

https://dx.doi.org/10.1021/acs.chemrev.0c00841
Chem. Rev. XXXX, XXX, XXX−XXX

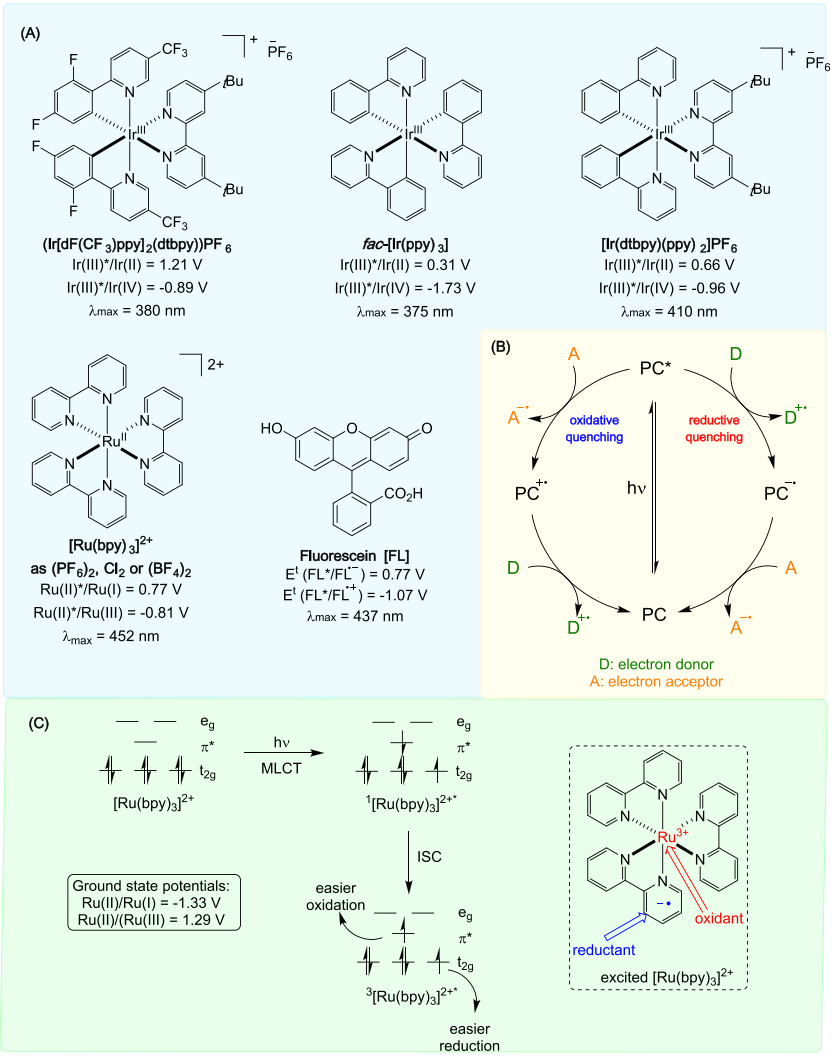

Figure 1. (A) Selected photocatalysts with their redox potentials (given in V vs SCE) and excitation wavelengths (reference for transition metal complexes,[38,39] fluorescein[42,47,48]). (B) General paradigm of photoredox catalysis by oxidative and reductive quenching pathways. (C) Structure of the excited state $*Ru(bpy)_3^{2+}$ and the electron configuration for O_h symmetry for the ground state, the excited singlet state, and the excited triplet state.[34,41,45] For comparison, the ground-state potentials were added.[41]

Scheme 3. Seminal Work by Che et al.[56,57]

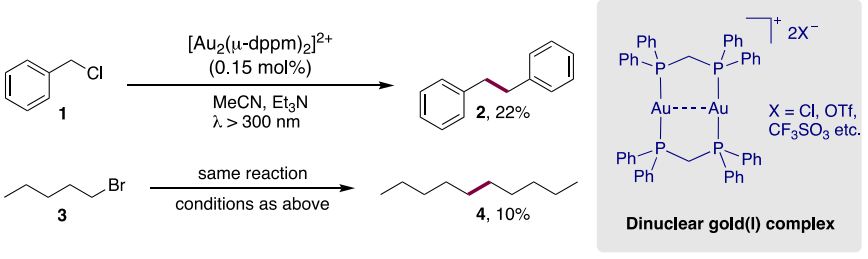

resulting in a change in oxidation state of the gold center. However, to the best of our knowledge, until Barriault's publication[59] from 2013, the direct use of gold complexes as photosensitizers has only been studied in rare examples and Che's intriguing reaction system for over 20 years did not concern the vision of chemists, and the same applies to the photosensitizer-free mononuclear gold(I)-catalyzed photoreactions published in 2016 by Huang et al.[60] All of these have evolved as a typical "black swan" events in synthetic chemistry.[61]

The most important features a photocatalyst should exhibit are (1) a long-lived excited state in order to react with the substrate molecules before relaxation to the ground state, (2) a strong reduction or oxidation potential in order to react with a range of substrates with different redox potentials, and (3) photoexcitation with light in the UV/vis range in order to gain selectivity and minimize undesired side reactions. On the basis of Che's studies, the dinuclear gold(I) catalysts holds all these characteristics: (1) excited state quantum yield of 0.23, (2) high redox potential of $[E^0(Au_2^{3+} \rightarrow Au_2^{2+*})] = -1.6$ to -1.7

https://dx.doi.org/10.1021/acs.chemrev.0c00841
Chem. Rev. XXXX, XXX, XXX−XXX

Scheme 4. Intramolecular Oxy- and Aminoarylation of Alkenes Combining Gold and Photoredox Catalysis and Selected Control Experiments

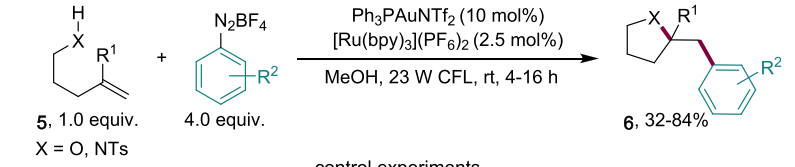

control experiments

For **6a**: X = O, R^1 = H, R^2 = H

Entry	[Au]	[Ru]	Light source	Yield (%)
1	$Ph_3PAuNTf_2$	$[Ru(bpy)_3](PF_6)_2$	CFL	88
2	$Ph_3PAuNTf_2$	-	CFL	4
3	-	$[Ru(bpy)_3](PF_6)_2$	CFL	0
4	$Ph_3PAuNTf_2$	$[Ru(bpy)_3](PF_6)_2$	dark	6

V vs SCE, and (3) photoexcitation in the UV/vis region: 290−320 nm in MeCN.[56,57] The gold photocatalyst was shown to act as both reductant (oxidative quenching) as well as oxidant (reductive quenching), and the mechanisms follow the general paradigm of a photoredox catalytic cycle (Figure 1B).[51,53] In the last years, the groups of Che, Barriault, and Hashmi aimed at deciphering the photochemical excitation pathway.[51,53,62,63] It was shown that the dinuclear gold(I) complex has a minimal aurophilic interaction in the ground state. Once excited with UVA light, an electron was raised from an antibonding $5d_z^2$ orbital into a $6s/6p_z$ bonding orbital (^{1}5dσ*6pσ) and after intersystem crossing (ISC) to its triplet state (^{3}5dσ*6pσ).[64] This triplet excited state was found to have a preference of increasing the coordination number at the gold center through an inner-sphere exciplex. This makes the excited dinuclear gold catalyst so unique and enables it to undergo redox processes with substrates, such as unactivated alkyl and aryl bromides, exhibiting a much higher redox potential ($E^0_{reduction}$ = −1.90 to −2.50 vs SCE (alkyl bromides) and $E^0_{reduction}$ = −2.05 to −2.57 vs SCE (aryl bromides).[65,66] In contrast to this, other commonly used Ru- or Ir-based photocatalysts (redox potentials see Figure 1A) operate through an outer-sphere metal-to-ligand charge transfer (MLCT) once they are excited, and therefore the cleavage of a C−Br bond of unactivated alkyl and aryl bromides becomes challenging.[34,38,67]

In this review, we will discuss the synthetic benefits and mechanistic aspects of gold in the field of photocatalysis: on the one hand, the mononuclear gold(I) going from a cocatalyst to the only actor in photochemical conversions, and on the other hand, the dinuclear gold(I) catalyst acting as a photocatalyst itself. Finally, also the few examples on the use of gold(III) catalysts in photocatalysis were briefly discussed. Not included in this review was the photochemistry of gold nanoparticles and mixed metal gold-containing nanoparticles.

2. MONONUCLEAR GOLD(I) COMPLEXES

2.1. Dual Gold/Photoredox Catalysis

2.1.1. Intra- and Intermolecular Nucleophilic Additions. The first combination of mononuclear gold chemistry and photoredox catalysis was published in 2013 by Glorius et al., reporting a gold-catalyzed intramolecular oxy- and aminoarylation of alkenes (**5**) with aryldiazonium salts in combination with a ruthenium photosensitizer: $[Ru(bpy)_3](PF_6)_2$ (Scheme 4).[68] The reaction involved the formation of a new C−Nu and C−C bond to give oxyarylated products (**6**) with a good functional group tolerance in moderate to very good yields. Further, it proceeded under mild reaction conditions using a 23 W household compact fluorescent lamp (CFL) as the light source. The necessity of both catalysts (gold and photosensitizer) for a successful reaction was confirmed by respective control experiments (entries 1−3), and the absence of light led to a dramatic drop in yield (entry 4). As shown in entry 2 in Scheme 4, only 4% yield of the desired product **6a** were obtained in the absence of a photosensitizer.

As illustrated in Scheme 5, the proposed mechanism started with the activation of the olefin by cationic gold(I)

Scheme 5. Proposed Reaction Mechanism of the Intramolecular Oxy- and Aminoarylation of Alkenes

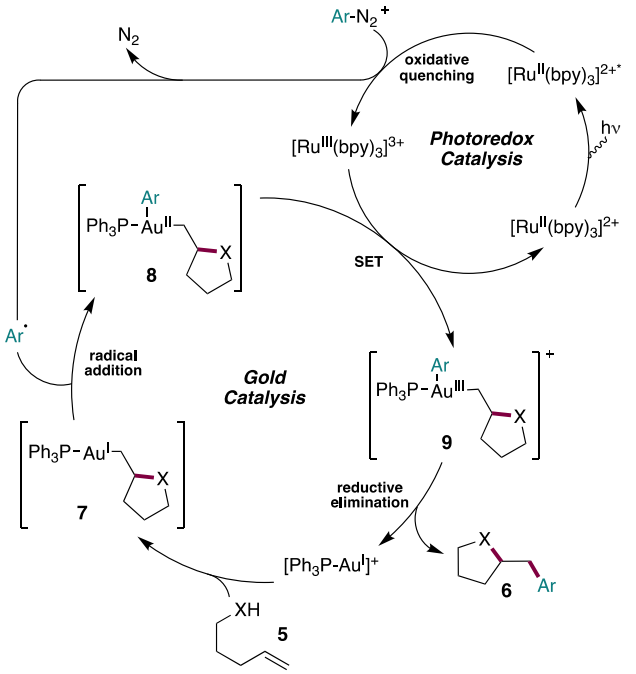

coordination and subsequent nucleophilic intramolecular 5-*exo-trig* ring-closure to form an alkylgold(I) intermediate (**7**). Concomitantly, the excited photocatalyst $[*Ru(bpy)_3(PF_6)_2]$ underwent an oxidative quenching by the aryldiazonium salt, generating a Ru(III) species and an aryl radical. The latter oxidized the alkylgold(I) intermediate (**7**) to give the arylgold(II)-alkyl species (**8**), which is further oxidized to the corresponding gold(III) intermediate (**9**) by single

https://dx.doi.org/10.1021/acs.chemrev.0c00841
Chem. Rev. XXXX, XXX, XXX−XXX

Scheme 6. Intermolecular Oxyarylation of Alkenes

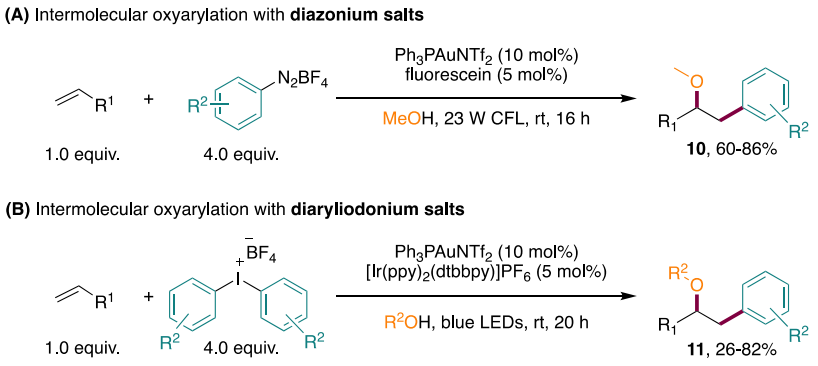

Scheme 7. Arylative Ring Expansion of Alkenyl and Allenyl Cycloalkanols with Aryldiazonium Salts and Selected Examples

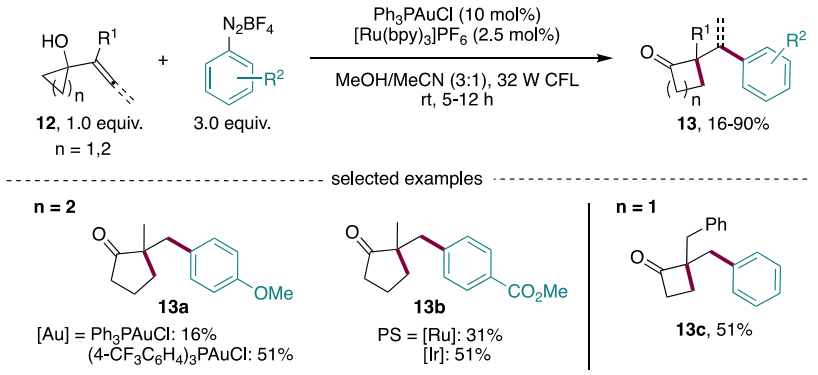

electron transfer (SET) to $[Ru(bpy)_3]^{3+}$. A final reductive elimination led to the desired arylated products (**6**) and regenerated the gold(I) catalyst. The redox potential for the suggested oxidation of gold(II) to gold(III) in the specific complexes used is still unknown, but it is assumed that the Ru(III) species is able to induce this step.

The same research group also developed the intermolecular version of the oxyarylation reaction of olefins leading to α-arylated ethers **10** and **11** (Scheme 6).[69] In this case, a less expensive organic dye, fluorescein (for redox potentials see Figure 1A), was used as suitable photosensitizer, and the solvent methanol functioned as both solvent and nucleophile. In addition, after extensive screening, the authors found that diaryliodonium salts were effective arylating agents in this reaction by using a relatively stronger reducing iridium photocatalyst ($[Ir(ppy)_2(dtbbpy)]PF_6$) under the irradiation of blue light-emitting diode strips (LEDs). It may presumably be explained by the maximum absorption of $[Ir(ppy)_2(dtbbpy)]PF_6$ at λ_{max} = 380 nm. In both cases, the mechanistic hypothesis was in accordance to the one presented in Scheme 5.

In 2014, Toste and co-workers developed the gold-catalyzed arylative ring expansion of alkenyl and allenyl cycloalkanols (**12**) with aryldiazonium salts, affording a wide array of functionalized cyclic ketones (**13**) in moderate to good yields (Scheme 7).[70] In this regard, the coordinatively saturated mononuclear Ph_3PAuCl was used in combination with the photosensitizer $[Ru(bpy)_3](PF_6)_2$. The group also detected that a diazonium salt bearing a comparatively electron-rich substituent, such as −OMe, resulted in lower yield with the use of Ph_3PAuCl (**13a**, 16%). A stronger electron-withdrawing group on the ligand of the gold catalyst $(4\text{-}CF_3C_6H_4)_3PAuCl$ improved the yield to 51%. Furthermore, changing the photosensitizer from $[Ru(bpy)_3](PF_6)_2$ to *fac*-$Ir(ppy)_3$, which possess a higher excited-state reduction potential, also influenced the outcome of the reaction. For example, when the electron-rich diazonium salts were employed, the yields dropped, however, for electron-poor surrogates, the yield improved significantly (**13b**, from 31% to 51% for 4-methoxycarbonylphenyldiazonium tetrafluoroborate). The authors did not speculate on the reason for the divergence in yield, however, the trend that acceptor substituents performed better than donor could correlate to the easier reduction of the respective diazonium salts bearing electron-withdrawing groups.

On the basis of their intensive time-resolved FT-IR spectroscopic experiments, Toste and co-workers proposed an alternative reaction pathway starting with the oxidation of the gold(I) complex by an aryl radical generated from excited Ru(II) photocatalyst (Scheme 8). The thereby formed gold(II) intermediate (**14**) was further oxidized by Ru(III) to give rise to the cationic arylgold(III) species (**15**). Here the gold(III) species acted as the Lewis acid (not the gold(I)) and coordinated to the double bond to promote the ring expansion. Final reductive elimination provided the arylated cyclic ketones and regenerated the gold(I) catalyst.

Thereafter, the group of Shin accessed the synthesis of 3-arylated butenolides (**18**) from *tert*-butyl allenoates (**17**) and aryldiazonium salts under both photoredox (A) and thermal (B) conditions (Scheme 9).[71] In case of conditions A, a combination of Ph_3PAuCl and AgOTf in situ form the respective cationic gold(I) complex, and $[Ru(bpy)_3](PF_6)_2$ was used as the dual catalyst system. Not surprising, when using the identical conditions or omitting the photocatalyst in the dark, no reaction occurred. In sharp contrast, heating the reaction mixture to 60 °C and employing Ph_3PAuCl solely, the

https://dx.doi.org/10.1021/acs.chemrev.0c00841
Chem. Rev. XXXX, XXX, XXX−XXX

Scheme 8. Mechanistic Proposal for the Arylative Ring Expansion of Alkenyl and Allenyl Cycloalkanols

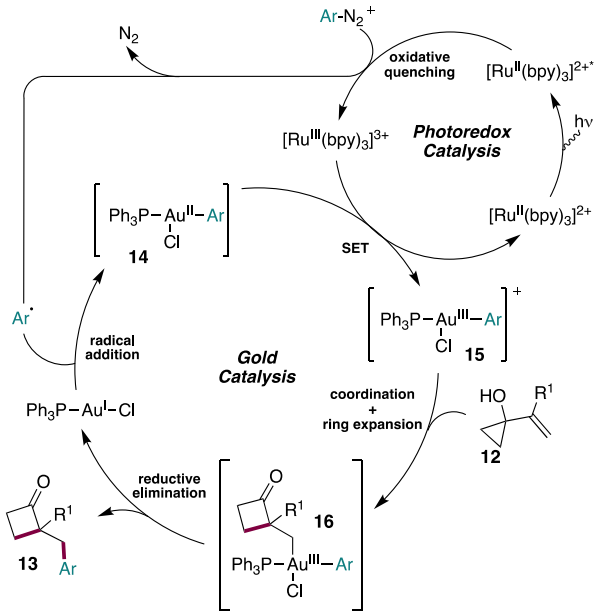

reaction proceeded smoothly in the dark. To study the respective mechanisms, the group examined the oxidation state of the gold catalyst under both photoredox (A) and thermal (B) conditions with XPS (X-ray photoelectron spectroscopy). With the result that for the photoredox conditions (A) an initial formation of the vinyl gold(I) species (**19**) was proposed, which was followed by the oxidative addition and reductive elimination to afford the desired butenolides (**18**). The mechanistic proposal for the thermal conditions (B) proceeded vice versa, an initial oxidation of the gold(I) catalyst to gold(III), followed by the π-activation.

Furthermore, the quantum yield of the photocatalytic reaction was studied and differentiated between the use of a coordinatively saturated and a cationic gold(I) complex. Applying a neutral gold(I) complex in a type of Ph_3PAuCl, the quantum yield was measured to be 0.31. In the case of a cationic gold(I) complex, generated in situ by the combination of Ph_3PAuCl and AgOTf, the quantum yield suggested a short radical chain process (Φ = 1.21). This was explained by the fact that a radical chain process contributed to the oxidation of gold(II) to gold(III).

A common mechanistic trend emerged for the understanding of dual gold/photoredox catalysis: (1) an initial formation of a vinylgold(I) intermediate by using a cationic gold(I) complex followed by an oxidative addition and (2) an initial oxidative addition to gold(I) and subsequent π-activation in the case of a neutral, coordinatively saturated gold(I) complex.

Contradictorily, Yu et al. pursued an in-depth theoretical study on the intramolecular oxyarylation of alkenes realized by Glorius.[72] Despite applying a cationic gold(I) catalyst, they revealed that the more favorable mechanism starts with the oxidation of the gold center and the cyclization was subsequently facilitated by the arylgold(III) intermediate.

After these milestones of accomplishing the mild oxidation of gold(I) to gold(III), significant efforts have been made to further explore the utilization of the merged gold/photoredox technique. In 2016, the groups of Shin,[73] Glorius,[74] and Alcaide/Alemendros[75] independently disclosed the arylative Meyer–Schuster rearrangement of propargylic alcohols (**23**) to furnish α-arylated enones (**24**), with an excellent functional group tolerance in moderate to very good yields (Scheme 10A–C).

Shin et al. mainly focused on the transformation of tertiary propargylic alcohols and availed a neutral, saturated gold(I) catalyst, reporting that a cationic gold(I) did not effectively suppress the protodemetalation, leading to a product mixture of **24a** (32%) and **25a** (38%) (Scheme 10A). The catalyst loading of the gold catalyst could be optimized to 2.5 mol % (instead of the commonly used 10 mol % for dual/gold systems). Glorius and co-workers observed the same trend, for their conditions the utilization of a cationic gold(I) complex completely shut down the desired product formation and 20% of the (through protodemetalation formed) enone (**25b**) was obtained (Scheme 10B). While mainly studying the reaction of secondary propargylic alcohols, they diastereoselectively received the *E*-isomer upon employing a base. In contrast to the two just described methods of *tandem* Meyer–Schuster arylation/rearrangement, Alcaide/Alemendros accounted a successful transformation to the desired cross-coupled product (**24c**) employing a cationic gold(I) complex (Scheme 10C, entry 1). Further, for their study on primary propargylic

Scheme 9. Gold-Catalyzed Coupling of *tert*-Butyl Allenoates and Aryldiazonium Salts under (A) Photoredox and (B) Thermal Conditions and Their Respective Key Intermediates

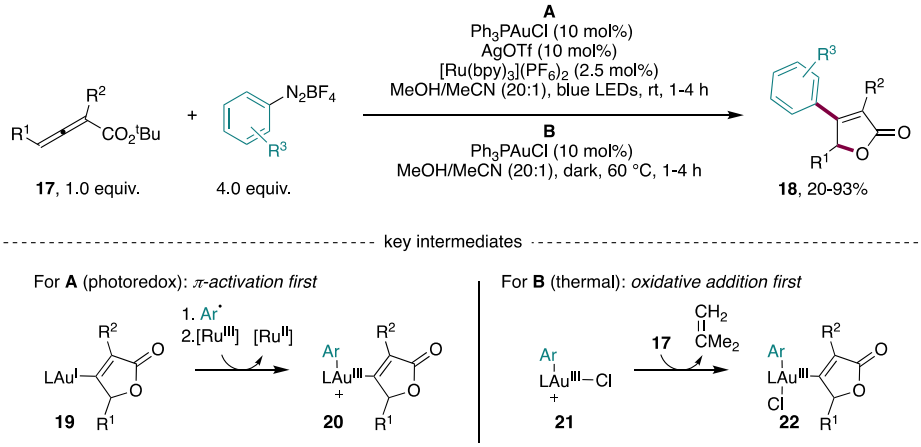

https://dx.doi.org/10.1021/acs.chemrev.0c00841
Chem. Rev. XXXX, XXX, XXX–XXX

Scheme 10. Arylative Meyer–Schuster Rearrangements by Shin, Glorius, and Alcaide/Alemendros

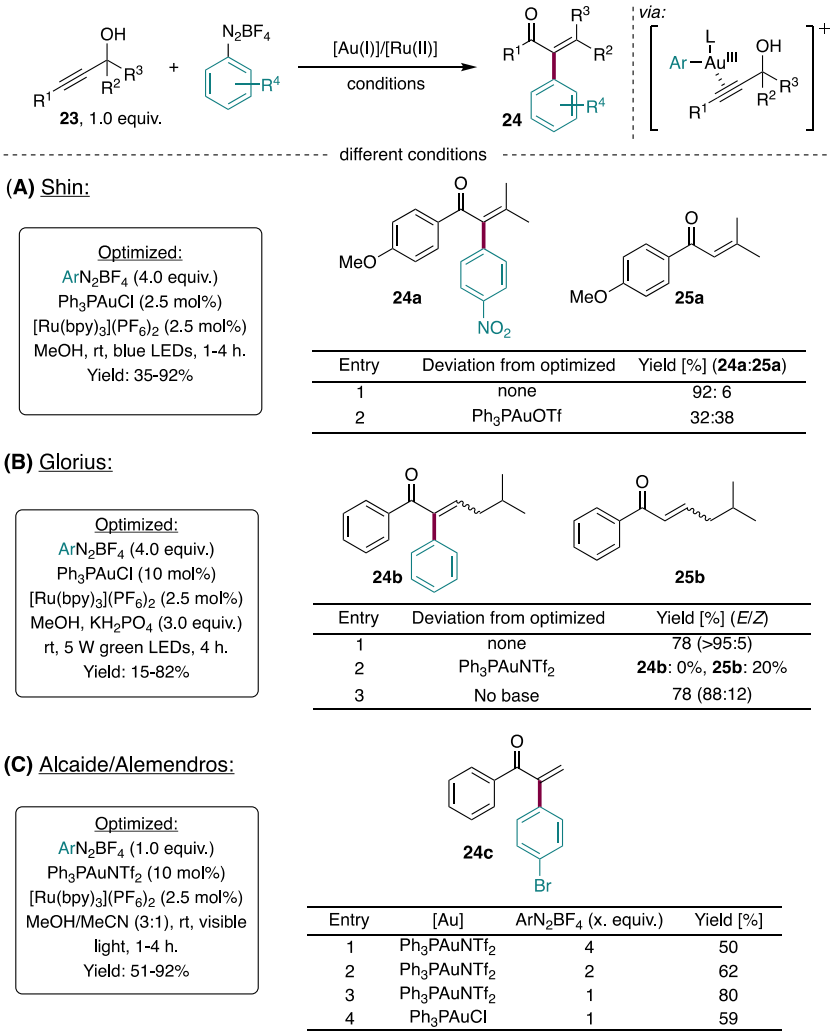

Scheme 11. Dual Gold/Photoredox Cyclization/Arylation Cascade to Benzofurans and Indoles

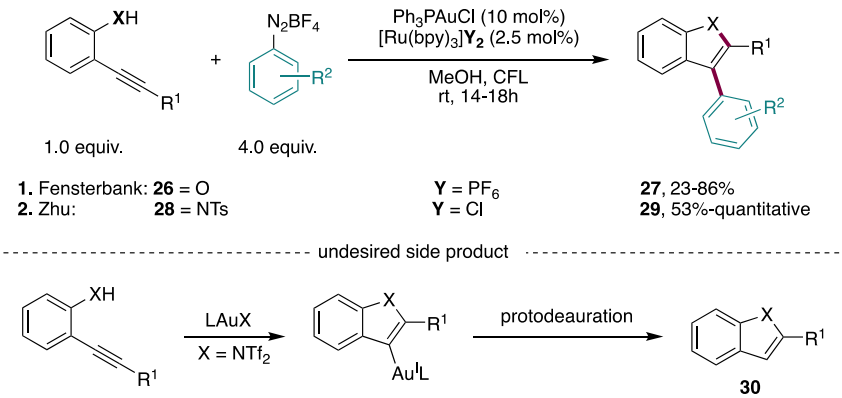

alcohols, they decreased the amount of aryldiazonium salts to only 1.0 equiv. (entries 2 and 3). Under otherwise equal conditions they showed, that the use of Ph_3PAuCl led to a drop-in yield to 59% (entry 4). Regardless of the choice of the electronic nature of the gold catalyst, the protocols concurrently suggest a photocatalytically generated arylgold(III) species activating the C–C triple bond.

These synergistic gold and photocatalysis techniques have also been applied for the construction of diverse arylated heterocycles by intramolecular ring closure of alkynes and allenols. In this realm, Fensterbank's group developed the cyclization of *o*-alkynylphenols (**26**) with aryldiazonium salts accessing structurally diverse benzofurans (**27**) in satisfying yields (Scheme 11).[76] Later, Zhu's group examined the synthesis of indoles starting from *N*-Ts-*o*-alkynylanilines (**28**) (Scheme 11).[77] Both protocols indicated that the use of a cationic gold(I) catalyst led to a very fast, intrinsic π-activation of the alkyne moiety followed by cycloisomerization and

https://dx.doi.org/10.1021/acs.chemrev.0c00841
Chem. Rev. XXXX, XXX, XXX–XXX

undesired protodeauration. This gave rise to the nonarylated benzofurans or indoles (**30**). However, by applying a neutral, saturated gold(I) catalyst, the protodemetalation seemed to be effectively suppressed.

At this point in 2016, it became already clear that mononuclear gold(I) photocatalysis with aryldiazonium salts does not necessarily need an additional photoredox catalyst (see discussion in section 2.2),[60] still, subsequent studies (in this discussion following this paragraph) often kept adding these photosensitizers.

Mechanistically, the corresponding arylgold(III) was formed first by stepwise oxidative addition (Scheme 12). The highly

Scheme 12. Mechanistic Hypothesis of the Arylative Cyclization to Benzofuran and Indol Derivatives

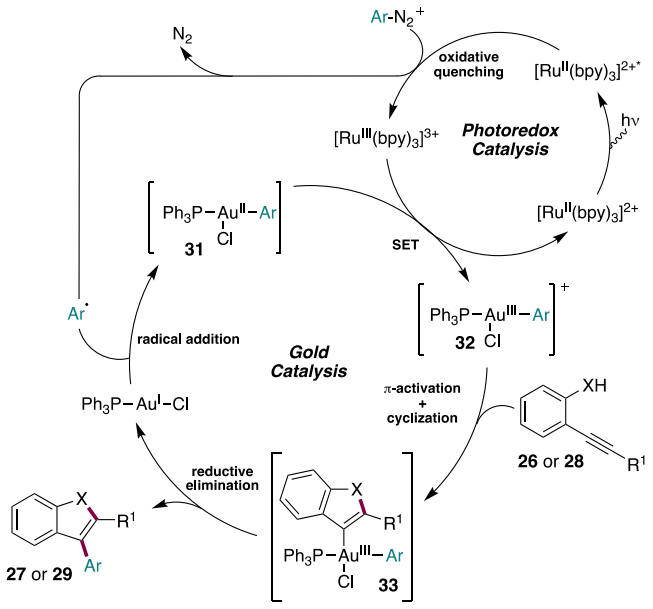

electrophilic arylgold(III) then activated the alkyne moiety to trigger the cyclization to vinylgold(III) intermediate, and a subsequent reductive elimination produced the benzofuran or indole derivatives.

An access to trisubstituted 2,5-dihydrofurans (**35**) was provided by Alcaide and Alemendros (Scheme 13).[78] A wide range of substituted allenols (**34**) were converted and directly arylated in the presence of aryldiazonium salts with the use of Ph_3PAuCl and $[Ru(bpy)_3](PF_6)_2$ in a solvent mixture of MeOH and MeCN under irradiation with compact fluorescent lamp (CFL light). In contrast to their previously described Meyer–Schuster arylation/rearrangement reaction,[75] a cationic gold(I) catalyst resulted in the undesired cycloisomerization adduct (**36a**) (entry 1). A possible explanation for this might be that in the case of using the cationic gold(I) catalyst in combination with substrate **34** the π-activation and subsequent cyclization proceeded faster. The thus formed vinyl gold(I) species could then be further oxidized, however, the formation of **36a** showed that in this case the protodeauration dominated. Furthermore, using a gold(III) catalyst did not deliver the desired product (**35a**), albeit **36a**, because the crucial oxidative addition of gold(I) to gold(II) by the aryl radical cannot take place, when the oxidation state of the starting gold catalyst is already +3 (entries 2 and 3).

Both aliphatic and aromatic allenols were well tolerated, delivering the desired products in moderate to excellent yields. Remarkably, a double cyclization/arylation process was received by an enantiopure bis(allenol) (**34d**) to bis(β-lactam-tethered 2,5-dihydrofuran) (**35d**) in a moderate yield of 49%. Interestingly, a selective cleavage of one of the ketal substructures occurred under the given reaction conditions. The authors initially considered both reaction mechanisms: nucleophilic addition first or oxidative addition first. However, the performed density functional theory (DFT) calculations revealed that the intramolecular nucleophilic attack of the alcohol was more efficient with arylgold(III) than that with gold(I) catalyst.

An intramolecular *ipso*-arylative cyclization to obtain spirocarbocycles (**39**) using the dual gold/photoredox technique was disclosed by Patil and co-workers by deploying 4-methoxyphenyl-3-arylpropiolates (**38**) and aryldiazonium salts (Scheme 14).[79] The influence of the electronic nature of the gold(I) catalyst was well demonstrated in this protocol. Intriguingly, a neutral, coordinatively saturated gold(I) catalyst bearing a phosphine ligand with an electron-donating substituent performed best (76%, entry 1) compared to triphenylphosphine (62%, entry 2) or an electron-withdrawing group on the ligand (53%, entry 3). It may be rationalized by a better stabilization of the gold(III) intermediate by electron-rich phosphine ligands. A cationic gold(I) catalyst of type $Ph_3PAuNTf_2$ delivered **39a** with a yield of 45% (entry 4). The proposed reaction mechanism proceeded via the arylgold(III) intermediate triggering the demethylative, dearomative *ipso*-cyclization (**40**) to the respective vinylgold(III) species (**41**) with the aid of water.

The most recent example in this research field was the arylative cyclization of 1,6-enynes (**42**) with aryldiazonium salts by the group of Echavarren (Scheme 15).[80] The initial obstacle of the major formation of nonarylated methoxycyclized product **44** had to be overcome. Curiously, using a phosphine gold(I) catalyst improved the selectivity toward the desired arylated product (**43a**). An intensive screening of the photocatalyst disclosed that a more oxidizing $[Ru(bpz)_3](PF_6)_2$ (bpz = 2,2′-bipyrazine) photocatalyst in combination with the electron-rich trimethylphosphine gold(I) catalyst performed best to selectively afford **43a** in 90% yield.

In this three-component reaction, not only the reaction scope regarding both substrates, 1,6-enyne and the aryldiazonium salt, can be investigated, but also the alcoholic solvent. The most exciting example was the tolerance for propargylic alcohol exhibiting a terminal alkyne, nevertheless, 60% of the product (**43b**) could be isolated (Scheme 16). Moreover, different 1,6-enynes were tested such as a phenyl-substituted or a *N*-tosyl-containing enyne. Both were tolerated well, giving (**43d**) and (**43e**) in a yield of 61% and 72%, respectively. Unfortunately, the employment of internal alkynes failed for this transformation. During their mechanistic studies, Echavarren and co-workers found that trimethylphosphine gold(I) chloride was unable to activate the alkyne, which might be a reason for the high selectivity for the formation of the desired product **43** over undesired nonarylated **44**.

Surprisingly, a stoichiometric oxidation attempt with the sole use of a gold(I) complex with aryldiazonium salt (*note*: *without photosensitizer*) was successful, showing that a direct interaction between gold and the catalyst was possible. However, all of their attempts with catalytic amounts of the gold(I) complex failed without a photosensitizer. On that account, a mechanism starting from the oxidation of gold(I) over gold(II) (**45**) to gold(III) (**46**) was postulated (Scheme 16). The latter

https://dx.doi.org/10.1021/acs.chemrev.0c00841
Chem. Rev. XXXX, XXX, XXX−XXX

Scheme 13. General Sequence, Selected Control Experiments, Key Intermediate, and Selected Examples for the Synthesis of Substituted 2,5-Dihydrofurans under Merged Gold/Photoredox Conditions

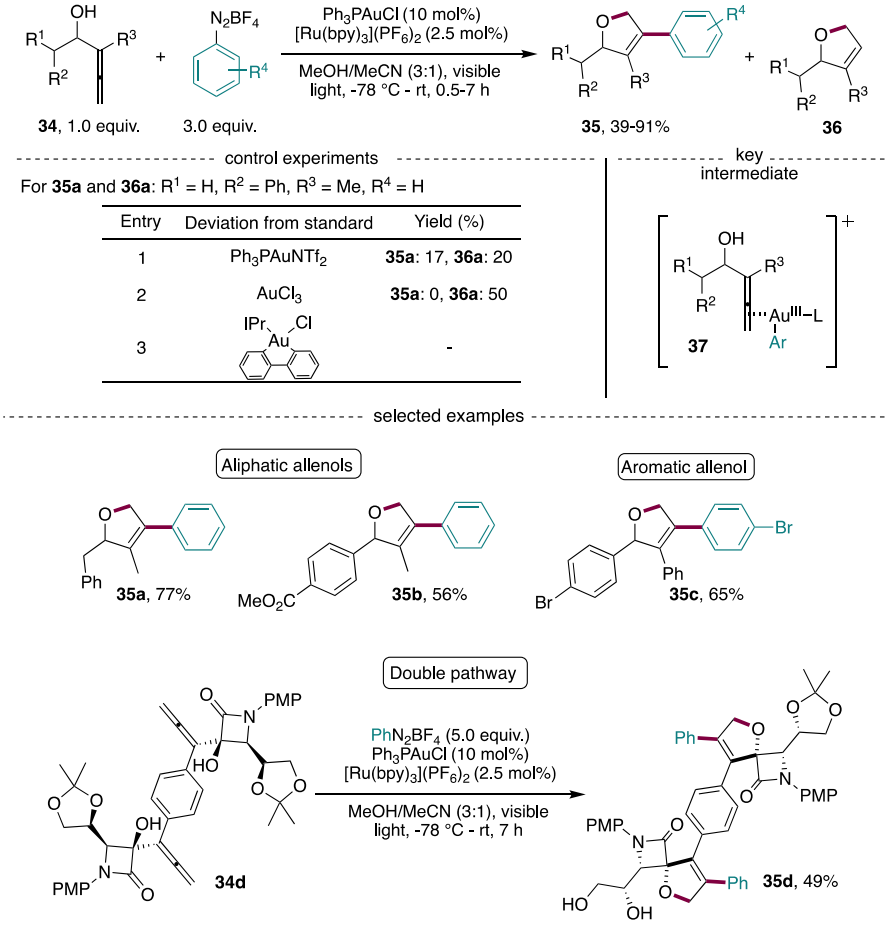

Scheme 14. Intramolecular *ipso*-Arylative Cyclization through Merged Gold/Photoredox Catalysis

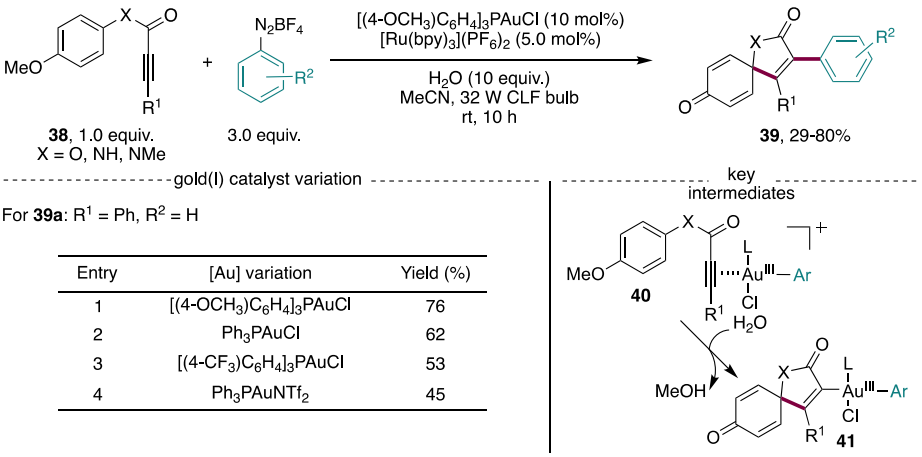

oxidation could proceed either by reduction of [Ru(III)] or by another equivalent of diazonium salt. Next, the electrophilic arylgold(III) complex (**46**) coordinated to the 1,6-enyne (**42**) to trigger a 5-*exo*-*dig* cyclization, which was followed by the addition of the alcohol to form the vinylgold(III) intermediate **48**. Finally, the product (**43**) was formed by reductive elimination under regeneration of the gold(I) catalyst. This approach gives access to cyclization products with opposite configuration of that provided by traditional redox-neutral gold-catalyzed alkoxycyclizations.[81,82]

2.1.2. C−C and C−X Cross Coupling Reactions. Along with the hitherto described nucleophilic additions, the merged gold/photoredox technique has also been used for a great number of C−C and C−X cross-coupling reactions. One of the first contributions in this field was reported by Toste et al., investigating the P−H arylation of phosphonates (**49**) (Scheme 17).[83] A broad reaction scope was studied, first varying the substitution of the aryldiazonium salts, with the result that electron-donating groups were better coupled with diethyl phosphite than electron-withdrawing groups (**50a** vs

https://dx.doi.org/10.1021/acs.chemrev.0c00841
Chem. Rev. XXXX, XXX, XXX−XXX

Scheme 15. Arylative Cyclization of 1,6-Enynes with Aryldiazonium Salts Using Dual Gold/Photoredox Conditions

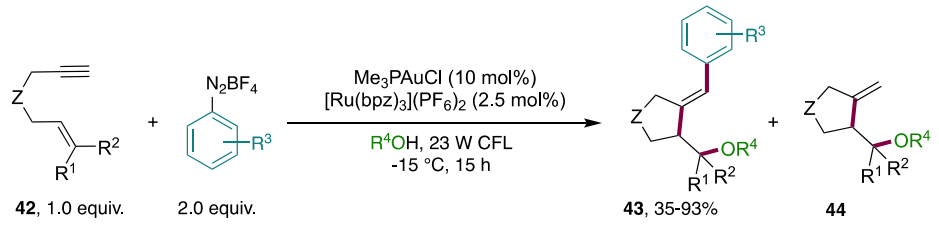

control experiments

For : **43a**, $R^1 = R^2 = Me$, $R^3 = H$, $R^4 = Me$, Z = $C(CO_2Me)_2$

Entry	Deviation from optimized	Yield (%) (**43a**:**44a**)
1	-	90:0
2	Ph_3PAuCl / $[Ru(bpm)_3](PF_6)_2$, rt	21:46
3	$Ph_3PAuNTf_2$ / $[Ru(bpm)_3](PF_6)_2$, rt	24:51
4	$Me_3PAuNTf_2$ / $[Ru(bpm)_3](PF_6)_2$, rt	70:11
5	$Me_3PAuNTf_2$ / $[Ru(bpz)_3](PF_6)_2$, rt	72:10

Scheme 16. Proposed Reaction Mechanism and Selected Examples for the Arylative Cyclization of 1,6-Enynes with Aryldiazonium Salts

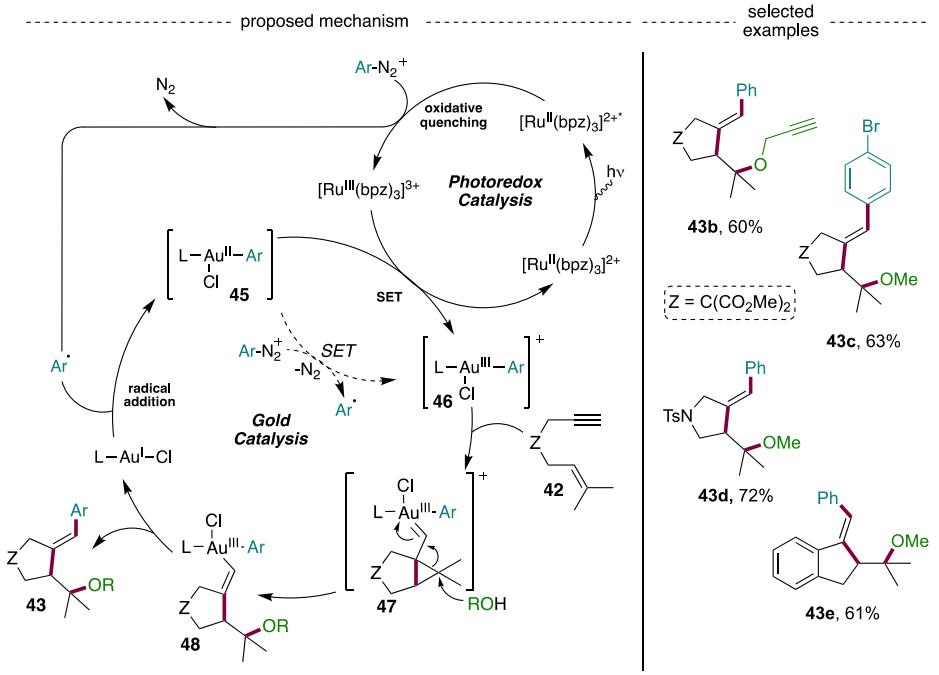

Scheme 17. P−H Arylation of Phosphonates via Gold and Photoredox Catalysis

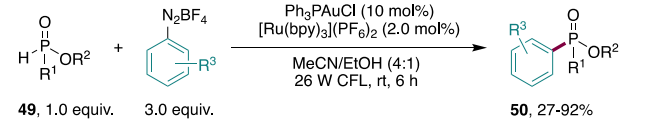

selected examples

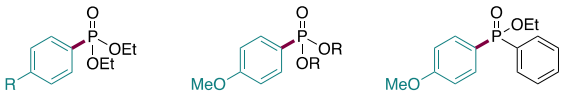

R = OMe, **50a**, 92%
= F, **50b**, 86%
= CF_3, **50c**, 40%

R = Me, **50d**, 90%
= ^{i}Pr, **50e**, 81%
= Bn, **50f**, 50%

50g, 43%

50c). Changing different types of phosphite compounds gave a better reaction outcome with alkyl groups than with a dibenzylphosphinate (**50d** vs **50f**). The conversion of phenylphosphinic acid in a three-component coupling with aryldiazonium salt and the alcoholic solvent (**50g**) further demonstrated the versatility of this method.

Later, the same group introduced the gold-catalyzed arylation of trimethylsilylalkynes (**51**) to afford functionalized internal arylalkynes (**53**) in moderate to excellent yields using a broad set of aryldiazonium salts and substituted trimethylsilylalkynes (Scheme 18 A).[84] In their report, the effect of the counteranion of the aryldiazonium salt was also examined. Tetrafluoroborate and tosylate performed well (entries 1 and 2), however, hexafluorophosphate had a detrimental effect on the reaction outcome (24%, entry 3). A sound explanation of the counteranion effect in gold photocatalysis is still unknown (for the influence in traditional gold catalysis, see refs 85−88). Further, investigating the role of the silyl moiety of alkynylsilane led to a dramatic drop in yield with increasing

https://dx.doi.org/10.1021/acs.chemrev.0c00841
Chem. Rev. XXXX, XXX, XXX−XXX

Scheme 18. C(sp)−C(sp^2) Cross-Coupling Reactions by (A) Toste and (B) Glorius

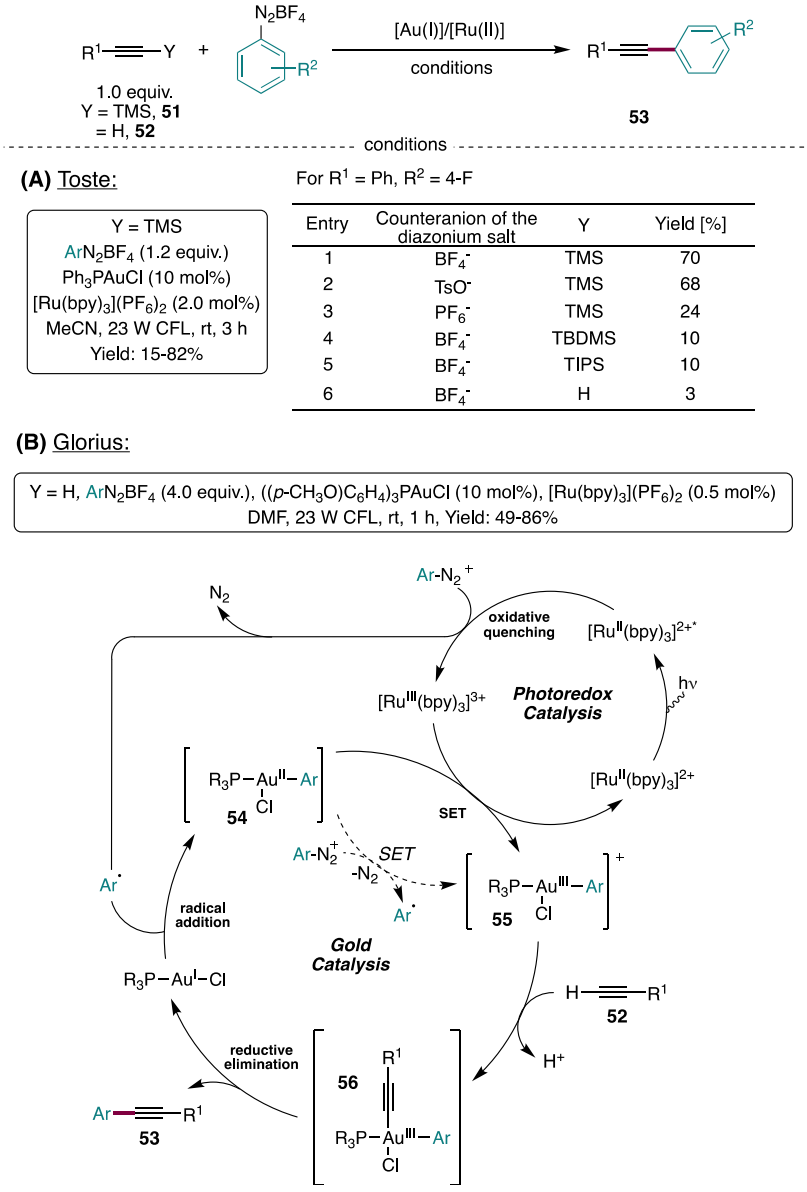

Entry	Counteranion of the diazonium salt	Y	Yield [%]
1	BF_4^-	TMS	70
2	TsO^-	TMS	68
3	PF_6^-	TMS	24
4	BF_4^-	TBDMS	10
5	BF_4^-	TIPS	10
6	BF_4^-	H	3

the steric hindrance of the silyl group (entries 4−5). When applying the corresponding terminal alkyne instead of trimethylsilylalkyne, only 3% of the desired product were obtained (entry 6). Despite the great synthetic potential of these two methods, the mechanistic discussion would be helpful for future reaction developments.

Almost simultaneously, Glorius and colleagues accessed these internal arylalkynes (**52**) by a direct C−H functionalization of terminal alkynes (Scheme 18B).[89,90] This success could potentially be attributed to three factors: (1) the amount of diazonium salt (1.2 equiv. versus 4.0 equiv.), (2) the solvent (MeCN versus DMF), or (3) the gold(I) catalyst (Ph_3PAuCl versus $((p\text{-}CH_3O)C_6H_4)_3PAuCl$).

The proposed mechanism was in accordance to the previously described sequences containing a nucleophilic addition of electrophilic arylgold(III) species (**55**) to the terminal alkyne. However, quantum yield measurement by chemical actinometry gave a value of 3.6. Thus, an innovative second SET process between the arylgold(II) intermediate (**54**) with another equivalent of diazonium salt delivering arylgold(III) species (**55**) and an aryl radical was proposed to occur (dashed arrows). The authors stated that this process would mainly contribute to the formation of gold(III) intermediate. In turn, this would also lead to the hypothesis that the photosensitizer in this case would mainly act as a radical initiator. In general, the above coupling of alkynes with aryldiazonium salts tolerating halide moieties complemented the traditional palladium-catalyzed Sonogashira−Hagihara cross-coupling.

Extending this strategy to C(sp^2)−C(sp^2) cross-coupling reactions, Fouquet et al.[91] and Lee et al.[92] concurrently studied the reaction of aryldiazonium salts with arylboronic acids under merged gold and photoredox catalysis to obtain substituted biaryls (**58**) (Scheme 19A). The group of Fouquet used $[Ru(bpy)_3](PF_6)_2$ or 9-mesityl-10-acridinium tetrafluoroborate as a photosensitizer and CsF as an additive to facilitate the transmetalation. Lee and co-workers applied $[Ru(bpy)_3](PF_6)_2$ as a photosensitizer and water instead of CsF. However, their respective mechanistic proposal contradicted (Scheme 19B).

https://dx.doi.org/10.1021/acs.chemrev.0c00841
Chem. Rev. XXXX, XXX, XXX−XXX

Scheme 19. Cross-Coupling of Aryldiazonium Salts with Arylboronic Acids and Their Mechanistic Proposals

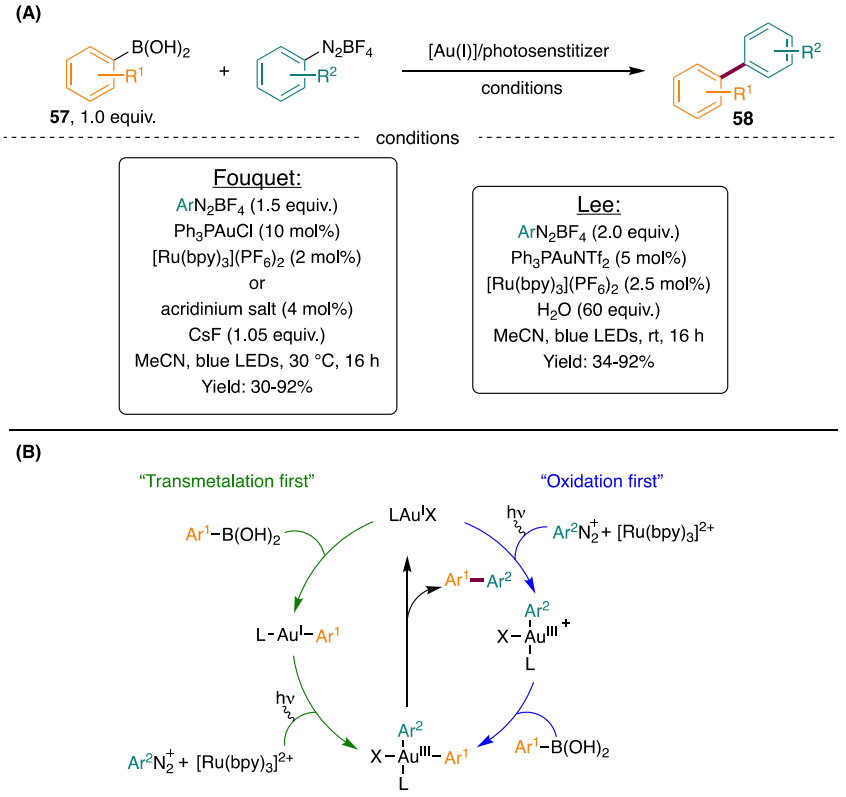

Scheme 20. Mechanistic Studies for the Reaction of Aryldiazonium Salts and Arylboronic Acids Using (P,N)AuCl

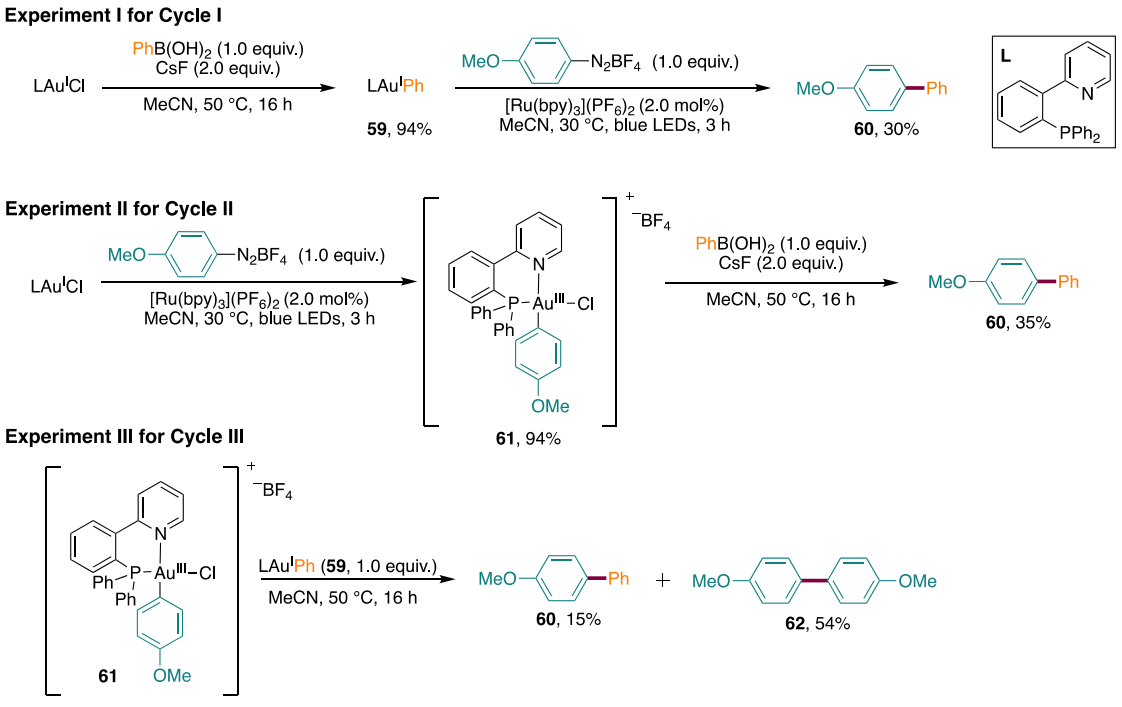

Fouquet used a coordinatively saturated gold(I) catalyst suggesting a "transmetalation first" mechanism. This resulted from ^{31}P NMR studies examining stoichiometric experiments using the generated $Ph_3PAu(I)Ar$ as basis. On the other hand, Lee and co-workers corroborated their mechanistic suggestion also on ^{31}P NMR spectroscopy analyzing stoichiometric and catalytic experiments of both Ph_3PAuCl and $Ph_3PAuNTf_2$ in the presence of the boronic acid in a solvent mixture of CD_3CN and D_2O. In case of neutral gold(I) complex (Ph_3PAuCl), no transmetalation was observed, whereas by using the cationic gold(I) complex ($Ph_3PAuNTf_2$), the transmetalated arylgold(I) species was detected. As a result, they concluded that a "transmetalation first" mechanism is favored when deploying the cationic gold(I) complex,

https://dx.doi.org/10.1021/acs.chemrev.0c00841
Chem. Rev. XXXX, XXX, XXX−XXX

Scheme 21. Proposed Reaction Mechanism of the Reaction of Aryldiazonium Salts and Arylboronic Acids Using (P,N)AuCl

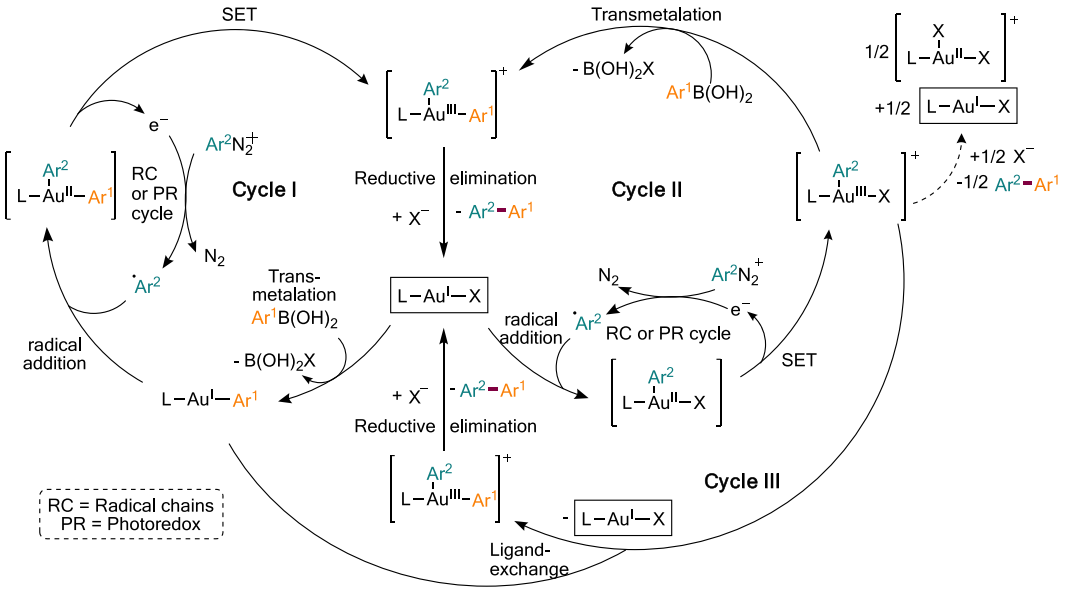

Scheme 22. Hiyama-like Desilylative Arylations of Allyltrimethylsilanes

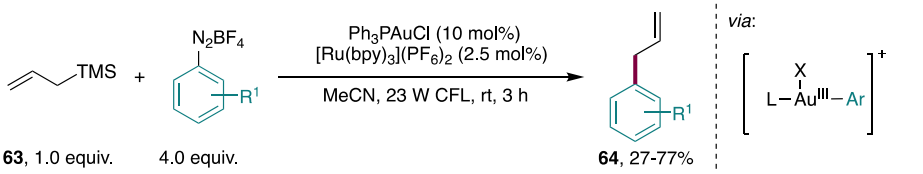

control experiments

For **64a**: R^1 = 4-Cl

Entry	[Au]	Yield [%]
1	Ph_3PAuCl	79
2	$Ph_3PAuNTf_2$	61
3	$Ph_3PAuOTf$	38
4	$((p\text{-}CH_3O)C_6H_4)_3PAuNTf_2$	60
5	$(C_6F_5)_3PAuNTf_2$	11

Entry	Counteranion of the diazonium salt	Silyl	Yield [%]
1	TsO^-	TMS	-
2	PF_6^-	TMS	49
3	CF_3OCO^-	TMS	68
4	BF_4^-	TES	70
5	BF_4^-	TBDMS	61
6	BF_4^-	TIPS	-

compared to an "oxidation first" pathway in the case of a coordinatively saturated gold(I) complex.

Further, Fouquet suggested that the use of either an electron-deficient aryldiazonium salt (4-NO_2) or an electron-rich aryldiazonium salt (4-OMe) influenced the reaction mechanism (Scheme 20). This assumption was studied by quantum yield measurements by chemical actinometry to give two different values: 1.4 for 4-methoxyphenyldiazonium tetrafluoroborate and 9.6 for 4-nitrophenyldiazonium tetrafluoroborate. Using the electron-deficient surrogate, the reaction also proceeded under thermal conditions (30 °C) in the dark, delivering the cross-coupled product with a yield of 57%. However, at 18 °C, the reaction was observed to only give traces of the cross-coupled product. As a result, this was the first observation that the mechanism (transmetalation first or oxidative addition first) was influenced by the electronic nature of the aryldiazonium salt.

To clarify the mechanistic understanding of the coupling of arylboronic acids and aryldiazonium salts using dual gold/photoredox catalysis, Fouquet and colleagues pursued further stoichiometric experiments on this topic. For example, a coordinatively saturated gold(I) complex with a (P,N) ligand (2-pyridylphenyl-diphenylphosphine) was applied, to stabilize the arylgold(III) intermediate (Scheme 21).[93]

Initially, a transmetalation as first step in the catalytic cycle was considered. For this purpose, a saturated gold(I) complex was reacted with phenylboronic acid in the presence of cesium fluoride in the dark at 50 °C, delivering the corresponding arylgold(I) complex (**59**) in 94% yield (experiment I, first step). This was not surprising because this transmetalation step is widely investigated in traditional homogeneous gold chemistry.[28,94,95] Addition of 4-methoxyphenyldiazonium tetrafluoroborate to arylgold(I) complex **59** in the presence of $Ru(bpy)_3(PF_6)_2$ and blue LEDs gave 30% of the cross-coupled product (**60**), in similar yield to the one obtained from the overall catalytic reaction (39%). This suggested a possible transmetalation first pathway (experiment I, second step). Next, the oxidation as the first step was evaluated by using LAuCl and aryldiazonium salt in the presence of Ru-photosensitizer and light irradiation (experiment II). The corresponding arylgold(III) complex (**61**) was formed in 94% yield. A following transmetalation onto Ar−Au(III) species-(**61**) was studied by applying phenylboronic acid in the presence of CsF, and the desired coupling product (**60**) was

https://dx.doi.org/10.1021/acs.chemrev.0c00841
Chem. Rev. XXXX, XXX, XXX−XXX

Scheme 23. Hiyama-like Desilylative Arylations of Aryltrimethylsilanes

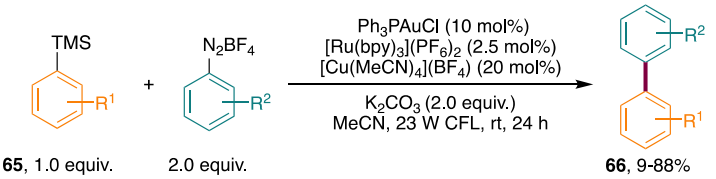

65, 1.0 equiv. 2.0 equiv. **66**, 9-88%

control experiments

For : **66a**: Benzofuran-TMS, R^2 = 4-Cl

Entry	Deviation from optimized	Yield [%]
1	-	65
2	$Ph_3PAuNTf_2$	21
3	$((p\text{-}CH_3O)C_6H_4)_3PAuCl$	17
4	$(C_6F_5)_3PAuCl$	10
5	CuBr	45
6	$Cu(OAc)_2$	50

Entry	Counteranion of the diazonium salt	Silyl	Yield [%]
1	TsO^-	TMS	-
2	PF_6^-	TMS	62
3	CF_3OCO^-	TMS	41
4	BF_4^-	TES	65
5	BF_4^-	TBDMS	59
6	BF_4^-	TIPS	62

delivered in 35% yield. This result potentially permitted the statement that an oxidation first mechanism was feasible (cycle II). At last, a ligand exchange between LAu(I)-Ar through transmetalation first and LAu(III)-Ar through oxidation first mechanism in the catalytic cycle was considered. Studying this, both complexes **59** and **61** were reacted in the dark at 50 °C, producing 15% of the cross-coupled product (**60**) (experiment III). This was an indication for the authors to postulate that this pathway might occur in the present catalytic cycle.

Concluding that the reaction of aryldiazonium tetrafluoroborate and arylboronic acids using a (P,N)AuCl complex in the presence of a photosensitizer proceeded via three mechanistic pathways: (cycle I) "transmetalation first", (cycle II) "oxidation first", or (cycle III) by involving a transmetalation between gold(I) and gold(III). Additional experiments could have possibly excluded the other pathways, which would have helped for a real clarification of the mechanistic understanding.

After the success of complementing the traditional Sonogashira–Hagihara and Suzuki–Miyaura cross-coupling reactions by the simple employment of a gold catalyst in combination with a photosensitizer and light irradiation, Patil and co-workers focused on the Hiyama-like reactions. One publication engaged the coupling of allyltrimethylsilanes (**63**) and aryldiazonium salts to afford allylarenes (**64**) when deploying coordinatively saturated gold(I) complex of type Ph_3PAuCl and $[Ru(bpy)_3](PF_6)_2$ as a photocatalyst (Scheme 22).[96] During the course of optimization they realized that the reaction outcome is also influenced by the counteranion of the cationic gold(I) complex. Bis(trifluoromethanesulfonyl)imide gave the desired product with a yield of 61% (entry 2), while triflate only provided 38% of expected product (**64a**) (entry 3). Moreover, an electron-rich substituted phosphine ligand led to 60% yield (entry 4), whereas an electron-withdrawing phosphine-ligated gold complex diminished the reaction efficiency (11%, entry 5). They also studied the influence of the counteranion of the aryldiazonium salt and the effect of the silyl group on the coupling. Surprisingly, they observed a contrary outcome compared to the coupling of TMS-alkynes presented in Scheme 18A. Here, the use of tosylate as counteranion completely shut down the reaction (entry 1) while hexafluorophosphate worked well to give the product (**64a**) in 49% yield (entry 2). Along with tetrafluoroborate (79%), trifluoroacetate had a positive effect on the reaction (68%, entry 3). In addition, TES and TBDMS gave **64a** in similar yields (entries 4 and 5), while with a TIPS-substituted allylsilane the conversion failed. It is important to note that the reaction only operated when using unsubstituted allylsilanes and did not work for simple terminal alkenes. The latter was explained due to the β-silicon effect. The authors proposed an "oxidation first" mechanism via a transmetalation to arylgold(III) intermediate. Also, they ruled out a radical chain process, as suggested by Glorius (Scheme 18B), by showing the necessity of a continuous irradiation by conducting a light on/off experiment. Albeit, the lifetime of most of the radical chains are in the subsecond time scale, while the experiment of switching the light source on and off are conducted in a time scale of minutes. Therefore, such an experiment is controversial and the results of it should be considered with caution.[97]

The other protocol of Patil and co-workers on this topic dealt with the reaction of aryldiazonium salts and aryltrimethylsilanes (**65**) using a ternary catalyst system composed of Ph_3PAuCl, $[Ru(bpy)_3](PF_6)_2$ and $[Cu(MeCN)_4](BF_4)$ (Scheme 23).[98] Interestingly, also in comparison to the previous observation, the application of other gold(I) catalysts, such as cationic or bearing phosphine-ligands with either electron-rich or electron-poor substitution, reduced the reaction outcome to its minimum (10–21%, entries 2–4). In addition, the reaction showed lower yields when changing to copper catalysts, such as CuBr or copper(II) acetate (entries 5–6), showing a dependency of the reaction on the copper catalyst. Studying the different counteranions of the aryldiazonium salt, a similar trend to the coupling of allylsilanes was depicted (entries 1–3). Furthermore, other silyl groups, such as triethylsilyl (TES), *tert*-butyldimethylsilyl (TBDMS), and triisopropylsilyl (TIPS) all gave product **66a** in similar yields as the coupling with aryltrimethylsilanes (entries 4–6).

Mechanistically, the only difference to the dual gold/photoredox catalytic system was a precedent transmetalation of arylsilanes to the copper catalyst (**70**), which then underwent transmetalation to the photocatalytically generated arylgold(III) intermediate (**69**) (Scheme 24). A quantum yield measurement gave a value of 0.3, which is consistent with there being no radical chain mechanism.

https://dx.doi.org/10.1021/acs.chemrev.0c00841
Chem. Rev. XXXX, XXX, XXX–XXX

Scheme 24. Postulated Reaction Mechanism for the Coupling of Aryltrimethylsilanes under Merged Gold/Photoredox Conditions

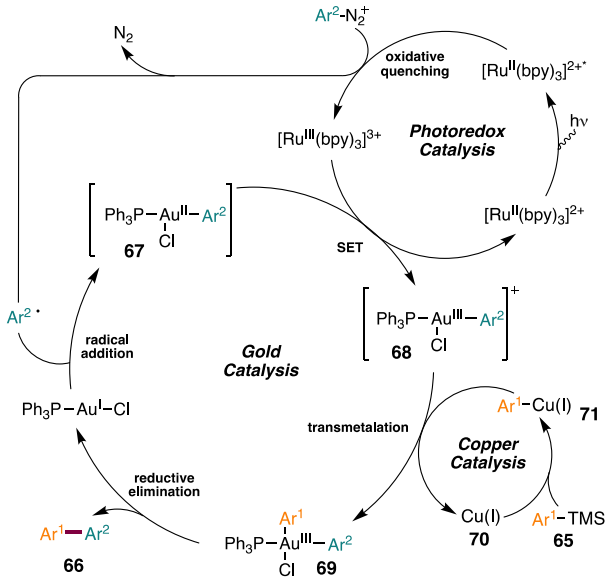

2.1.3. Combination of Nucleophilic Addition and Cross-Coupling Reaction. Inspired by Toste's work on the arylation of TMS-alkynes,[84] Alcaide and co-workers designed a domino double arylation strategy of TMS-terminated alkynols (**72** or **77**) (Scheme 25 and Scheme 26).[99] With their one-pot, two-step method, a wide range of triand tetra-substituted *α,β*-unsaturated ketones (**73**, Scheme 25), as well as 2,3-diarylbenzofurans (**79**, Scheme 26) could be easily accessed applying cooperative gold/photoredox catalysis. With the optimized reaction conditions from their previous work on the monoarylative Meyer–Schuster rearrangement (Scheme 10C),[75] namely $Ph_3PAuNTf_2$ and $[Ru(bpy)_3](PF_6)_2$ under visible light irradiation in a solvent mixture of MeOH and MeCN, and 6.0 equiv. of the aryldiazonium salt, they immediately received the desired enone (**73a**) in a yield of 82% (Scheme 25, entry 1). Toste and co-workers found that the choice of catalyst for the coupling of TMS-alkynes was the saturated gold(I) complex, Ph_3PAuCl.[84] In the present discussed protocol, the application of Ph_3PAuCl reduced the yield to 40% (entry 2). By changing the silyl group from TMS to TIPS, only trace amounts of **73a** were afforded (10%, entry 3). To benefit from this inert reactivity, Alcaide and Alemendros implemented a TMS/TIPS diynol (**75**) and obtained a chemoselective coupling of TMS-alkyne with the inviolate TIPS-alkyne remaining in the product (**76**). This domino double arylation was suggested to proceed via two consecutive gold/photoredox cycles. The first cycle arylated the TMS-terminated alknyols **72** to give key intermediate **74**, which enters a second cycle to produce the desired *α,β*-unsaturated ketones **73**.

Interestingly, when the optimized reaction conditions were applied to obtain 2,3-diarylbenzofurans (**79**), only the monoarylated 2-arylbenzofurans (**78**) were produced (Scheme 26). However, with the neutral Ph_3PAuCl under otherwise identical reaction conditions, the double arylations proceeded. This phenomena of fast nucleophilic addition and subsequent protodeauration by using a cationic gold(I) complex was also already observed by Fensterbank et al. for the monoarylation of *o*-alkynylphenols.[76]

With the aim to incorporate two different aryl groups in the domino 2-fold arylation of TMS-alkynols, they managed to optimize the one-pot conditions starting with 1.5 equiv. of the first aryldiazonium salt under a strict temperature control to a maximum of −20 °C (Scheme 27). Upon addition of a second, different aryldiazonium salt, the different arylated *α,β*-unsaturated ketones (**83**) were obtained in moderate yields.

For a successful reaction outcome, a fast chemoselective arylation of the TMS-alkyne (**74** and **80**) had to occur before the Meyer–Schuster-type rearrangement or oxycyclization commenced. Thus, the substrates traversed two of the normal cycles, each consisting of (1) aryl radical generation, (2) oxidation of gold(I), (3) *π*-coordination, and (4) reductive elimination. The first cycle contained a chemoselective transmetalation of TMS-alkyne substructure to gold(III) acetylide to produce the internal, arylated alkyne (**74** and **80**). The second cycle underwent a cyclization to afford a vinyl

Scheme 25. Domino Double Arylation Strategy of Propargylic Alcohols

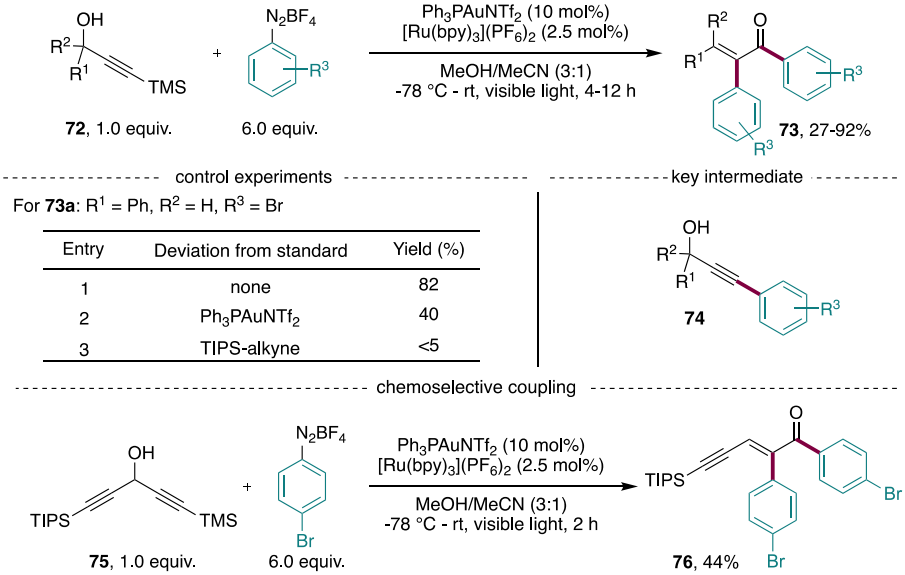

https://dx.doi.org/10.1021/acs.chemrev.0c00841
Chem. Rev. XXXX, XXX, XXX−XXX

Scheme 26. Domino Double Arylation Strategy of *o*-Trimethylsilylalkynylphenols

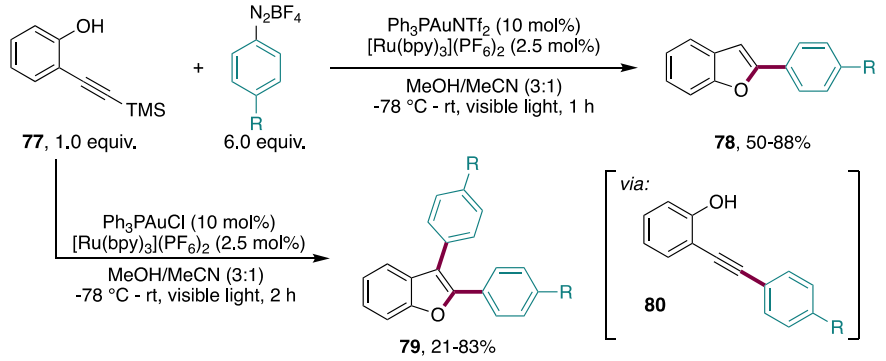

Scheme 27. Domino Two-Fold Arylation of TMS-Alkynols

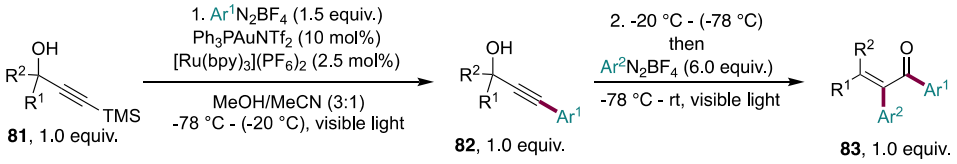

Scheme 28. Overview of Feasible Syntheses of Various Benzo-fused Heterocycles

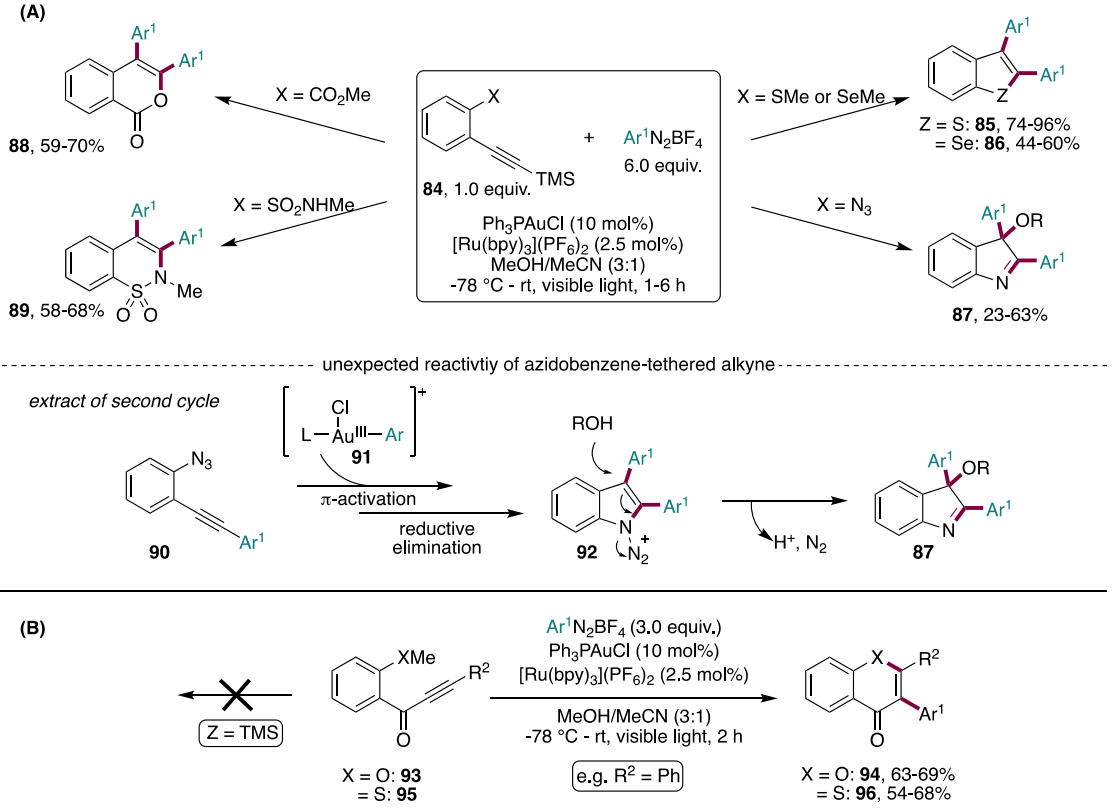

gold(III) intermediate, whereupon the products were afforded (**73** and **79**).

This method of domino diarylations containing a TMS-alkyne substructure was further expanded by the same group, furnishing a wide range of different benzo-fused heterocycles.[100] Under the deployment of the optimized conditions for the synthesis of 2,3-diarylbenzofurans,[99] **85**−**89** could be successfully prepared (Scheme 28A). The formation of 2,3-diarylbenzoselenophene (**86**) was less efficient than the sulfur-based surrogate (**85**). Considering that an azide-moiety functions as a versatile nitrogen source, they aimed to obtain 2,3-diarylated indole derivatives.[101−104] Instead, they observed the formation of functionalized 3*H*-indoles (**87**), which revealed the participation of the methanol as nucleophile. Mechanistically, this unexpected product formation derived from an initial coupling of the TMS-alkyne moiety to internal alkyne (**90**). The latter enters a second cycle and was activated by the in situ formed cationic arylgold(III) intermediate (**91**). A 5-*endo-dig* azacyclization and subsequent reductive elimination furnished intermediate (**92**). At last, the alcohol solvent

https://dx.doi.org/10.1021/acs.chemrev.0c00841
Chem. Rev. XXXX, XXX, XXX−XXX

Scheme 29. Bis-arylative Cyclization (A) Homoprogargyl Sulfonamides and (B) *o*-Ethynylaniline with Aryldiazonium Salts

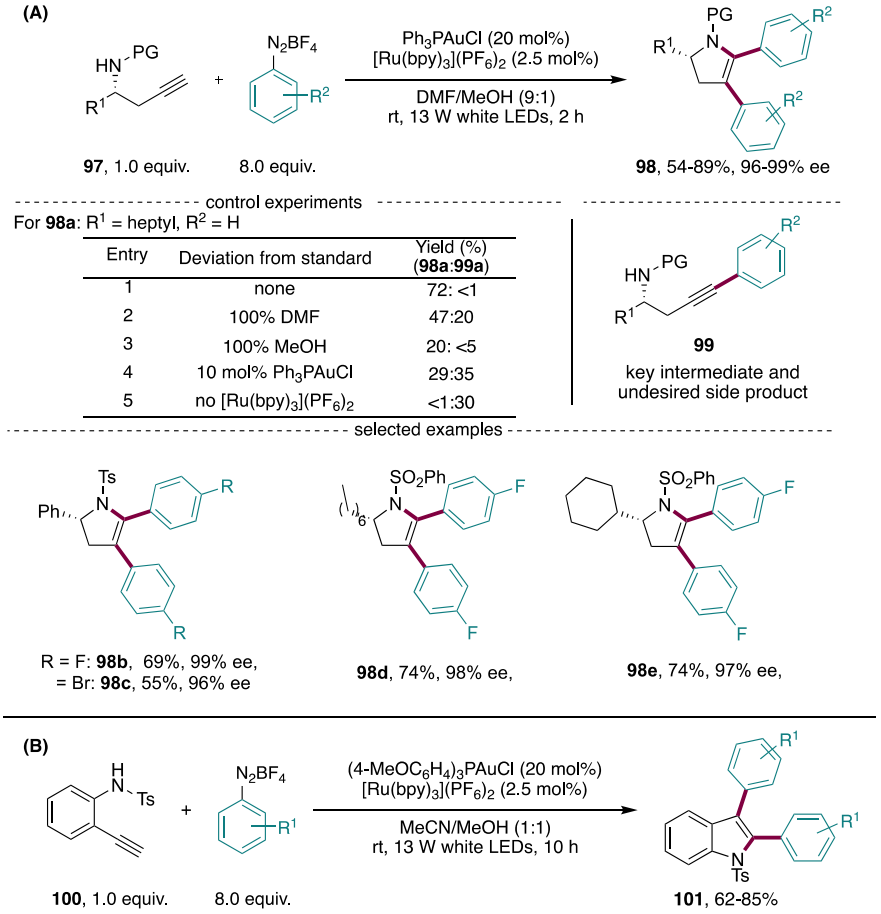

Scheme 30. Thio- and Trifluoromethylthio-sulfonylation of Substituted Styrenes

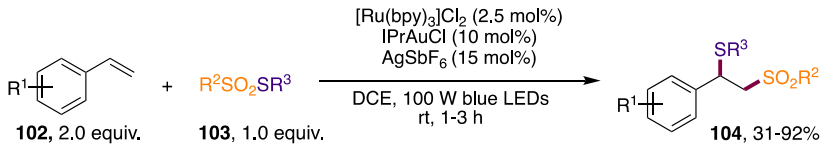

control experiments

For **104a**, R^1 = H, R^2 = Ph, R^3 = CF_3

Entry	Deviation from standard	Yield [%]
1	-	94
2	Ph_3PAuCl as [Au]	56
3	no $AgSbF_6$	< 5
4	21 W blue LEDs	68
5	3 W blue LEDs	-

attacked and a concomitant nitrogen release was triggered under formation of product (**87**). Additionally, this protocol was also compatible for the construction of six-membered benzo-fused heterocycles, such as isocoumarins (**88**) and benzosultams (**89**) from ester and sulfonamide precursors, respectively.

Remarkably, an attempt to convert substrates **93** and **95** with a contiguous ketone group in the TMS-alkyne substructure failed to afford the desired double arylation. By replacing the TMS with a phenyl group (R^2) and then aiming, a simple monoarylation to benzo-fused heterocycles **94** and **96** was successful. This clearly demonstrated that the Hiyama–Sonogashira-type reaction did not take place with an alkynone framework present.

Shortly thereafter, Zhu and Ye realized a dual gold/photoredox-catalyzed bis-arylative cyclization of chiral homopropargyl sulfonamides (**97**) to obtain enantioenriched 2,3-dihydropyrroles (**98**) in good to excellent yields (Scheme 29A).[105] During the course of their optimization, it was found that the optimal solvent consisted of a mixture of DMF and MeOH (9:1), using the individual solvents solely, a product mixture or low yields were obtained (entries 2 and 3). Furthermore, the usually applied 10 mol % of the gold(I) catalyst led to a product mixture of the targeted (**98a**) and the monoarylated uncyclized side product (**99a**) (entry 4). By using the double amount, 20 mol % of gold catalyst, **98a** was delivered in 72% yield (entry 1). To compare these conditions to the once applied by Glorius for the coupling of terminal

https://dx.doi.org/10.1021/acs.chemrev.0c00841
Chem. Rev. XXXX, XXX, XXX−XXX

Scheme 31. Structures of Tiflorex, Toltrazuril, and Vaniliprole

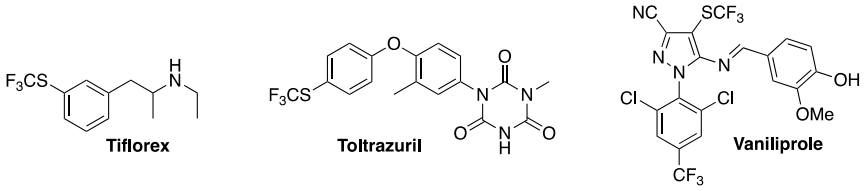

Scheme 32. (A) Selected Examples for the Thio- and Trifluoromethylthio-sulfonylation of Substituted Styrenes. (B) Post Functionalization

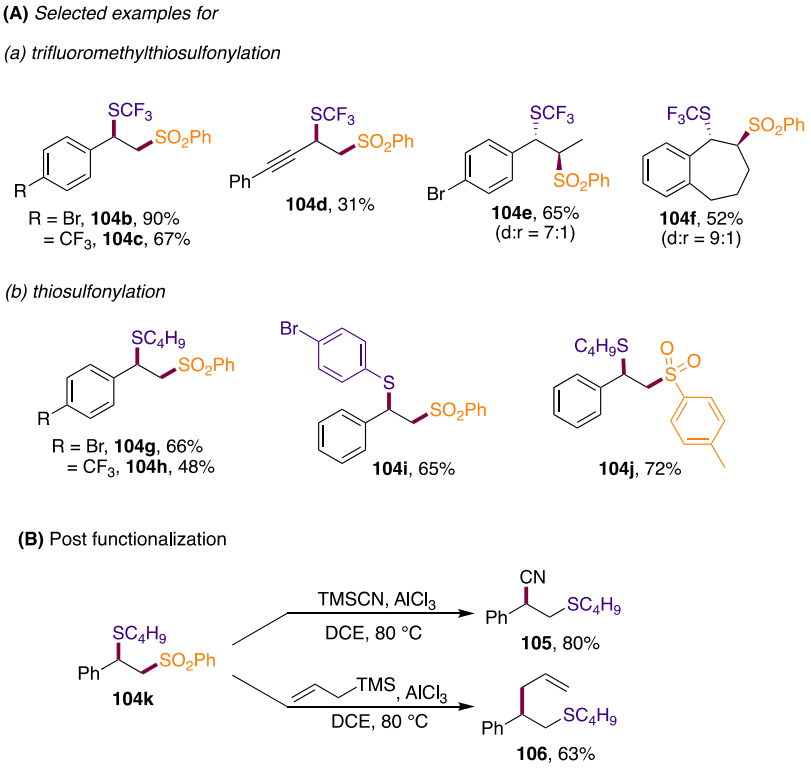

alkynes (Scheme 18B),[89] DMF was the solvent of choice and an electron-rich phosphane-ligated gold(I) catalyst performed best.

Interestingly, under irradiation of white light (λ = 390−700 nm), and in the absence of the photosensitizer, only the monoarylated product (**99a**) was observed (entry 5). A broad set of functional groups by variation of both the aryldiazonium salts and homopropargyl sulfonamides was studied. In all cases, the enantiopurity was maintained throughout the reaction and no loss in ee could be achieved (96−99% ee) and no epimerization was detected. Next, the application of *o*-ethynylaniline (**100**) to synthesize 2,3-arylindoles (**101**) was tested (Scheme 29B). For an effective transformation, the conditions needed to be adjusted and then relied on the use of 20 mol % of the electron-rich phosphane-ligated gold(I) catalyst, also used by Glorius. The mechanism for both substrates was in accordance to the proposal by Alcaide for their domino bis-arylations: first the arylation of the terminal alkyne (**99**) and then arylative cyclization in the second cycle.

2.1.4. Dual Gold/Photoredox Catalysis without Aryldiazonium Salts. With the aim of expanding the scope of possible coupling partners in the light-mediated gold(I)/gold(III) catalysis to other than aryldiazonium salts, the research group of Xu disclosed an intermolecular thio- and trifluoromethylthio-sulfonylation of substituted styrenes (**102**) (Scheme 30).[106] Interestingly, they found that the best catalyst system for this photoredox process was a mixture of the NHC gold(I) complex IPrAuCl (10 mol %), $AgSbF_6$ (15 mol %), and $Ru(bpy)_3Cl_2$ (2.5 mol %) (entry 1). Using a gold(I) catalyst bearing a phosphine ligand lowered the yield of **104a** to 56% (entry 2). The presence of the silver salt had a tremendous effect on the reaction outcome (entry 3). The power of the blue LEDs also influenced the reaction substantially. A change from 100 to 21 W diminished the yield to 68% (entry 4), however, a 3 W blue LED lamp completely paralyzed the reaction (entry 5).

By either applying $PhSO_2SR$ (with R = aryl or alkyl) for thiosulfonylations or $PhSO_2SCF_3$ for the trifluoromethylthiosulfonylations delivered the difunctionalized alkenes, regioselectively and in good diastereoselectivity, with a broad functional group tolerance (Scheme 32A). In particular, an alkene connected to an alkyne moiety was successfully converted to give **104d** in a yield of 31%. Internal alkenes, both acyclic and cyclic (**104f**), could be easily converted. From a synthetic point of view, a method to concomitantly introduce trifluoromethylthio (SCF_3) and sulfonyl groups is very attractive. The SCF_3 group represents a key motif in

https://dx.doi.org/10.1021/acs.chemrev.0c00841
Chem. Rev. XXXX, XXX, XXX−XXX

pharmaceutical and agrochemical products, such as tiflorex, toltrazuril, and vaniliprole (Scheme 31).[107−109]

The sulfone synthon can be readily transformed into other functional groups,[110,111] for example, via Julia olefination into alkenes.[112] Further, the authors presented two examples for the functionalization of the sulfonyl group by employing TMSCN and allylsilane in the presence of aluminum chloride. The products **105** and **106** were obtained in 80% and 63% yield (Scheme 32B).

Several mechanistic experiments indicated that $IPrAuSCF_3$ was a key intermediate in the catalytic cycle. In addition, the benzenesulfonyl radical was proven by the addition to a radical scavenger. Stern−Volmer fluorescence quenching experiments were performed and revealed that only $IPrAuSbF_6$ was able to quench the excited Ru-photocatalyst. A reduction of the cationic gold−NHC complex to IPrAu(0) was hinted by a determined reduction peak at −0.11 V vs SCE by cyclic voltammogram (compared to excited photocatalyst: $E_{1/2}^{III/II*} = -0.81$).[34] Therefore, the authors proposed a tentative reaction mechanism which started with the excitation of the $Ru(bpy)_3Cl_2$ using a 100 W blue LED lamp (Scheme 33). The

Scheme 33. Postulated Reaction Mechanism for the Thio- and Trifluoromethylthio-sulfonylation of Substituted Styrenes

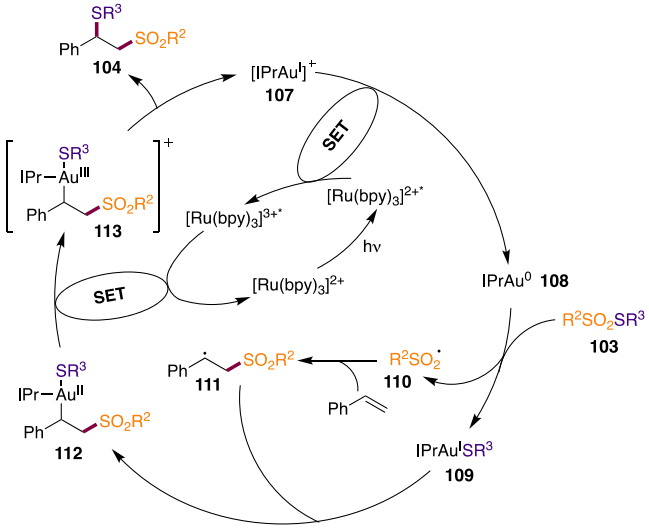

excited photocatalyst reduced the cationic gold(I) catalyst ($IPrAuSbF_6$, **107**) to highly active gold(0) (**108**). The latter was then enabled to reduce the $PhSO_2SR^3$ reagent (**103**) to form $IPrAu(I)SR^3$ (**109**) and the corresponding benzenesulfonyl radical (**110**). Next, the sulfonyl radical added to the alkene moiety of the styrene derivative to afford a benzyl radical **111**, determining the regioselectivity. This radical then oxidized $IPrAu(I)SR^3$ to alkylgold(II) species **112**, which was further oxidized by $[Ru]^{3+}$ to regenerate the photocatalyst. Final reductive elimination of the gold(III) intermediate (**113**) delivered the targeted products (**104**) and the gold(I) catalyst. This mechanistic pathway involved the participation of four different oxidation states of gold from 0 to +III, which was unprecedented.

In 2019, the research group of Fensterbank mobilized iodoalkynes (**115**) for the photosensitized alkynylative cyclization of *o*-alkynylphenols (**114**) (Scheme 34).[113] The employed iodoalkynes are much less reactive than aryldiazonium salts, and therefore the mode of activation of the gold(I) complex had to differ in order to promote the C−C bond formation. In turn, the application of organic iodides in the field of oxidative gold catalysis is already thoroughly studied in the absence of light and highlighted by the works of Ribas,[114] Russel,[115] and Amgoune/Bourissou.[116,117] In these systems, the oxidation of the gold center was achieved by either use of a directing group[114] or with special bidentate ligands.[115−117] The thus obtained gold(III) complexes were also reacted with a nucleophile to obtain cross-coupling products,[114−116] and further, one example showed to function in a catalytic fashion.[116] Fensterbank et al. desired to promote the oxidative addition of the gold(I) complex by photosensitized energy transfer rather than an electron transfer on which all of the previously described methods with aryldiazonium salts relied on. After extensive screening the appropriate reaction conditions were: 5.0 mol % of $(4\text{-}CF_3\text{−}C_6H_4)_3PAuCl$, 1.0 mol % of $Ir[dF(CF_3)ppy]_2(dtbbpy)PF_6$, 10 mol % of 1,10-phenanthroline, and 2.5 equiv. K_2CO_3 in MeCN under irradiation with blue LEDs. The electron-withdrawing group on the phosphane ligand produced the desired product (**116**) more selective than neutral Ph_3PAuCl. The reason for this was explained by the higher electrophilicity of $(4\text{-}CF_3\text{−}C_6H_4)_3PAuCl$. The addition of 1,10-phenanthroline showed to have a huge impact on the outcome of the reaction. However, an explanation remained elusive; a hypothesis would be a potential halogen bonding between the additive and the iodoalkyne because 1,10-phenanthroline exhibits halogen-bonding donor abilities.[118]

With the optimized reaction conditions in hand, the group focused on the evidence of a participating photosensitized energy transfer. At first, the vinylgold(I) intermediate (**117**) was synthesized in a stoichiometric fashion, however, under different conditions than the ones used in the catalytic cycle. In the experiment, a silver salt was added to in situ generate the corresponding cationic gold(I) to activate the π-bond for the *O*-cyclization. Further, triethylamine was used as base instead of potassium carbonate. Next, fluorescence quenching experiments of [Ir] were conducted, and it was shown that upon increasing the concentration of vinylgold(I) complex **117**, the fluorescence of the excited triplet [Ir]-catalyst decreases. Further, the presence of **117** decreased the luminescence lifetime of the excited triplet [Ir]-catalyst. These studies showed that the vinylgold(I) complex (**117**) acted as an effective quencher of the excited [Ir]-catalyst. Also, reacting **117** with the iodoalkyne solely with light, the corresponding product (**116a**) was obtained in 33% yield. However, in the presence of the photosensitized [Ir] catalyst, **116a** was afforded in 95% yield after 3.5 h. This demonstrates the enhancement of the reactivity when [Ir] was applied.

The bimolecular quenching rate constants were determined to be under the control of molecular diffusion. This observation suggested the presence of a Dexter energy transfer. Recorded transient absorption spectra of [Ir] with different amounts of vinylgold(I) complex (**117**) showed that, with an excess of **117** the excited triplet [Ir] signal decreased and a novel signal appeared which was vaguely attributed to the excited triplet state of **117** (^{3}**117**). Their mechanistic investigations were also supported by density functional theory (DFT) calculations, confirming the experiment evidence.

On the basis of the performed experiments, the authors proposed a mechanism starting from the formation of the vinyl gold(I) intermediate (**117**) by a gold(I) promoted 5-*endo*-*dig*

https://dx.doi.org/10.1021/acs.chemrev.0c00841
Chem. Rev. XXXX, XXX, XXX−XXX

Scheme 34. Photosensitized Alkynylative *O*-Cyclization Using Gold Catalysis

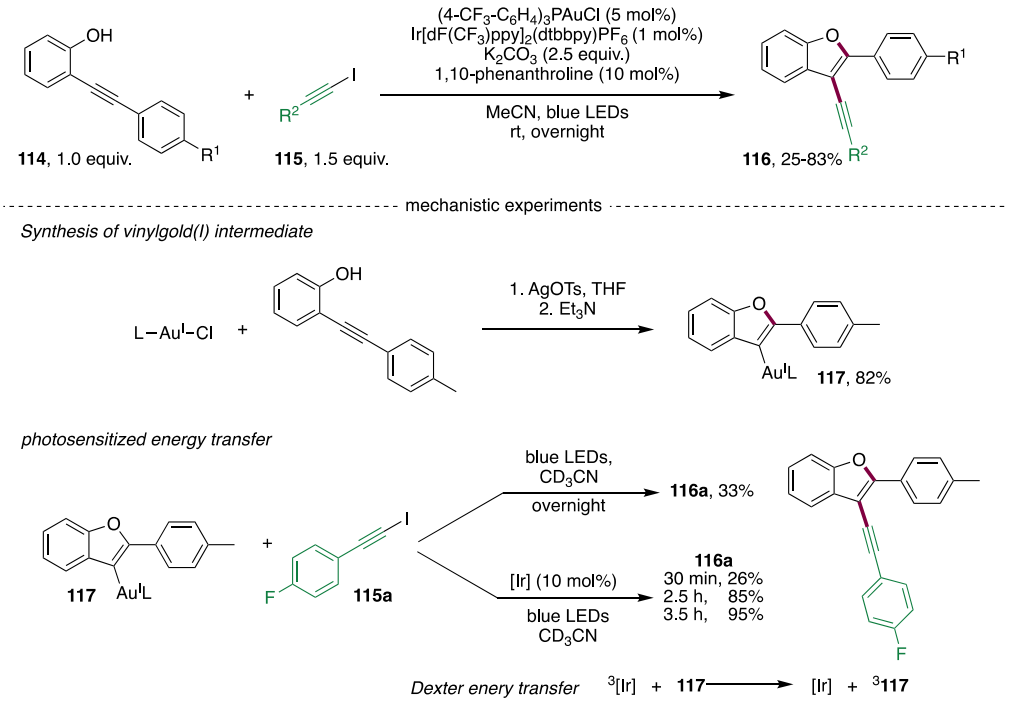

Scheme 35. Proposed Reaction Mechanism via an Energy Transfer

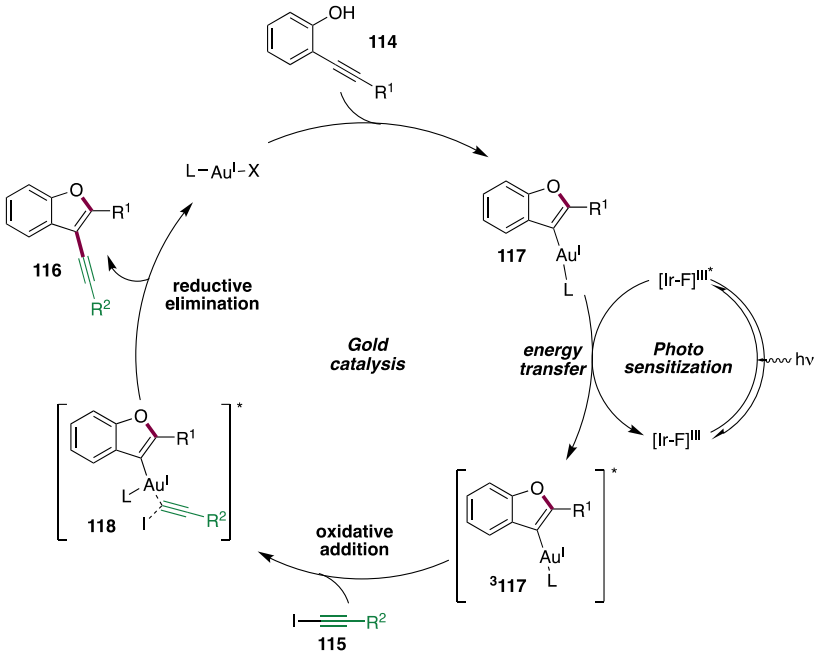

O-cyclization in the presence of a base (Scheme 35). In parallel, [Ir] was excited by blue LEDs and the thus formed excited triplet [Ir]-complex transferred the energy to vinylgold-(I) to forge a triplet excited state of vinylgold(I) intermediate (^{3}**117**). The latter was prone to undergo oxidative addition with the iodoalkyne. Subsequent reductive elimination delivered desired alkynylated benzofuran (**116**). It is important to mention that during the process of an energy transfers, the oxidation state of the metal centers do not change, while in the electron transfer, redox-processes with a change in oxidation state are enclosed.

2.2. Photosensitizer-Free Gold-Catalyzed Photoreactions

2.2.1. Nucleophilic Addition and Cross-Coupling Reactions. The research field of photosensitizer-free gold-catalyzed photoreactions arose in 2016 when Hashmi and co-workers developed the 1,2-difunctionalization of alkynes using aryldiazonium salts to access α-aryl ketones (**120**) in moderate to very good yields (Scheme 36A).[60] The initial aim was to conduct the reaction under the dual gold/photoredox conditions, ideally in combination with the dimeric gold photosensitizer. During the course of the investigations, they were surprised to find that the sole use of a mononuclear

https://dx.doi.org/10.1021/acs.chemrev.0c00841
Chem. Rev. XXXX, XXX, XXX−XXX

Scheme 36. Photosensitizer-Free Gold-Catalyzed 1,2-Difunctionalization of Alkynes with Aryldiazonium Salts

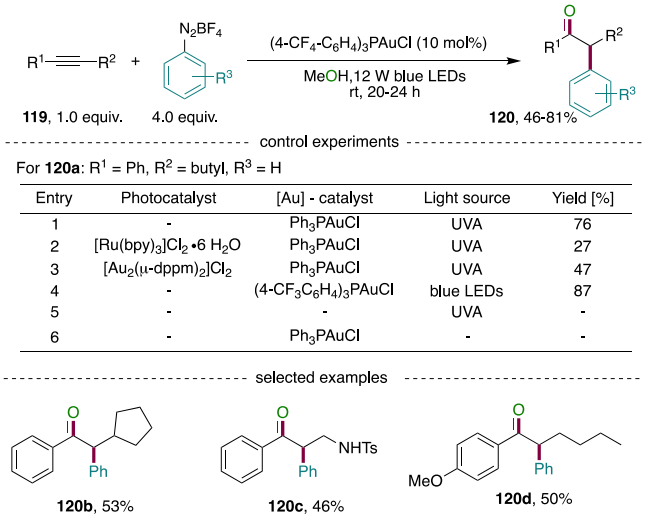

gold(I) catalyst delivered the desired α-aryl ketone (**120a**) in 76% yield (entry 1) and that the presence of a photosensitizer even had a negative effect on the reaction outcome (entries 2−3). The more electron-poor phosphine ligand together with blue LEDs as the light source were revealed to give the best results (87%, entry 4). Control experiments demonstrated the necessity of the light and the gold catalyst (entries 5−6).

The hydration of alkynes represents a well-established field in homogeneous gold catalysis.[119−121] Further, a gold-catalyzed trifunctionalization of alkynes with boronic acids and Selectfluor as external oxidant and fluorinating reagent was reported by Hammond and Xu et al.[22] Thus, the difunctionalization of alkynes offered a vastly improved route in gold catalysis to α-aryl ketones.

The authors proposed a highly speculative reaction mechanism based on the fact, that the coordinatively saturated gold(I) catalyst and the aryldiazonium salts do not absorb the light of blue LEDs (Scheme 37A). Therefore, it was suggested that a SET from gold(I) to the aryldiazonium salt generated an aryl diazo radical (**121**) and a gold(II) species (**122**). Oxidative recombination of the latter led to species **123**, and subsequent light-assisted nitrogen elimination in combination with alkyne coordination gave arylgold(III) intermediate (**124**). Up to here, the mechanism is only speculated and no proof exists for the existence of intermediate **123**. Methanol was then added to the activated alkyne to form a vinyl gold(III) species (**125**). Reductive elimination regenerated the gold(I) catalyst and afforded the arylated enol ether (**126**), which upon hydrolysis formed α-aryl ketones (**120**). The hydrolysis was proven by an isotope labeling experiment with $H_2{}^{18}O$ as an additive, and the ^{18}O-labeled α-aryl ketone was obtained in 61% yield. The slight decrease in yield was explained by the fact that the aryldiazonium salt tends to decompose with an excess of water. In addition, a light on/off experiment was conducted and showed that the transformation required continuous light irradiation. As already mentioned above, this result in principle should be interpreted with caution.[97] Because an attempt to directly isolate intermediates from the reaction mixture failed, a P,N-bidentate ligand was applied to improve the stability of possible intermediates (Scheme 37B). Thus, the first direct evidence of gold(III) species being formed in gold-catalyzed photoreactions with

Scheme 37. Highly Speculative Mechanism for the Photosensitizer-Free 1,2-Difunctionalization of Alkynes and Gold(III) Isolation Attempt

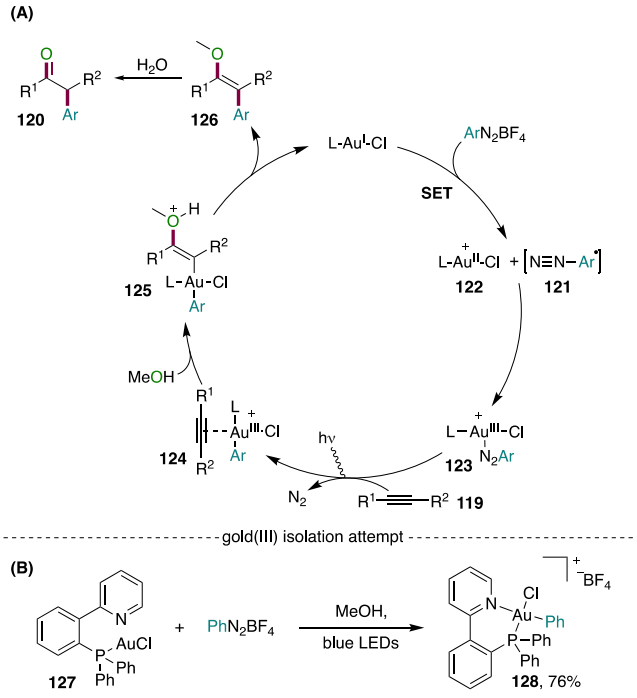

aryldiazonium salts was provided by the isolation of complex **128**. This in 2016 experimentally confirmed the feasibility of oxidizing the gold(I) to gold(III) without the necessity of a photocatalyst.[122]

In the same protocol, Hashmi and co-workers also explored the applicability of the photosensitizer-free light-induced gold-catalyzed method to a few already published methods using a photosensitizer. As illustrated in Scheme 38, the intramolecular

Scheme 38. Combination of the Photosensitizer-Free Method with Already Reported Reactions

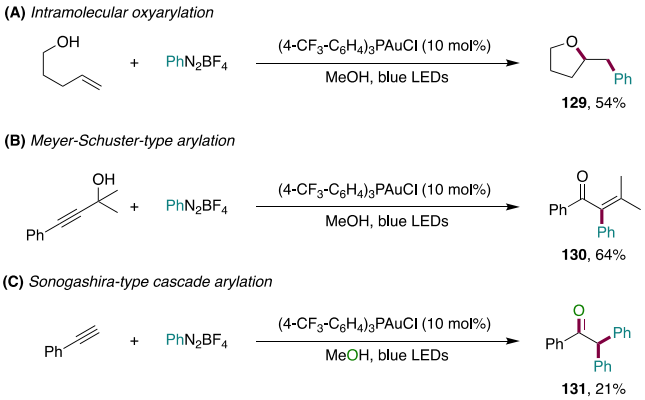

oxyarylation of 4-penten-1-ol afforded **129** with a yield of 54%. The Meyer−Schuster-type arylation without a photosensitizer produced **130** with a yield of 64% and a Sonogashira-type cascade arylation gave **131** with a low yield of 21%. These results contradicted the earlier described necessity of a photosensitizer. The exact mechanism of the photosensitizer-free gold-catalyzed photoreactions is still not published in the literature, different explanations for the successful conversions

https://dx.doi.org/10.1021/acs.chemrev.0c00841
Chem. Rev. XXXX, XXX, XXX−XXX

can be considered. Apart from the power of the light source, the energy of the light source, also the photochemical activity of a donor−acceptor complex formed by the aryldiazonium salt and a gold(I) compound and related possibilities are conceivable.

The groups of Zhu and Zhang mimicked the reaction mechanism of the photosensitizer-free 1,2-difunctionalization of alkynes theoretically with a special focus on the light-induced step (Scheme 39).[123] On the basis of various density functional theory (DFT) calculations, the most probable reaction mechanism was initiated by a charge-transfer complex of gold(I) catalyst and diazonium salt (**132**) acting as a photosensitizer. The excited charge transfer complex (**132***) underwent a SET with another equivalent of the diazonium salt, whereby diazo radical **134** and gold(II) intermediate **135** were generated. After denitrification of the diazobenzene radical, the aryl radical was formed and added to the gold(II) center to give the cationic gold(III) intermediate (**136**), which was suggested to further react with the alkyne, in the same manner as already proposed by Hashmi et al.[60] Also considered was a possible direct addition of an aryl radical (but it is not discussed how this would be formed) to the gold(I) center to obtain gold(II), which can then abreact in two different manners. First, through a direct oxidation by another equivalent of diazonium salt or detouring via a π-coordination of gold(II) to the alkyne, which was then oxidized in the same fashion. Interestingly, the addition of diazonium radical to gold(I) or gold(II) centers were considered less plausible, stating that the Au−N bond in the gold(I or II)-N_2Ph complex was labile. This initiation proposal contradicted the speculations made by Hashmi and co-workers.

Scheme 39. Theoretical Proposal for the Initiation of the Photosensitizer-Free 1,2-Difunctionalization of Alkynes

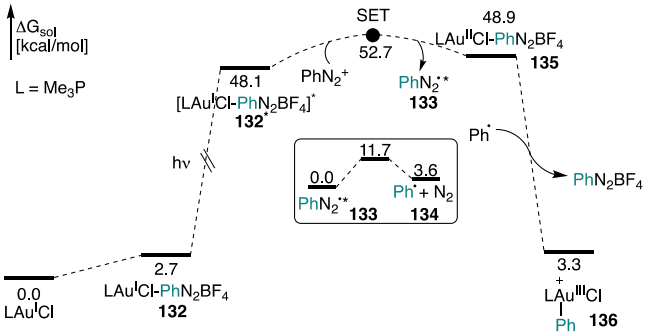

On the basis of the success of the photosensitizer-free conditions, Hashmi et al. disclosed the cross-coupling of aryldiazonium salts with aryl boronic acids, a gold-catalyzed Suzuki-type coupling (Scheme 40).[124] It is interesting to note that the electronic nature of the gold catalyst and the solvent influenced the reaction outcome tremendously. Applying Ph_3PAuCl in MeCN, only traces of the desired product (**138a**) were formed (entry 1), while the relatively electron-poor phosphine $(4\text{-}CF_3\text{−}C_6H_4)_3P$ resulted in an increased yield of 51% (entry 2). A drop in yield was observed when using the cationic pendant $(4\text{-}CF_3\text{−}C_6H_4)_3PAuNTf_2$ (entry 3). Curiously, the identical condition as for the latter described method,[60] MeOH in combination with $(4\text{-}CF_3\text{−}C_6H_4)_3PAuCl$, was identified to be the optimum (entry 4).

This method allowed an alternative route to a variety of substituted biaryls in moderate to excellent yields with a broad functional group tolerance. Boronic acids bearing electron-withdrawing substituents on the phenyl ring reacted more efficiently than those with electron-donating groups. The same trend was observed when varying the substituents on the aryldiazonium tetrafluoroborate. Besides boronic acids, arylboronic pinacol esters could also be readily converted.

Notably, the counteranion of the aryldiazonium salt effected the reaction outcome. A change from tetrafluoroborate (Scheme 41, entry 1) to bis(trifluoromethylsulfonyl)imide (NTf_2) completely shut down the reaction (entry 2). However, the addition of an external fluoride source, such as CsF, afforded the product in 36% yield (entry 3). Thus, it was hypothesized that a fluoride source was needed to activate the boronic acid for a transmetalation. A possible, still highly speculative, mechanism was proposed, which started with the same path as the previous described process.[60] A gold-induced SET to the aryldiazonium salt which after subsequent steps and light irradiation gave the cationic arylgold(III) intermediate (**139**). Instead of a π-activation, a BF_4^--assisted transmetalation of an arylboronic acid (**140**) occurred to give a diarylgold(III) species (**141**). Finally, reductive elimination

Scheme 40. Photosensitizer-Free Gold-Catalyzed Coupling of Boronic Acids and Aryldiazonium Salts

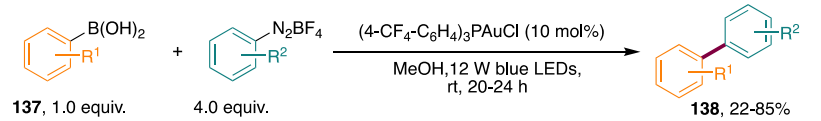

selected optimization experiments

For **138a**: R^1 = 4-CO_2Me, R^2 = H

Entry	[Au] - catalyst	solvent	Yield [%]
1	Ph_3PAuCl	MeCN	traces
2	$(4\text{-}CF_3C_6H_4)_3PAuCl$	MeCN	51
3	$(4\text{-}CF_3C_6H_4)_3PAuNTf_2$	MeCN	22
4	$(4\text{-}CF_3C_6H_4)_3PAuCl$	MeOH	85

selected examples

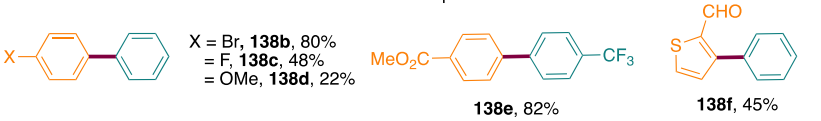

https://dx.doi.org/10.1021/acs.chemrev.0c00841
Chem. Rev. XXXX, XXX, XXX−XXX

Scheme 41. Mechanism and Influence of the Counter Anion for the Cross-Coupling of Arylboronic Acids and Aryldiazonium Salts

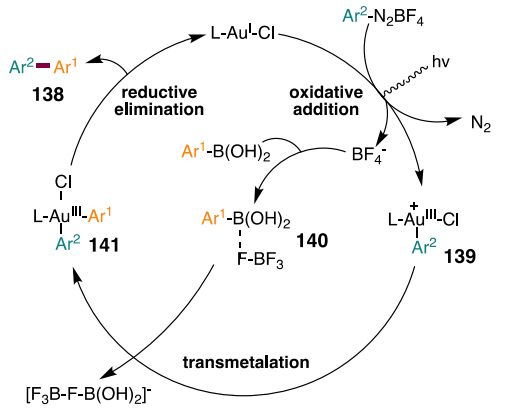

counteranion effect

Entry	Counterion of the diazonium salt	Additive	Yield [%]
1	BF_4^-	-	95
2	NTf_2^-	-	-
3	NTf_2^-	CsF (2.0 equiv.)	36

delivered the desired biaryls (**138**) and regenerated the gold(I) catalyst.

The success of the C(sp^2)−C(sp^2) coupling showed that besides nucleophilic additions, transmetalations also could proceed readily without the use of a photosensitizer or an external oxidant. In a later work, Hashmi and co-workers reported on the light-induced gold-catalyzed chemoselective Hiyama arylation of B,Si-bifunctionalized reagents (**142**) with aryldiazonium salts to afford a broad range of biarylboronates (**143**) (Scheme 42).[125] For this coupling, the reaction conditions were further optimized to the use of a cationic gold(I) catalyst, namely $Ph_3PAuNTf_2$, MeCN as solvent, and a reduced amount of aryldiazonium salt (1.2 equiv. instead of 4.0 equiv.). Under blue LED light irradiation, a wide range of aryldiazonium salts were investigated and converted with various BMIDA, BPin, and Bnep containing B,Si-bifunctionalized aromatics to give biarylboronates in moderate to very good yields. Herein, the same trend was observed: low yields for strongly electron-donating diazo compounds. Besides the site-selective coupling of TMS, other trialkylsilyl-substituted arylboronates were also well tolerated (**145**, **147**).

The possibility of maintaining not only organoboron moieties, but also bromo, iodo, and also triflate groups during the reaction revealed the synthetic potential for post modification. Taking advantage of the good synergism of gold catalysis with another catalytic system, this method was also applied in iterative one-pot reactions (Scheme 43), for example, a gold-catalyzed site-selective arylation using an aryldiazonium salt and a subsequent amination via copper catalysis to **148**. Further, the combination of gold catalysis and palladium catalysis to obtain **149**, demonstrated the versatility for a rapid construction of complex target molecules.

On the basis of conducted control experiments, kinetic studies, and ^{31}P NMR spectroscopy, the authors proposed a possible reaction mechanism (Scheme 44). Irradiation of blue LEDs opened up two considered pathways: (1) either gold-activated diazonium salts being able to promote the oxidative

Scheme 42. Selective Hiyama Arylations to Access Biarylboronates

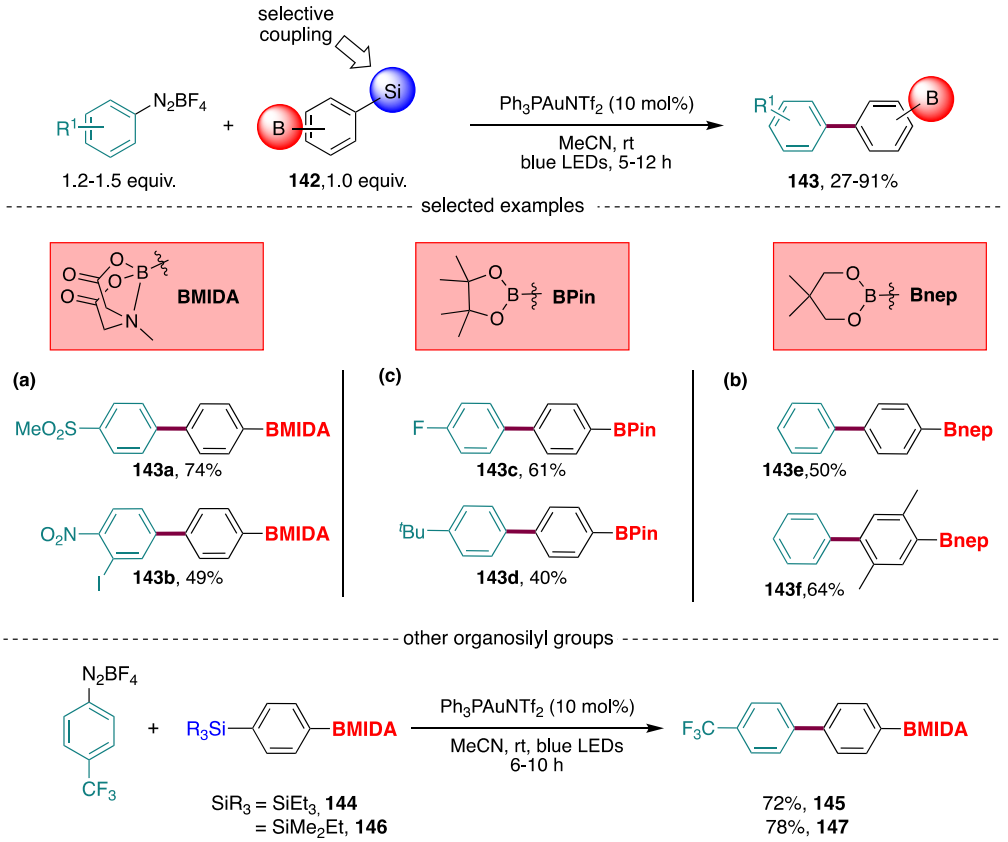

https://dx.doi.org/10.1021/acs.chemrev.0c00841
Chem. Rev. XXXX, XXX, XXX−XXX

Scheme 43. Selected Examples for Iterative One-Pot Reactions

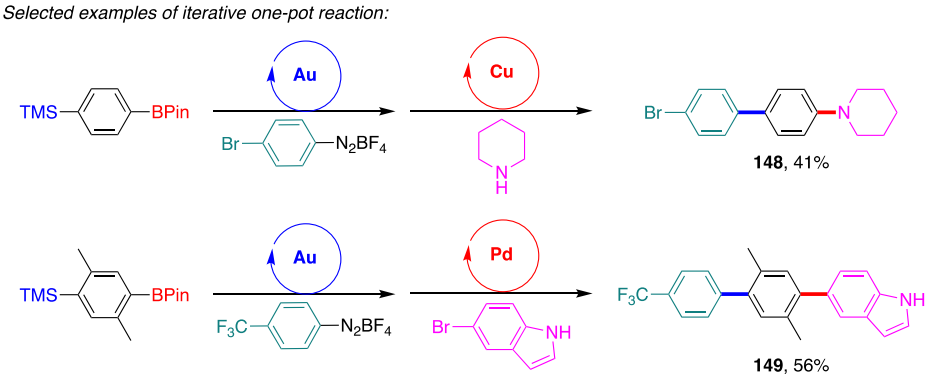

Scheme 44. Mechanistic Proposal for the Chemoselective Arylation of B,Si-Bifunctionalized Reagents

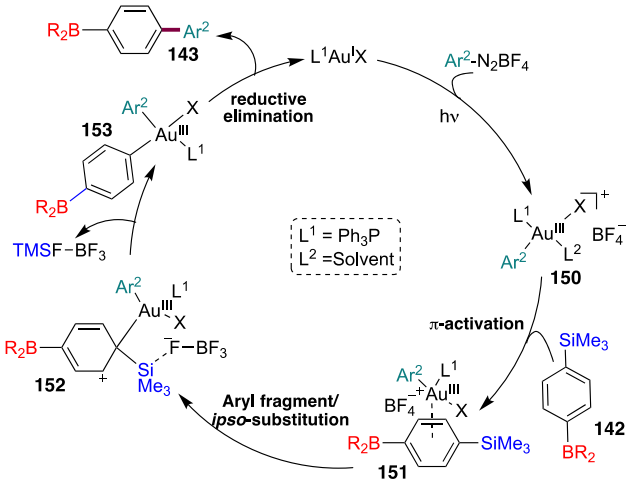

addition to gold(I) or (2) an aryl radical addition and subsequent SET to gold(II) intermediate, both generating the cationic arylgold(III) species (**150**). The latter coordinated to the B,Si-bifunctionalized substrate (**151**) to initiate a BF_4^- anion-assisted aryl *ipso*-substitution. A finale reductive elimination afforded the desired biarylboronate (**143**).

Interestingly, the BF_4^- anion also promoted the transmetalation of arylboronic acids in the photosensitizer-free gold-catalyzed photoreactions.[124] Thus, the electronic nature of the applied gold(I) catalyst and the solvent might influence the obtained chemoselectivity.

Thereafter, the group of Hashmi aimed at further expanding the scope of possible transmetalating reagents (Scheme 45),[126] at first by applying their optimized conditions for the coupling of arylboronic acids and aryldiazonium salt: 4.0 equiv. of aryldiazonium salt, $(4\text{-}CF_3\text{-}C_6H_4)_3PAuCl$, MeOH, and blue LEDs. With this, the method could be broadened to other organoboron species, such as MIDA boronate (**154**) and potassium trifluoroboronate (**155**), which reacted smoothly to deliver the corresponding biaryls in moderate to excellent yields. Also, trimethoxysilane (**156**) and bis(catecholato)-silicate (**157**) were tested to couple under these conditions and could readily be transformed.

For the selective coupling of aryltrimethylsilanes bearing boron substituents with aryldiazonium salts, the reaction conditions could be further optimized to the use of 1.2 equiv. of aryldiazonium salt, $Ph_3PAuNTf_2$, MeCN, and blue LEDs.[125]

Therefore, the authors applied these conditions for the coupling of an array of aryltrimethylsilanes without boron substituents (**158**) and also varied the electronic nature of the aryldiazonium salt (Scheme 46A). The arylation of the heteroaromatic 2-trimethylsilylbenzofuran to deliver **159a** and **159b** in good yields of 71% and 79% were the two most representative examples. In particular, the two products were also afforded by the group of Patil by using not only a photosensitizer but also a copper salt, however, even with a slightly decreased yield (61% for **159a**, 62% of ethyl ester of **159b**).[98] Next, the coupling of alkynyltrimethylsilanes (**158**) was examined and afforded the respective internal alkynes (**161**) in moderate to very good yields (Scheme 46B). The yield of **161a** showed a significant increase compared to the identical product obtained by Toste and co-workers using a

Scheme 45. Expansion of the Scope of Transmetalating Reagents MIDA Boronate, Potassium Trifluoroboronate, Trimethoxysilane, and Bis(catecholato)-silicate

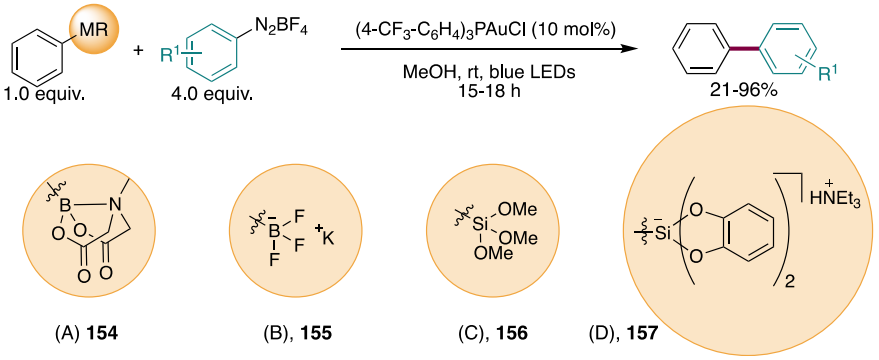

https://dx.doi.org/10.1021/acs.chemrev.0c00841
Chem. Rev. XXXX, XXX, XXX−XXX

Scheme 46. Photosensitizer-Free Cross-Coupling of (A) Aryltrimethylsilanes and (B) Alkynyltrimethylsilanes

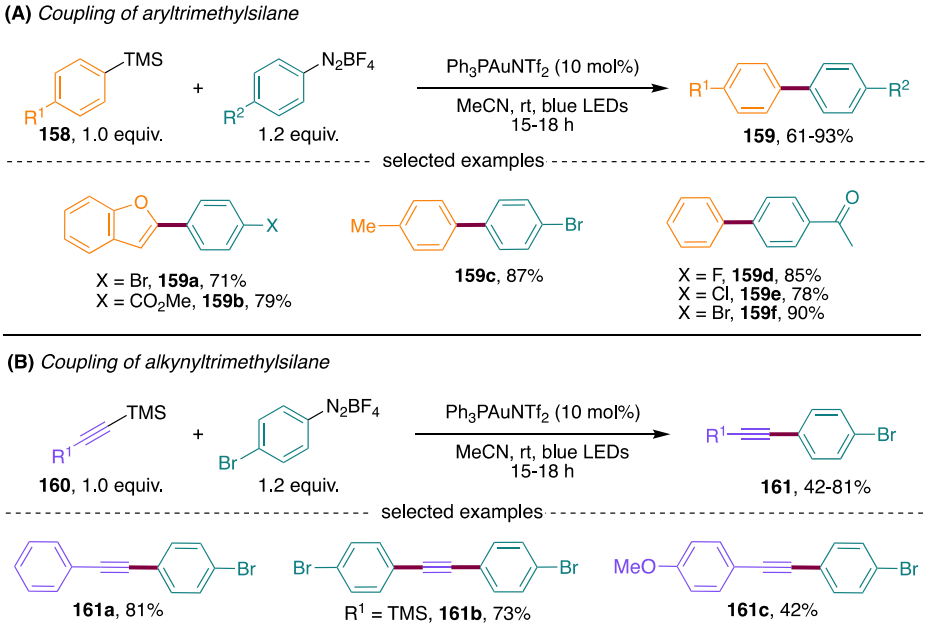

photosensitizer, 68%.[84] These examples highlight the improved efficiency of the photosensitizer-free method which are economically also very attractive.

In a photosensitizer-free study of the gold(I)-catalyzed reaction of *o*-alkynylphenols (**162**) with aryldiazonium salt, Hashmi and Klein revealed that a change in reaction outcome can be reached by either conducting the reaction in the dark or irradiation with blue LEDs (Scheme 47).[127] In the absence of

Scheme 47. Photosensitizer-Free Gold-Catalyzed Reaction of *o*-Alkynylphenols with Aryldiazonium Salt in the Dark and with Blue LED Irradiation

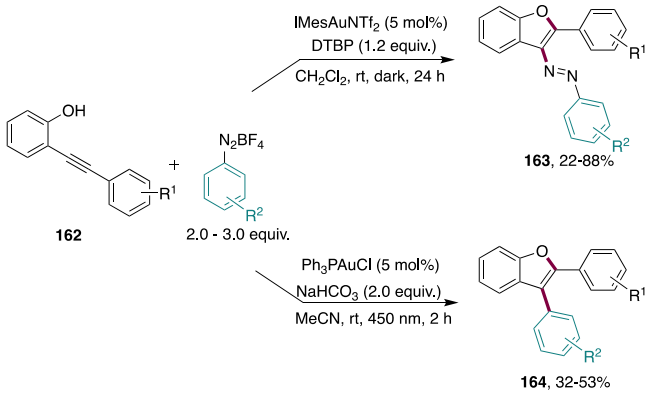

light, by using the NHC–Au complex, $IMesAuNTf_2$, 2,6-di-*tert*-butylpyridine (DTBP) as base, and DCM as solvent, azobenzofurans (**163**) were afforded. Whereas with Ph_3PAuCl and $NaHCO_3$ in MeCN under blue LED irradiation, arylated benzofurans (**164**) were obtained.

Mechanistic experiments indicated that the light-induced oxidative addition of aryldiazonium salt to either Ph_3PAuCl or $Ph_3PAuNTf_2$ in the presence of a base ($NaHCO_3$) did not take place within a time period of 2 h. Next, the vinylgold(I) intermediate was synthesized from the cationic gold(I) complex and the corresponding *o*-alkynylphenol under basic conditions.[28] Nevertheless, a stoichiometric transformation of the vinylgold(I) intermediate with an aryldiazonium salt under both optimized reaction conditions (dark and light) was observed. The two reactions showed full conversion, giving the azobenzofuran (**163**) in 46% yield and the arylated benzofuran (**164**) in 65% yield. The authors assumed that under the given conditions, the formation of cationic gold(I) intermediate was possible, which is a requirement for the "nucleophilic addition first" mechanism. Thus, a mechanism for both pathways, light (A) and dark (B), was proposed, which started with the π-activation of the cationic gold(I) to trigger a 5-*endo-dig* cyclization (**166**, **169**) (Scheme 48). Subsequent deprotonation by the base delivered vinyl gold(I) complex (**167**, **170**). At this point, the two pathways differed. In the absence of light, the diazonium salt reacted as a *N*-electrophile and under N_2-retention the azobenzofuran (**163**) was formed. Under light irradiation, the diazonium salt acted as a *C*-electrophile to give arylated benzofuran (**164**) under N_2-extrusion.

The authors again pointed out that both the substrate and the catalyst do not absorb the light of blue LEDs. Therefore, the proposed light-consuming step, the oxidation of vinylgold(I) intermediate by aryldiazonium salt, was studied by density functional theory (DFT) calculations. These suggested that the vinylgold(I) intermediate formed a donor–acceptor complex with the aryldiazonium salt. This associate complex exhibited a low-lying S_1 excited state of 45.8 kcal/mol, which corresponded to the charge transfer from the HOMO, located at the electron-rich vinyl gold(I) substructure to the LUMO, located on the diazonium salt. Further, an energetically lower lying triplet state T_1 with an energy of 13.2 kcal/mol was found. In this triplet state, the spin density was distributed over the vinyl gold(I) complex and the diazonium salt fragment, increasing the C–N bond distance. However, the reaction mixture was irradiated with a 450 nm light source, while the associate donor–acceptor complex showed its maximum of absorbance between 200 and 400 nm. Therefore, the exact mode of photochemical activation should be in-depth elucidated in the future.

An inspiring visible light-promoted gold-catalyzed fluoroarylation of allenoates was realized by the research group of Feng

https://dx.doi.org/10.1021/acs.chemrev.0c00841
Chem. Rev. XXXX, XXX, XXX–XXX

Scheme 48. Mechanistic Hypothesis for the Photosensitizer-Free Gold-Catalyzed Reaction of *o*-Alkynylphenols with Aryldiazonium Salt in the Dark (Path A) and with Blue LED Irradiation (Path B)

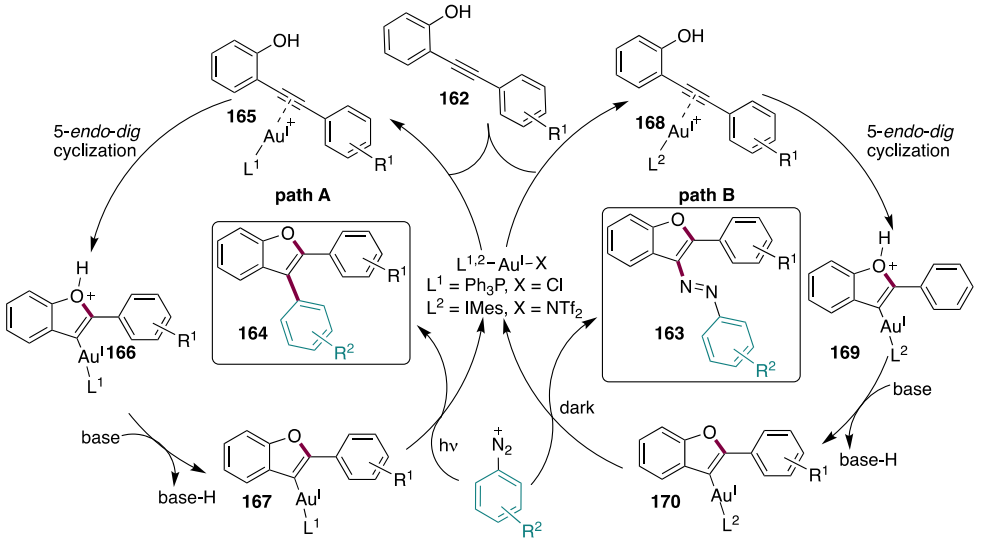

Scheme 49. Fluoroarylation of Allenoates (DCE = 1,2-Dichloroethane)

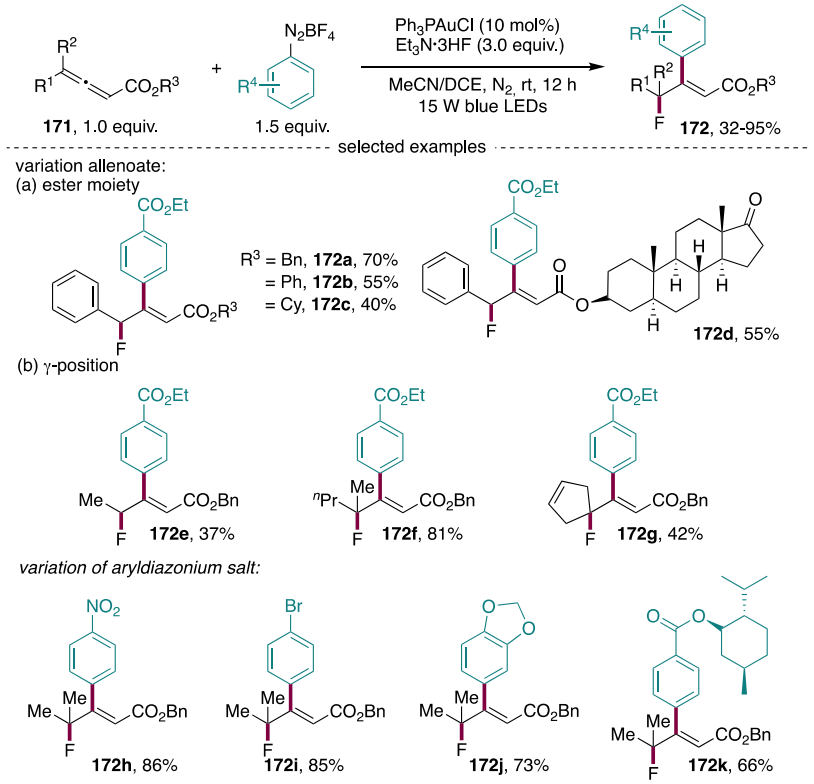

constructing a broad set of *β*-fluoroalkyl-containing cinnamate derivatives (**172**) (Scheme 49).[128] The aryl group stemmed from the use of aryldiazonium salts and the nucleophilic fluorine source was $Et_3N{\cdot}3HF$. Fluoride as nucleophile serves as a tool to mildly add fluorine to multiply bonds.[129−131] On the contrary, electrophilic fluorination reagents[132−135] such as Selectfluor,[136] in combination with gold as a catalyst, has a detrimental effect on functional group tolerance.[22,24] The present method followed a highly regioselective and stereoselective manner with a *Z*-configuration of the aryl and ester functionality. Interestingly, the addition of a photosensitizer did not significantly influence the reaction outcome. However, it was also stated that in some cases the presence of such a photocatalyst was beneficial, albeit neglecting the occasions. The authors provided a remarkable reaction scope by varying both the ester moiety of allenoates (e.g., **172a−172d**) and the *γ*-position (e.g., **172e−172g**). Besides phenyl at the *γ*-position, single acyclic alkyl (**172e**) and dialkyl (**172f**) and cyclic alkyls (**172g**) were also well tolerated. Additionally, the substituents of the aryldiazonium salts were modified (e.g., **172h−172k**) and even a natural products derived diazonium salts, such as L-menthol, were readily converted (**172k**).

https://dx.doi.org/10.1021/acs.chemrev.0c00841
Chem. Rev. XXXX, XXX, XXX−XXX

Scheme 50. Tentative Mechanism of the Fluoroarylation of Allenoates

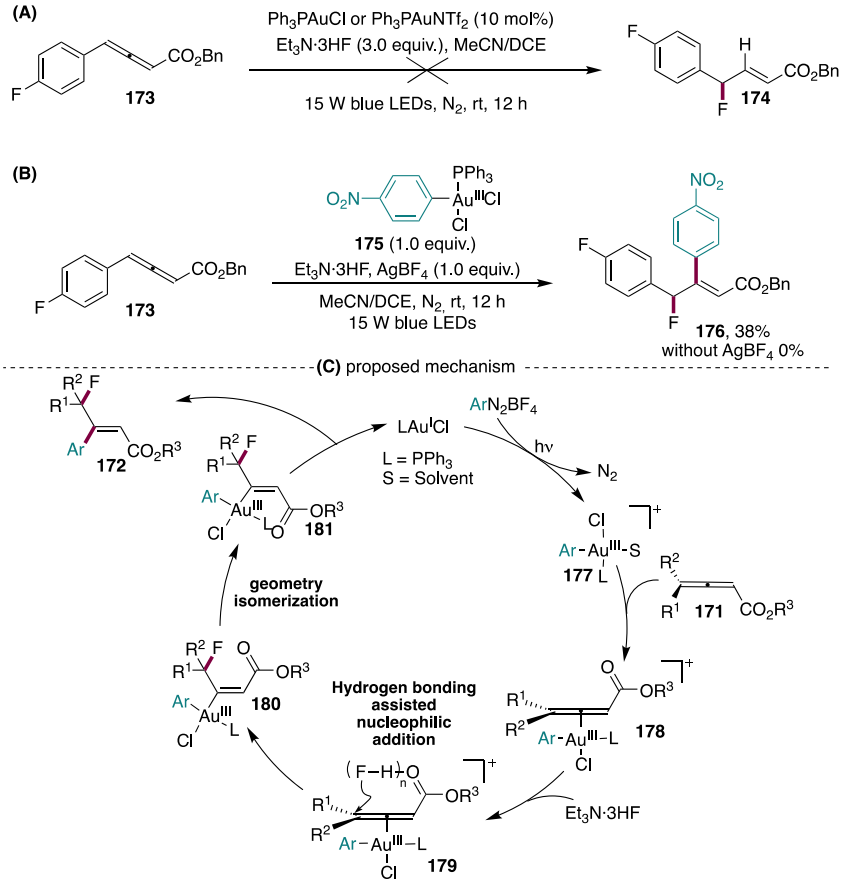

Scheme 51. Chemoselective Arylation of Arylgermanes Using Electron-Poor Aryldiazonium Salts

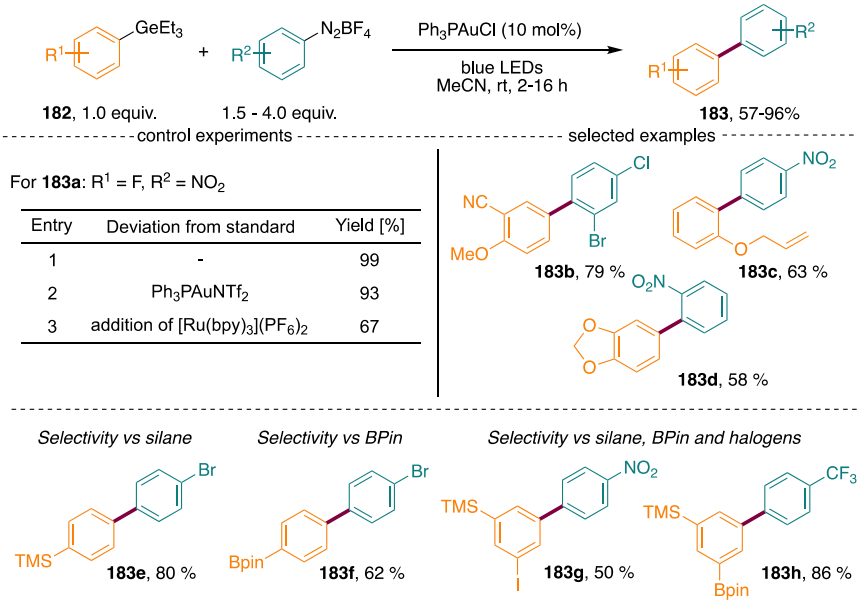

Entry	Deviation from standard	Yield [%]
1	-	99
2	$Ph_3PAuNTf_2$	93
3	addition of $[Ru(bpy)_3](PF_6)_2$	67

Replacing the ester group of the allenoate with a cyano, phenyl, alkyl, or sulfone group or a change to terminal alkenes inhibited the reaction. This indicated, along with the *Z*-configuration of the aryl and ester group, that the ester moiety could function as a directing group. To investigate the mode of activation of the allenoate, either by gold(I) or by gold(III), a control experiment between allenoate **173** and $Et_3N{\cdot}3HF$ was conducted in the absence of the diazonium salt (Scheme 50A). According to literature protocols,[129,130] this should result in a hydrofluorination product; however, **174** was not observed. This indicated that the π-activation proceeded via gold(III), which was in contrast to the arylation of allenoates using the dual gold/photoredox technique.[71] To corroborate this hypothesis, the corresponding gold(III) complex (**175**) was

https://dx.doi.org/10.1021/acs.chemrev.0c00841
Chem. Rev. XXXX, XXX, XXX−XXX

Scheme 52. Computational Mechanistic Studies on the Arylation of Aryl Germanes

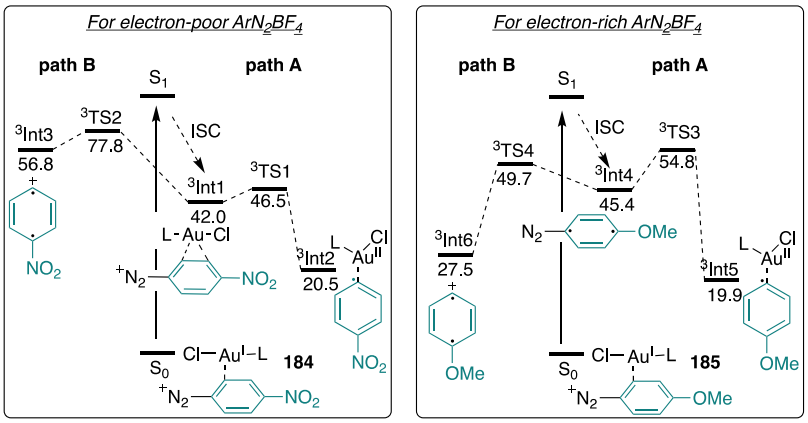

Scheme 53. Chemoselective Arylation of Arylgermanes Using Electron-Rich Aryldiazonium Salts

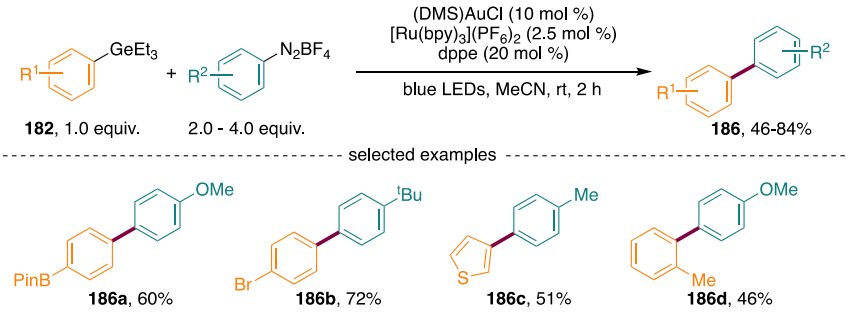

synthesized and stoichiometrically applied to allenoate **173** to afford the product **176** in 38% yield (Scheme 50B). To evaluate the regio- and stereoselectivity of this reaction, an enantiomerically enriched ethyl 4-phenyl-buta-2,3-dienoate (65% *ee*) was deployed to the standard reaction conditions, and 52% of the desired product with 43% *ee* were obtained. As a result, it was hypothesized that the distal double bond was functionalized in a concerted fashion, whereby the activation of the allenic moiety by arylgold(III) happened opposite to the ester group. Concomitantly, the HF was activated through a hydrogen bonding with the ester and the nucleophilic attack occurred on the other side. To this end, a mechanism was postulated which was initiated by a light-promoted oxidative addition of the aryldiazonium salt to gold(I) to form arylgold(III) intermediate (**177**) (Scheme 50C). After coordination of the gold(III) complex to the allenoate (**178**), HF entered the cycle and a subsequent hydrogen bonding assisted nucleophilic addition generated aryl,alkyl gold(III) (**180**). Double-bond isomerization and reductive elimination delivered the desired fluoroarylated product (**172**).

Very recently, Schoenebeck et al. developed a selective arylation of aryl germanes (**183a**) in the presence of C-BPin, C-TMS, C−I, C−Br, and C−Cl, which offered a versatile tool for a rapid diversification (Scheme 51).[137] For a successful coupling of electron-poor aryldiazonium salts, the sole gold-catalyzed method was utilized, while the reaction with electron-rich diazo species required a photocatalyst for an efficient coupling. At first, the authors focused on the coupling of electron-poor groups. During the optimization, it was found that 10 mol % of Ph_3PAuCl effectively catalyzed the reaction under blue LED irradiation (99% yield, entry 1). The electronic nature of the gold catalyst, if neutral or cationic, did not significantly influence the reaction outcome (entry 2). The presence of 2.5 mol % of $[Ru(bpy)_3](PF_6)_2$ decreased the yield of the desired product to 67% (entry 3). A wide variety of different substitutions of electron-poor aryldiazonium salts and aryl germanes was explored, showing a broad functional group tolerance. In particular, it was also focused on the efficient coupling of *ortho*-substitutions, for example, delivering **183b**−**183d** in a good yield. The coupling of aryl germanes bearing TMS, BPin or halogens could be chemoselective achieved to obtain diverse functionalized products (e.g., **183e**−**183h**). This was owed to the higher reactivity of the $GeEt_3$ scaffold.

Curiously, under these conditions, electron-rich aryl diazonium salts, such as 4-methoxyphenyl diazonium tetrafluoroborate, did not lead to the product, and the starting materials were not consumed. To understand the electronic influence on the mechanistic pathway computational studies were performed. Interestingly, the authors immediately considered an associate formation of the gold catalyst and the aryldiazo compound (**184** vs **185**) (Scheme 52). In this regard, they revealed that the excited diazonium−gold complex would undergo *intersystem crossing* (ISC) to the triplet state. Three different theoretical methods were used to determine the vertical excitation wavelength of the associate complexes. For electron-poor diazonium salts and gold, they were calculated to be 513 nm (B3LYPD3), 329 nm (ωB97xD), or 342 nm (CAM-B3LYP). In case of the electron-rich pendant and gold, the excitation wavelengths were 374 nm (B3LYPD3), 289 nm (ωB97xD), or 292 nm (CAM-B3LYP). Important to note here is that blue LEDs (λ_{max} = 475 nm) were used to drive the reaction. From the triplet state, two mechanistic pathways were suggested to be feasible. Either addition of the diazonium salt to gold under nitrogen loss and generation of the respective gold(II) species (path A) or the associate complex dissociated, leading to the decomposition of

https://dx.doi.org/10.1021/acs.chemrev.0c00841
Chem. Rev. XXXX, XXX, XXX−XXX

the aryl diazonium salt (path B). The question on how the reaction proceeded once the gold(II) intermediate was formed was not answered. While the favored pathway for electron-poor ArN_2BF_4 was the formation of the gold(II) intermediate (path A), the electron-rich surrogates preferentially dissociated, leading to undesired byproducts (path B).

On the basis of the results obtained by Fouquet et al., the addition of a photosensitizer would significantly increase the yields in gold-catalyzed arylations of boronic acids, especially with electron-rich diazonium salts,[91] Schoenebeck and co-workers applied photocatalyst $[Ru(bpy)_3](PF_6)_2$ for the coupling of electron-rich diazo species. This led to an increase of the homocoupling of aryl germanes. After screening of various ligands for the gold catalyst to smoothly drive the reaction, it was found that the bidentate ligand dppe in combination with DMSAuCl presented the optimal conditions for the coupling of electron-rich diazonium salts (Scheme 53). Thus, the substrate scope was studied tolerating various functional groups (e.g., **186a−186d**).

To illustrate the synthetic modularity of their method to chemoselectively couple $GeEt_3$ over TMS, BPin, or halogens, polyfunctionalized substrates (e.g., **187**) were applied and subsequently diversified in a highly selective manner by rapid arylation or alkylation methods (Scheme 54).

Scheme 54. Highly Selective, Sequential Coupling of Polyfunctionalized Starting Materials

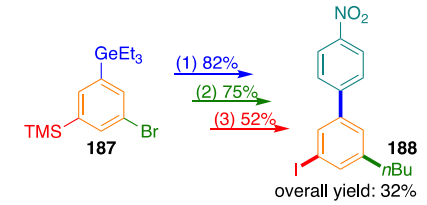

(1) $ArGeEt_3$ (0.3 mmol, ArN_2BF_4 (0.36-0.45 mmol) Ph_3PAuCl (10 mol%), MeCN, blue LEDs
(2) ArBr (0.2 mmol), AlkZnCl/LiCl (0.46 mmol), Pd^{I}-I-dimer (2.5 mol%)
(3) ArTMS (0.3 mmol), NIS (0.6 mmol), *p*TsOH (0.6 mol), $CHCl_3$

2.2.2. Direct Excitation of Diazonium Salt Precursors.

In 2017, Wong and co-workers disclosed a gold-catalyzed photoreaction of silyl-substituted alkynes (**190**) and blue LED light-absorbing quinoline-substituted aryl diazonium tetrafluoroborates (**189**), giving rise to a broad array of silyl-tethered quinolizinium compounds (**191**) in satisfactory yields (Scheme 55).[138] Most of the alkyne difunctionalization reactions undergo an *anti*-nucleophilic addition;[60,69,73−76,127] the present work however, achieved a *syn*-insertion pathway to *cis*-functionalization products. While optimizing the reaction conditions, the authors were surprised to find that using the identical conditions as Toste et al. for the coupling of TMS alkynes,[84] just without a photosensitizer, the desired *syn*-insertion proceeded readily to give **191a** in 71% yield; no direct coupling of the alkyne was obtained. Further, the reaction was remarkably regioselective, giving no regioisomer (**193**). Along with trimethylsilyl-substituted alkynes, the increase in steric bulkiness was also studied. The application of a triethylsilyl group furnished the desired quinolizinium in a comparatively lower yield (45%), while *tert*-butyldiphenylsilylalkyne was not tolerated at all. Terminal alkynes and internal alkynes were also not compatible with this method. To further highlight the chemoselectivity toward silyl-tethered alkynes, an alkyne bearing an internal and a trimethylsilylalkyne moiety was tested and only the trimethylsilylethynyl *cis*-difunctionalized product (**194**) was received.

To investigate the mechanism, a broad set of stoichiometric experiments were conducted. An oxidative addition of gold(I) catalyst in the presence of the aryldiazonium salt and light irradiation was demonstrated by ^1H NMR and ^{31}P NMR spectroscopy and by direct detection of the corresponding cationic arylgold(III) intermediate by ESI-MS analysis. In addition, UV/vis absorption properties were examined and again showed that the mononuclear gold(I) catalysts, in this case Ph_3PAuCl, do not absorb the light of blue LEDs. Interestingly, the quinoline-substituted aryl diazonium tetrafluoroborate (**189**) exhibited a tail of the lowest energy absorption peak above 395 nm. This suggested a direct excitation of the aryldiazonium compound. To support this hypothesis, the authors measured the fluorescence quenching of the diazonium salt upon addition of the gold(I) catalyst, Indeed, a quenching occurred. Moreover, the excited state

Scheme 55. *cis*-Difunctionalization of Silyl-Substituted Alkynes

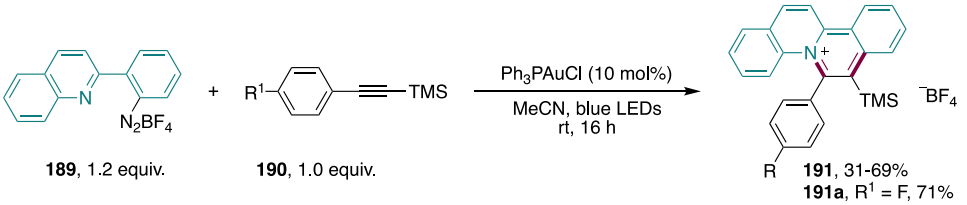

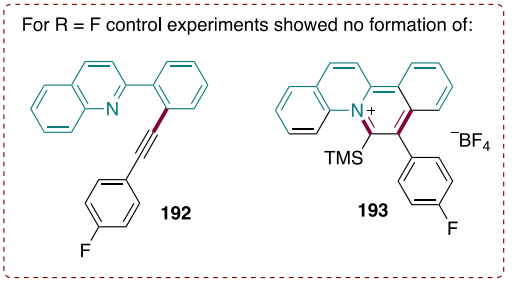

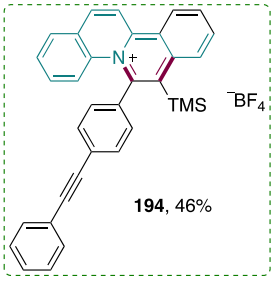

https://dx.doi.org/10.1021/acs.chemrev.0c00841
Chem. Rev. XXXX, XXX, XXX−XXX

Scheme 56. Mechanism of the *cis*-Difunctionalization of Silylalkynes

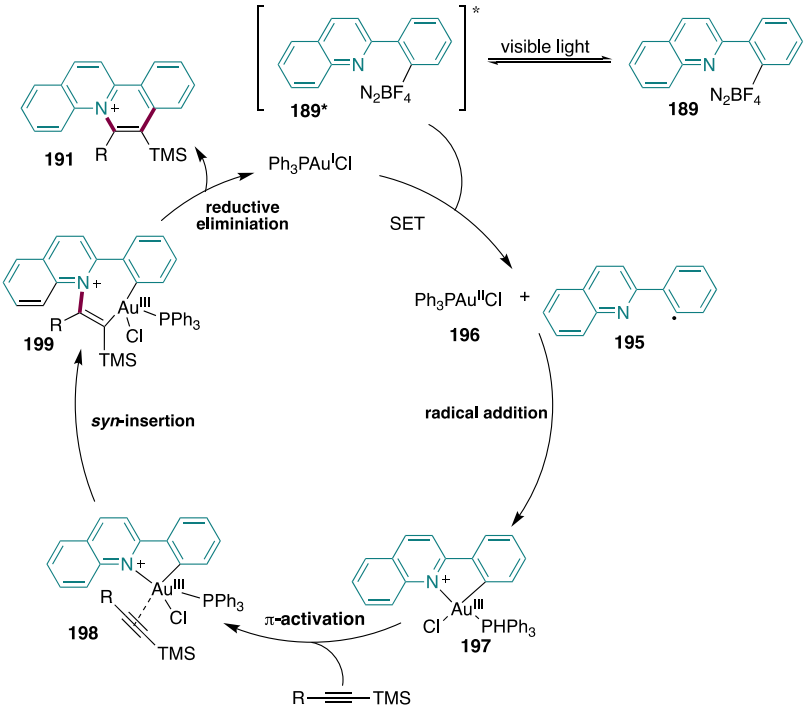

reduction potential of the aryldiazonium salt was 3.28 V, which was clearly higher than the redox potential of the Au(I)/Au(III) couple (E^0 = 1.41 V).[21] This indicated that the gold(I) catalyst could be easily oxidized by the excited aryldiazonium salt (**189***). Thus, the proposed mechanism was initiated by a direct excitation of the diazonium salt, which was subsequently reduced by SET from gold(I) catalyst to generate an aryl radical (**195**) and gold(II) intermediate (**196**) (Scheme 56). After recombination of the latter two, the resulting gold(III) complex (**197**) activated the silylalkyne. The Au−N bond was regioselectively inserted to form a *cis* vinylgold(III) complex (**199**). Final reductive elimination delivered the desired quinolizinium compounds (**191**) and regenerated the gold(I) catalyst. The quantum yield was measured to be 0.91, indicating that a radical chain mechanism was not prominent. In contrast to the other photosensitizer-free gold-catalyzed photoreactions, here the aryldiazonium derivative was capable of absorbing the light.

This mechanism was theoretically investigated by Zhu and Zhang using density functional theory (DFT) calculations.[139] They observed that not only the diazonium salt itself absorbed the light of blue LEDs but also a complex between the diazo compound and the catalyst Ph_3PAuCl (Scheme 57). Even though both could potentially initiate the reaction, the associate complex (**200**) was excluded to produce the key intermediate in the efficient operating catalytic cycle. This was owed to the low concentration of the complex compared to the abundant noncoordinated diazonium salt. Thus, they suggested a mechanism starting from the excitation of the diazonium salt (^{1}**191**) to its singlet excited sate (^{1}**191***), which decayed to its triplet form (^{3}**191**). In the next step, the gold(I) catalyst transferred an electron to the triplet diazo compound to afford the corresponding diazo radical and gold(II) intermediate. Oxidative recombination of both then gave the arylgold(III) species, essentially suggesting the same mechanism as already proposed by Wong et al.[138]

Scheme 57. DFT Calculations of the Oxidation of Gold(I) for the *cis*-Difunctionalization of Silylalkynes and the Considered Associate of Aryldiazonium Salt and Gold Catalyst

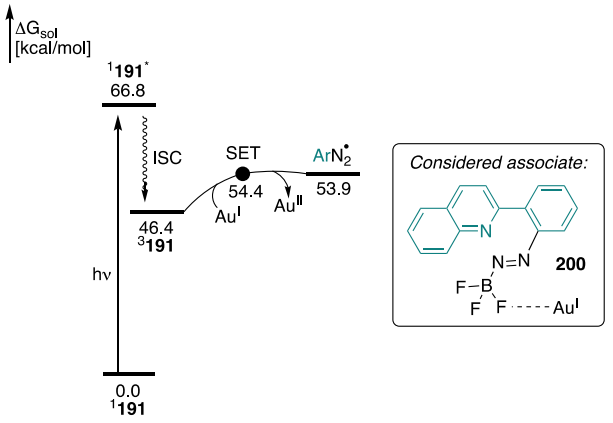

In general, quinoliziniums were investigated in alkaloid chemistry and applied as efficient DNA intercalators.[140−142] With the aim of exploring these cationic aromatic heterocycles in more depth, Wong et al. studied their absorption and emission properties.[138] Surprisingly, these compounds possessed the lowest energy absorption maxima at λ_{abs} > 395 nm, full color tunable emission properties in the visible light region (λ_{em} = 450−640 nm), and quantum yields up to 0.59. With these properties in hand, Wong and co-workers envisioned to apply their newly synthesized quinolizinium compounds as photosensitizers for photooxidative amidation of aldehydes (**202**) and secondary amines (**203**) (Scheme 58). During the course of the optimization, they even found that the catalytic activities were superior than the other tested organophotocatalysts and revealed that the compounds exhibited tunable and high excited state reduction potentials (E_{red}* =

https://dx.doi.org/10.1021/acs.chemrev.0c00841
Chem. Rev. XXXX, XXX, XXX−XXX

Scheme 58. Application of Quinolizinium Salts Prepared by Gold Photoredox Catalysis and Used As Photocatalyst for the Amidation of Aldehydes

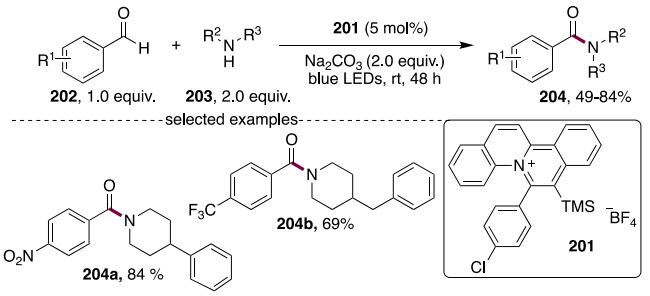

1.97−2.23 V). With the optimized reaction conditions in hand, they elegantly demonstrated the substrate scope of the reaction by varying both aldehydes and secondary amines and obtained the corresponding amides (**204**) in up to 84% yield.

In a next study by Protti and Bandini, bench-stable arylazosulfones (**206**) were applied in gold-catalyzed visible light-driven Suzuki-type coupling reaction (Scheme 59).[143] These molecules represent a class of compounds that upon visible light irradiation undergo homolytic cleavage of the N−S bond, triggering a N_2-extrusion, whereby aryl radicals are formed.[144,145] The optimal reaction conditions for this transformation were: 5 mol % of Ph_3PAuCl, 20 mol % of 2,2′-bipyridine (bpy), 2.0 equiv. of NaOAc, a solvent mixture of MeCN and MeOH (3:1), and using blue LEDs as the light source. Interestingly, along with the isolation of 61% of the cross-coupled product, 20% of the homocoupling product, derived from the arylazosulfones, were detected. The reaction exhibited a broad functional group tolerance, providing the desired products in moderate yields. The limitation in yield was probably owed to the significant formation of the homocoupling product. Along with the reported methods using a photosensitizer[91−93] and the photosensitizer-free version,[124] this protocol offered a third route for light-assisted gold-catalyzed Suzuki-type reactions, however, with the difference that the arylazosulfones were directly excited by light. With this as the first step in the catalytic cycle, the gold(I) center was proposed to react with the aryl radical to gold(II) intermediate (**207**), which is further oxidized by the methanesulfonyl radical (**206**). Next, the base-triggered transmetalation of the boronic acid to cationic gold(III) intermediate (**208**) took place, followed by the reductive elimination. In competition with this cycle was the homocoupling product formation (dashed arrows). This was proposed to result from a reaction of the gold(II) intermediate (**207**) with another equivalent of aryl radical to give diarylgold(III) (**210**). After reductive elimination the gold(I) catalyst was regenerated and the undesired homocoupled product (**211**) was afforded. The unambiguous presence of aryl radicals was proven by a TEMPO trapping experiment.

2.3. Stoichiometric Access to Gold(III) Complexes with Light

The combination of gold and light has also been used to simply and rapidly access gold(III) complexes. One of the first examples in this research field was provided by Toste and co-workers studying the photoinitiated oxidative addition of CF_3I to gold(I) complexes and the resulting reductive elimination to form Aryl-CF_3 bonds.[146] By irradiating diverse arylgold(I) phosphane complexes with a Hg vapor lamp (λ_{max} = 313 nm, 450 W) and 25 equiv. of trifluoromethyl iodide in DCM several stable gold(III) complexes **212** were obtained in moderate to very good yields within a reaction time of 5 min (Scheme 60).

Scheme 60. Photoinitiated Oxidative Addition of CF_3I to Arylgold(I) Phosphane Complexes

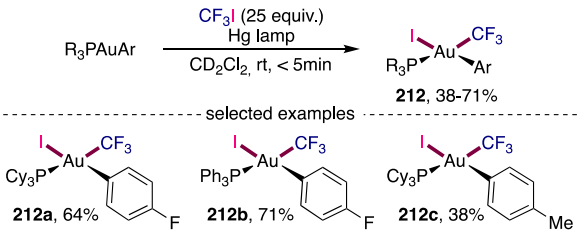

Scheme 59. Coupling of Arylazosulfones and Boronic Acids and the Mechanistic Proposal

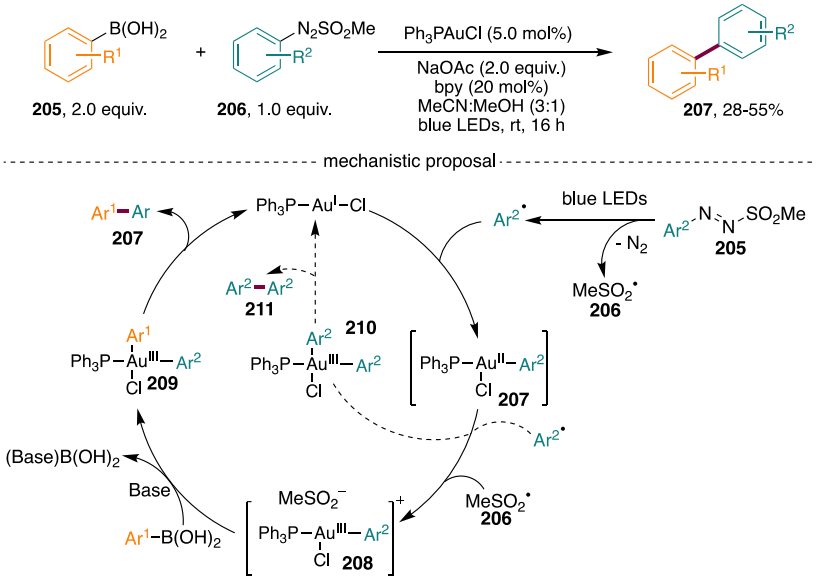

https://dx.doi.org/10.1021/acs.chemrev.0c00841
Chem. Rev. XXXX, XXX, XXX−XXX

The stoichiometric oxidative addition of alkyl iodides to gold(I) complexes is by far not a new topic and has already been observed by Kochi, Puddephatt, and Schmidbaur in the 1970s.[147−153] While these methods do not mention the dependence on light, the oxidative addition by Toste by using CF_3I was distinctly light dependent. To investigate a possible reaction mechanism, the participation of a radical chain mechanism was proven by quantum yield measurements. On the basis of a successful reaction outcome when employing a nonabsorbing gold(I) complex, $Cy_3PAu(I)Me$, they revealed that the reaction had to be initiated by the absorption of CF_3I. Accordingly, the suggested mechanism involved the formation of trifluoromethyl radical by homolysis of excited CF_3I, which oxidized gold(I) complexes under the generation of radical anion $[CF_3]^{\bullet-}$ (Scheme 61). The latter underwent another

Scheme 61. Suggested Mechanism of the Photoinitiated Oxidative Addition of CF_3I to Arylgold(I) Phosphane Complexes

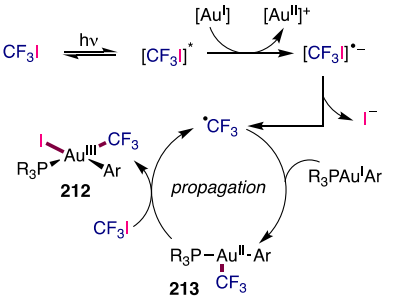

homolysis to generate iodide and trifluoromethyl radicals, which again oxidized gold(I) to gold(II). Another equivalent of CF_3I then oxidized gold(II) (**213**) to the desired gold(III) complexes (**212**) under formation of further CF_3 radicals initiating the next radical chain.

The authors also studied the thermal reductive elimination of the obtained gold(III) complexes (**212**). Surprisingly, in toluene at 110 °C, the corresponding iodoarene (**214**) was obtained (Scheme 62A). However, in the presence of a silver salt, the corresponding trifluoromethylated arene (**215**) could be afforded under the formation of AgI (Scheme 62B).

In the context of Hashmi et al.'s mechanistic study on the 1,2-difunctionalization of alkynes, a first direct evidence of a gold(III) species being formed through oxidative addition of aryldiazonium salts and gold(I) complexes with a P,N bidentate ligand was provided (Scheme 37B).[60] As a follow

Scheme 62. Reductive Elimination Studies of the Obtained Gold(III) Complexes

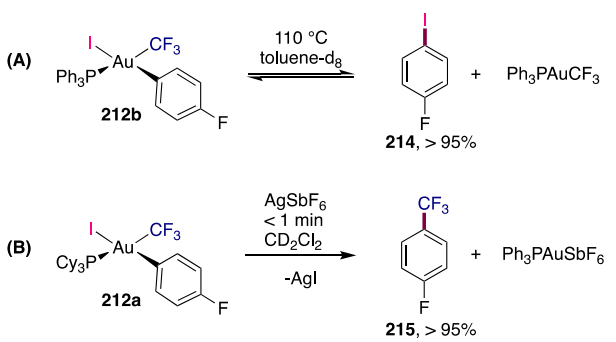

up study, the same group applied this method to a broader set of various aryldiazonium salts and gold(I) complexes (Scheme 63).[122] This protocol provided a general and very practical

Scheme 63. General Access to Organogold(III) Complexes by Oxidative Addition of Aryldiazonium Salts to Gold(I) Precursors

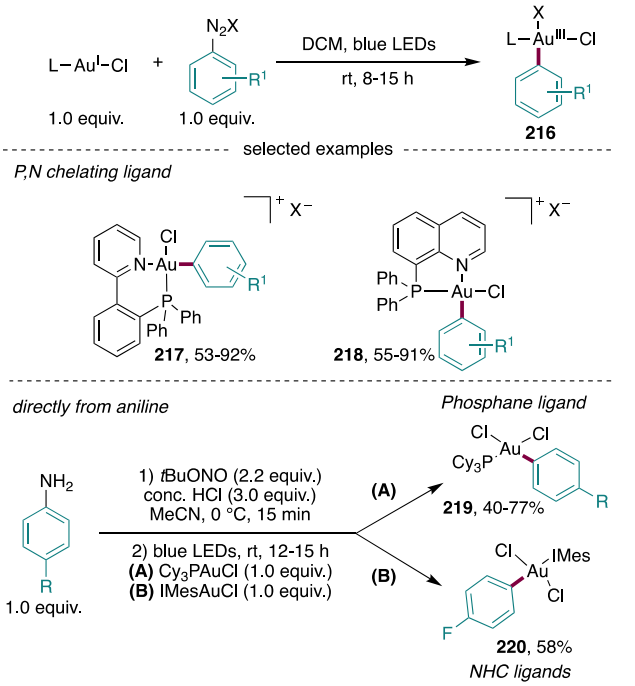

route to the synthesis of organogold(III) compounds bearing different chelating P,N ligands (**217** and **218**), phosphanes (**219**), and *N*-heterocyclic carbenes (NHC) ligands (**220**). The cationic gold(III) complexes were obtained in six-membered chelate complexes (**217**), as well as in five-membered chelate gold(III) complexes (**218**), depending on the type of P,N ligand. In this connection, the thermodynamically more stable isomer was formed, the aryl substituent *trans* to the pyridine *N*-atom, the weaker donor, and the halo-ligand were *trans* to the phosphorus(III), the strongest donor. The neutral gold(III) complexes bearing nonchelating tris-(cyclohexyl)phosphane (**219**) or NHC ligand (**220**) were synthesized in a one-pot, two-step fashion, directly from commercially available anilines.

Thereafter, Glorius and co-workers disclosed experimental evidence for the formation of gold(III) complexes under the merged gold/photoredox conditions in the presence of photocatalyst $[Ru(bpy)_3(BF_4)_2]$ (Scheme 64).[154] A wide range of cationic *C*,*N*-cyclometalated gold(III) complexes (**222**) from 2-(pyridine-2-yl)phenyldiazonium tetrafluoroborate (**221**) and gold(I) complexes bearing different phosphane (e.g., **222a**, **222b**) and NHC ligands (e.g., **222c**) under green LED irradiation were afforded. In these complexes, the chloride ligand was *trans* to the bipyridyl *C*-atom and the phosphane or NHC ligand was *trans*-oriented to the pyridine *N*-atom. Interestingly, very strong electron-deficient ($(MeO)_3P$) or bulky ligands ($(o\text{-tolyl})_3P$, tBu_3P and XPhos) uniformly gave unsatisfying results.

A mechanistic proposal for the photoredox-assisted stoichiometric oxidative addition to gold(I) complexes is illustrated in Scheme 65. The excited photocatalyst reacted

https://dx.doi.org/10.1021/acs.chemrev.0c00841
Chem. Rev. XXXX, XXX, XXX−XXX

Scheme 64. Access to Cationic *C,N*-Cyclometalated Gold(III) Complexes via Stoichiometric Dual Gold/Photoredox Conditions

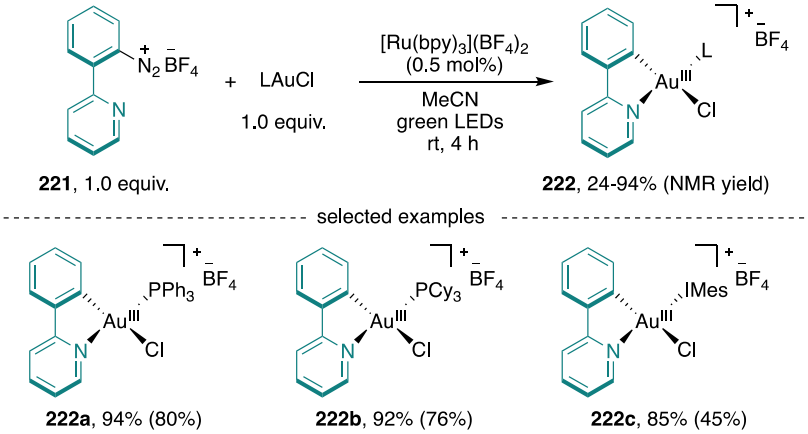

Scheme 65. Postulated Mechanism of the Stoichiometric Oxidative Addition to Gold(I) Complexes

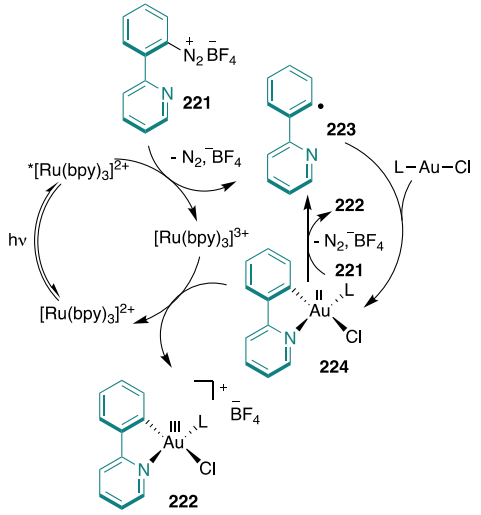

with the aryldiazonium salt (**221**) in a SET to deliver the aryl radical (**223**) and $[Ru]^{3+}$. In the next step, the aryl radical added to the gold(I) center to form the corresponding gold(II) intermediate (**224**). A quantum yield measurement delivered a value of 57, which indicated that a radical chain greatly contributed to the mechanism. Thus, it was suggested that the gold(II) species would predominantly undergo a SET with another equivalent of aryldiazonium salt to deliver the desired cationic gold(III) complex (**222**) and an aryl radical. However, every now and then a SET from the gold(II) species (**224**) to $[Ru]^{3+}$ had to occur to initiate a new radical chain, also under formation of the desired product (**222**).

In a next study, the group of Toste again highlighted that cationic gold(III) complexes could be the key intermediates in dual gold/photoredox catalysis.[155] This protocol provided mechanistic support for the formation of gold(III) species during gold-catalyzed $C(sp^2)–CF_3$ and $C(sp^2)–N$ coupling. The core of this report focused on the mechanistic study on the trifluoromethylation of aryldiazonium salts starting from $IPrAuCF_3$ in the presence of blue LED light irradiation and a ruthenium photocatalyst. The electronic effect of the *para*-substituent of the diazo compound on the reaction was studied and showed that the conversion of electron-deficient groups was more efficient (**222a**, **222b**) than for the electron-rich surrogates (**225d**) (Scheme 66).

Scheme 66. Electronic Effect on the Stoichiometric Trifluoromethylation of $IPrAuCF_3$

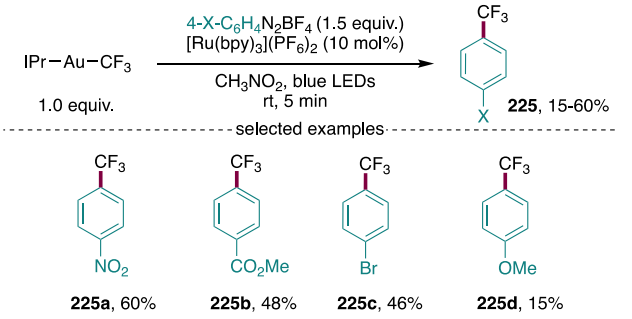

Control experiments revealed the necessity of the light and the photocatalyst for a successful transformation. These requirements were also proven by UV/vis absorption spectroscopy, with the result that only the photocatalyst absorbed the light of the blue LEDs. In addition, a Stern–Volmer fluorescence quenching experiment revealed that only the aryldiazonium salt interacted with the excited photocatalyst. Therefore, the proposed reaction mechanism involved the aryl radical addition to $IPrAu(I)CF_3$ to form gold(II) intermediate **226**, which underwent a SET with another equivalent of aryldiazonium salt to access the cationic gold(III) species **227** under generation of an aryl radical (Scheme 67). This chain mechanism was consistent with the value 6.6 as the quantum yield for this process. It can be assumed that the oxidation of gold(II) (**226**) to gold(III) (**227**) was just mainly accomplished by the aryldiazonium salt and that the radical chain from time to time needed to be reinitiated by regeneration of the photosensitizer (gray, added by the authors of this review).

By applying both $IPrAuCF_3$ or IPrAu-succinimide in the presence of 1.5 equiv. of aryldiazonium tetrafluoroborate and water (to prevent the reductive elimination), the corresponding gold(III) aquo complexes were isolated (**228** and **229**) (Scheme 68A). In their geometry, the aquo ligand was *trans* to the aryl ligand and thus the CF_3 or succinimide *trans*-oriented to the NHC (IPr) ligand. The authors beautifully addressed the lack of examples for C–N reductive elimination from gold(III) complexes and provided a first stoichiometric

https://dx.doi.org/10.1021/acs.chemrev.0c00841
Chem. Rev. XXXX, XXX, XXX–XXX

Scheme 67. Proposed Reaction Mechanism for the Stoichiometric Trifluoromethylation of Diazonium Salts by IPrAuCF$_3$

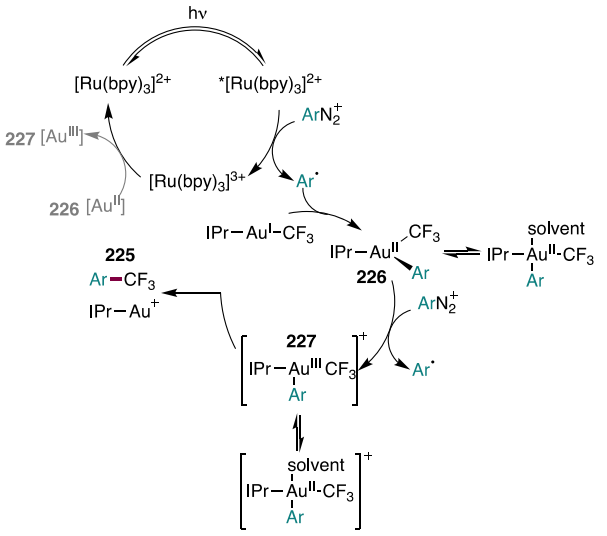

Scheme 68. (A) Synthesis of Gold(III) Aquo Complexes and (B) a First Attempt for Stoichiometric C–N Coupling

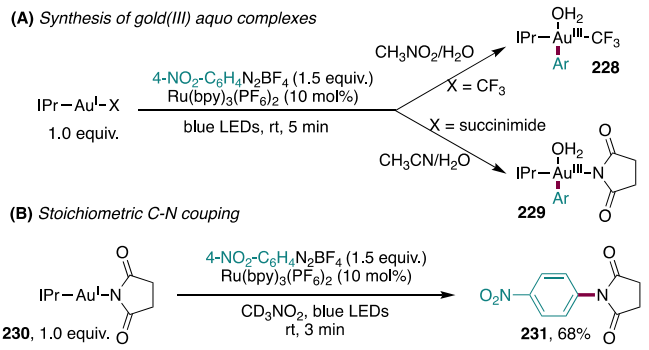

example of a C(sp^2)-succinimide coupling reaction under the dual gold/photoredox technique (Scheme 68B). However, to be of use for organic chemists, both trifluoromethylation and succinimide coupling should in the future be achieved in a catalytic fashion.

The most recent example in this realm was achieved by Hashmi and co-workers reporting on the photosensitizer-free synthesis of pincer [C^N^C]gold(III) complexes (**233**) through oxidative addition of aryldiazonium salts (**232**) to a gold(I) center (Scheme 69).[156] This route was a great achievement in the field of gold pincer complexes because, so far, these complexes were obtained through a transmetalation of highly toxic organomercury compounds.[157−160] This work provided a simple mercury-free photochemical path, starting from diazonium salts of type **232** and DMSAu(I)Cl. In the presence of blue LED irradiation and the organic base 2,6-di-*tert*-butyl-4-methylpyridine (DTBMP), the gold(I) was oxidized to the corresponding cationic gold(III) intermediate, which was followed by a base-assisted C−H activation to afford the desired [C^N^C]gold(III) complexes (**233**) in moderate to very good yields. Remarkably, in the case of unsymmetrically substituted arene systems, two possible positions for the final C−H activation were offered, however, only **233a** as sterically less hindered isomer was obtained. Further, alkyne substitution **233b** as well as a thiophene backbone **233c** were well tolerated.

Starting from a gold(I) source already bearing a strong binding ligand, such as IMesAuCl, the corresponding complex **235** was furnished with 65% yield (Scheme 70A). Another advantage of this route was the use of DMSAuCl as the gold(I) precursor, which allowed a postfunctionalization through chloride replacement; this is demonstrated for complex **237** (Scheme 70B).

3. DINUCLEAR GOLD CATALYST

3.1. Electron Transfer Reactions

More than 20 years after C.-M. Che first reported on the preparation and the photophysical properties of the dinuclear gold(I) complex $[Au_2(\mu\text{-dppm})_2]^{2+}$,[56,57] Barriault and co-workers detected the potential of this complex and tested its applicability to the reductive cleavage of alkyl and aryl bromides. As a benchmark reaction, the authors selected the intramolecular cyclization of unactivated alkyl bromides (**238**) (Scheme 71).[59] While optimizing the reaction conditions, it

Scheme 69. Photosensitizer-Free Synthesis of [C^N^C]Gold(III) Complexes

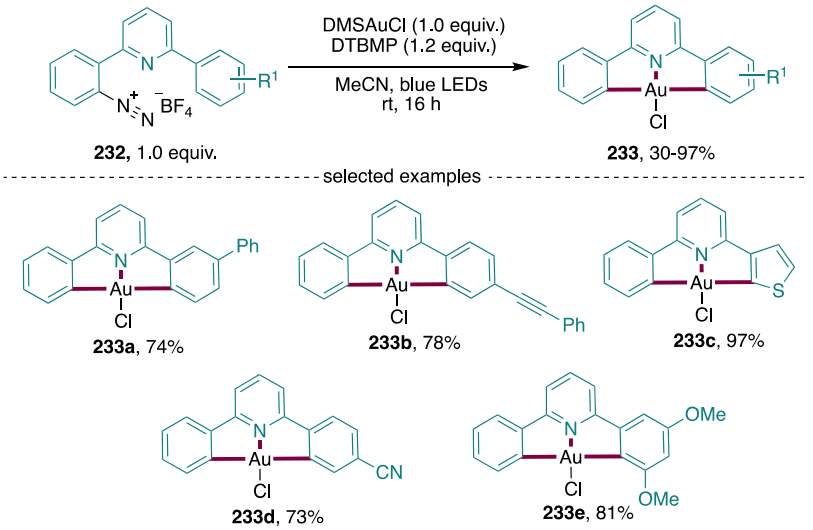

https://dx.doi.org/10.1021/acs.chemrev.0c00841
Chem. Rev. XXXX, XXX, XXX−XXX

Scheme 70. Application of the Photosensitizerf-Free Method towards [C^N^C]Gold(III) Complexes

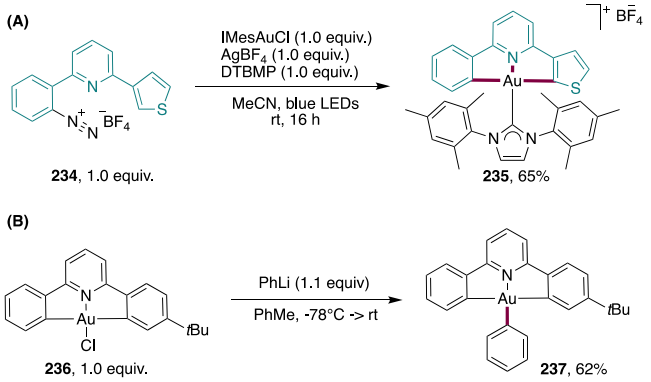

Scheme 71. Intra- and Intermolecular Cyclization of Unactivated Alkyl and Aryl Bromides

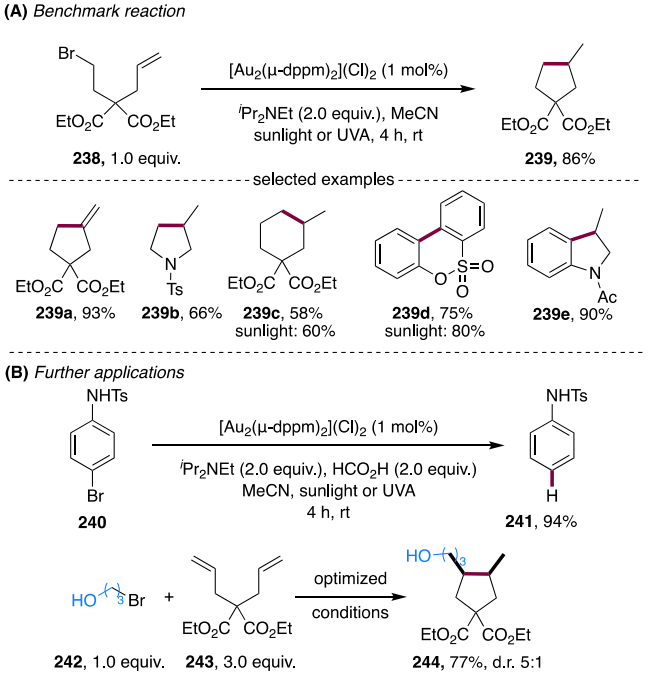

was found, that the tertiary amine base DIPEA functioned as a sacrificial electron and hydrogen donor. Further, the counteranion of the dimeric gold(I) catalyst did not seem to influence the reaction outcome significantly. Control experiments showed that the reaction distinctly required the combination of light irradiation and the catalyst. These reactions were carried out under irradiation with sunlight, however, UVA (315−400 nm) proved to be a good surrogate. The scope of the cyclization of alkyl and aryl bromides was broadly explored, with a yield ranging from 58 to 93% showing a good functional group tolerance. In the presence of formic acid, aryl bromide **240** was reductively dehalogenated to give sulfonanilide **241** in 94% yield. This method was an exceptional achievement because typical methods to form alkyl or aryl radicals from carbon−halogen bonds depended on the use of hazardous and/or toxic chemicals or radical initiators (e.g., azobis(isobutyronitrile) (AIBN), $K_2S_2O_8$, or organostannanes).[161−163] In addition, the authors showed that their benchmark reaction did not operate with the use of iridium-based photocatalyst ($[Ir(ppy)_2(dtbbpy)]PF_6$ and *fac*-$[Ir(ppy)_3]$). At last, also intermolecular reactions succeeded, for example, the reaction of 1-bromopropanol to diallylated malonate (**243**) to give *cis*-substituted cyclopentane **244**. Mechanistically, the presence of a tertiary amine base indicated that both oxidative and reductive quenching are likely to occur but was not further discussed.

In a next report, Barriault et al. disclosed an elegant one-pot reductive oxygenation reaction that combined their previous method of photomediated dinuclear gold-catalyzed reduction of alkyl bromide with a novel photochemical bromination of alcohols (Scheme 72).[164] The transformation of alcohols into

Scheme 72. Deoxygenation of Alcohols via Radical Bromination

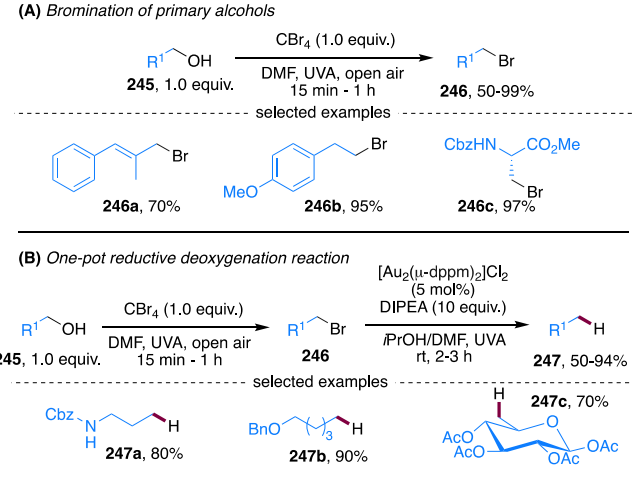

halides is a common process in synthetic organic chemistry, the most reliable among these is the Appel reaction.[165] The method presented by Barriault benefited from the sole use of CBr_4 in DMF under light irradiation, whereby the Vilsmier−Haack reagent was formed (unlike Stephenson et al.,[166] who used [Ru]-photosensitizer for this step). Accordingly, although limited to primary alcohols, the corresponding alkyl bromides **246** were obtained in yields of 50−99%, and the conversion showed a very good functional group tolerance (Scheme 72A). With this in hand, the authors focused on the one-pot, two step radical halogenation and reduction process (Scheme 72B). After extensive solvent screening, *i*PrOH turned out to be necessary, not only as a cosolvent but also as a hydrogen donor for the gold-catalyzed reduction process. Again, the scope with regard to diverse alcohols was explored and delivered the desired products **247** in excellent yields ranging from 50% to 94%. Among other functional groups, the reaction tolerated *N*-benzyloxycarbonyl (Cbz) (**247a**), *O*-benzyl (Bn) (**247b**) and the tetra-*O*-acetylated glucose (**247c**). Since the pioneering work of Barton and McCombie,[167] the research field of radical reductive deoxygenation of alcohols has been of great interest, however, most of them require rather toxic and hazardous radical initiators.[168−170]

The mechanism reposed on the finding of Nishina et al.[171] in combination of the work of the group of Stephenson.[166] In particular, the irradiation of CBr_4 promoted the homolytic cleavage of a C−Br bond to form the tribromomethane radical (Scheme 73). The latter added to DMF, which was followed by an oxidation by CBr_4 or O_2 to deliver the Vilsmeier−Haak-type reagent (**250**). In combination with the alcohol, intermediate **251** was generated, which underwent nucleophilic

https://dx.doi.org/10.1021/acs.chemrev.0c00841
Chem. Rev. XXXX, XXX, XXX−XXX

Scheme 73. Proposed Mechanism of Deoxygenation of Alcohols

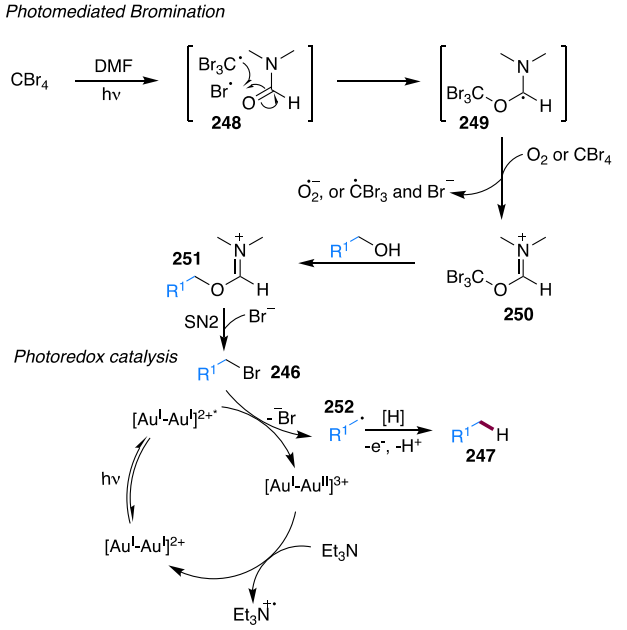

replacement with a bromide anion to deliver the intermediary alkyl bromide (**246**). After addition of DIPEA, *i*PrOH and catalytic amount of the dinuclear gold(I) catalyst, the mixture was irradiated by light, whereby the gold(I) catalyst was excited. After oxidative quenching by alkyl bromide, the corresponding alkyl radical (**252**) was generated. In the presence of a proton donor, in this case DIPEA or *i*PrOH, the targeted product (**247**) was formed. At last, the gold catalyst was regenerated by reduction of the sacrificial electron donor, the trialkylamine DIPEA.

In continuation of their work, Barriault and co-workers applied the combination of UV-light irradiation with the dinuclear gold photocatalyst $[Au_2(\mu\text{-dppm})_2]^{2+}$ for the intramolecular radical cyclization onto indoles (**253**) (Scheme 74).[172] During the optimization of the reaction conditions, it

Scheme 74. Intramolecular Radical Cyclization onto Indoles

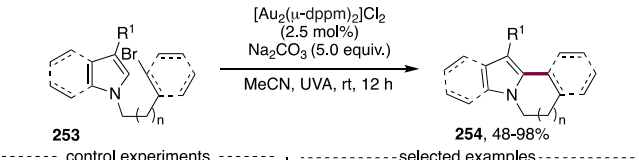

control experiments

For **254a**, R1 = H

Entry	Base, time	Yield [%]
1	DIPEA, 1 h	42
2	TMEDA, 1 h	10
3	DABCO, 1 h	-
4	Na_2CO_3, 1 h	41
5	Na_2CO_3, 12 h	98

selected examples

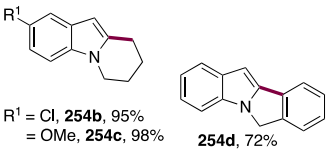

became apparent that these types of reaction did not necessarily require a tertiary amine base (entries 1−3). While employing the inorganic base, sodium carbonate, the best conversion of the starting material was observed (entry 4), increasing the reaction time from 1 to 12 h, delivered the exclusive formation of **254a** (entry 5). This synthetic protocol offered a mild alternative to already reported routes on oxidative radical additions to indoles.[173,174] It provided **254** in very good yields by tolerating diverse functional groups without a lack in yield (**254b** vs **254c**), such as aldehyde, ester, cyano, methoxy, and pyridine. The ring size of the adjacent cycle depended on the chain length of alkyl bromide. An oxidative quenching pathway was suggested for this transformation, most probably due to the absence of a tertiary amine base as sacrificial electron donor.

In 2018, this methodology was elegantly applied in the total synthesis of pyrroloazocine indole alkaloids, particularly gradilodines and lapidilectines, by the group of Echavarren (Scheme 75).[175] By using the identical conditions of Barriault et al., sole diastereomer **256** was accessed in 91% yield.

By utilizing the dinuclear gold photocatalyst, Hashmi et al. investigated the C(sp^3)-H alkynylation of tertiary aliphatic amines (**257**) (Scheme 76).[176] In this case, the applied tertiary alkylamine functioned as both sacrificial electron donor and reactant. Interestingly, the reaction did not work with bromoalkynes and was highly depended on the counteranion of the dinuclear gold catalyst. The application of a different photocatalyst, such as $[Ru(bpy)_3]Cl_2$ and $[Ir(ppy)_3]$, had a detrimental effect on the reaction. A variety of substituted iodoalkynes (**258**) and tertiary aliphatic amines (**257**) were examined. In doing so, mainly the methyl group adjacent to the nitrogen of the amine was coupled instead if the methylene or methine group (e.g., **259a**−**259g**). Further, upscaling the reaction to gram scale (for **259e**) did not significantly influence the outcome.

An array of various mechanistic experiments, among these radical trappings, indicated the generation of an alkynyl radical. An important experiment leading to this assumption was that by decreasing the concentration of tertiary amine, an increased formation of the homodimerization and hydrogen abstraction of the iodoalkyne was detected. On the basis of these results and in combination with a literature report on the visible light-mediated C(sp^3)-H arylation of tertiary amines with 1,4-dicyanobenzene by MacMillan et al.,[177] a tentative mechanism was proposed (Scheme 77). Initially, the gold photocatalyst was excited and thus enabled to reduce the C(sp)−I bond under the formation of a highly speculative alkynyl radical (**260**). The oxidized gold complex was regenerated by a SET from tertiary amine (**257**) to afford the amine radical cation **261**, which under hydrogen abstraction forms the aminoalkyl radical (**262**). A radical−radical recombination produced the desired product (**259**). The selectivity for the preferred cross-recombination of the two different radicals rather than a homocoupling, was explained by the "persistent" radical effect.[178−180]

The utilization of dinuclear gold photocatalyst has not only influenced typical organic chemistry but was also used in the field of radical photopolymerization. In this instance, Lalevée, Fensterbank, Goddard, and Ollivier studied the photoredox-catalyzed atom transfer radical polymerization (ATRP) of methyl methacrylate (MMA, **264**) induced by a photoreduction of ethyl α-bromophenylacetate (**263**).[181] Interestingly, two consecutive polymerizations with two different monomers was achieved. First, a polymerization using MMA as monomer afforded polymer **265** (PMMA) and a second polymerization with addition of benzyl methacrylate (BnMA, **266**) (Scheme 78). This demonstrated that the Br-terminus of one polymer can be further activated by light irradiation and dinuclear gold(I) catalyst for further polymerizations. A previous report showed that *fac*-Ir(ppy)$_3$ as photocatalyst for

https://dx.doi.org/10.1021/acs.chemrev.0c00841
Chem. Rev. XXXX, XXX, XXX−XXX

Scheme 75. Application of the Dinuclear Gold Catalyst in the Total Synthesis of Lapidilectines and Gradilodines

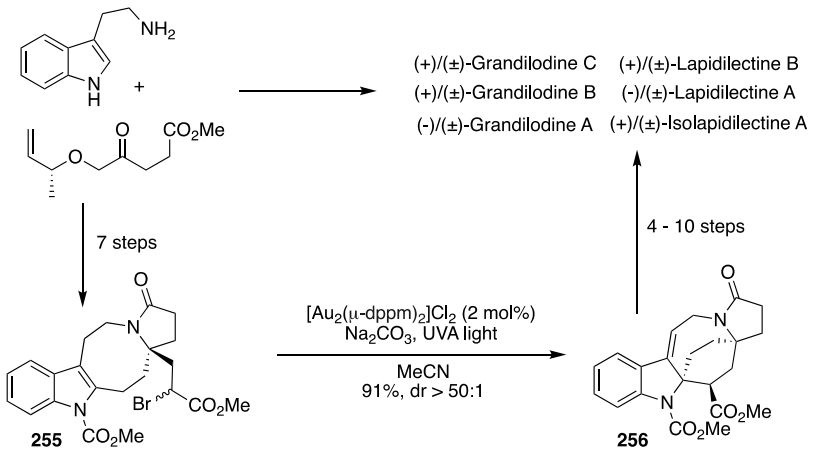

Scheme 76. Alkynylation of Tertiary Amines by Applying the Dinuclear Gold Photocatalyst

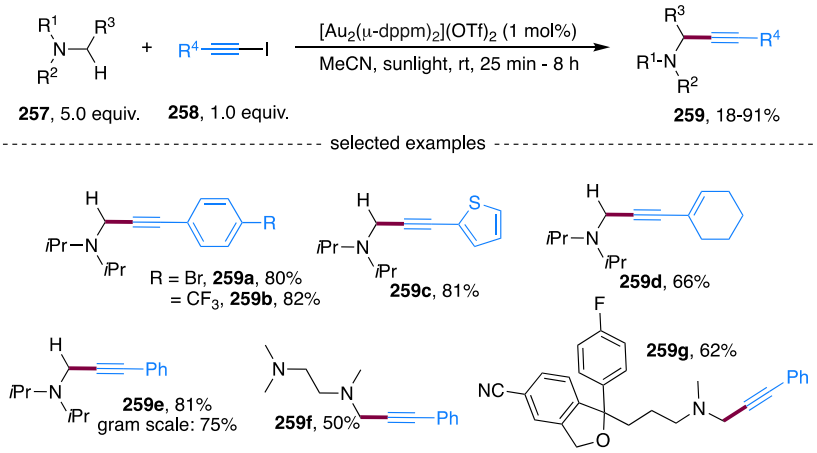

Scheme 77. Tentative Mechanism for the Alkynylation of Tertiary Amines

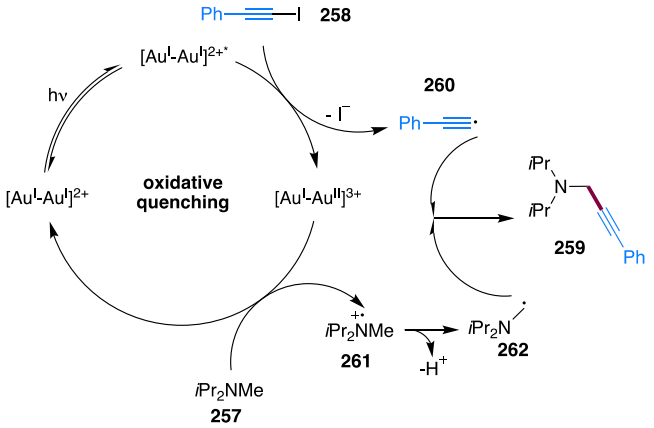

Scheme 78. Dinuclear Gold(I) Catalyst Applied in Light-Induced Atom Transfer Radical Polymerization (ATRP)

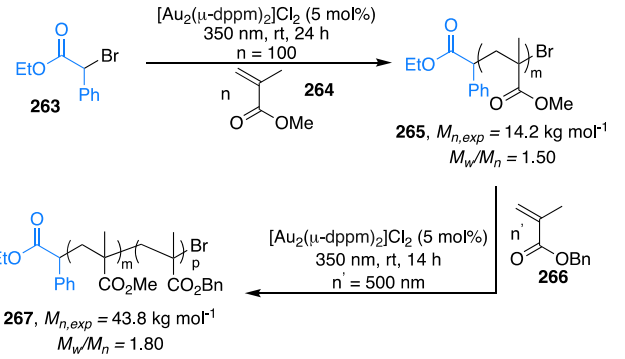

polymerization was very efficient,[182] however, a comparison was drawn and distinctly revealed that the dinuclear gold catalyst improved the efficiency.

A highly selective visible light-mediated gold-catalyzed difluoroalkylation and perfluoroalkylation of hydrazones was explored by the group of Hashmi.[183] Both aromatic aldehydes and their synthetic equivalent, here, hydrazone[184−187] and the difluoromethylene/polyfluorinatedalkyls are valuable building blocks for organic synthesis and drug discovery.[188,189] The optimized reaction conditions for the coupling of hydrazone **268** and (bromodifluoromethyl)phosphonate **269** consisted of 2.0 mol % of $[Au_2(\mu\text{-dppm})_2](OTf)_2$ and 3.0 equiv. of 2,6-lutidine as a base to neutralize the in situ formed HBr, MeCN as solvent, and irradiation with UVA light. The scope with respect to phosphonyldifluoromethylation of *N*-morpholine hydrazones (Scheme 79A) was explored, and a wide variety of functional groups were well tolerated. For coupling of various benzaldehyde hydrazones (**271**) with ethyl bromodifluoroacetate and perfluoroalkylation of hydrazones, imidazole as the base was used. As exemplified in Scheme 79B, all of the studied

https://dx.doi.org/10.1021/acs.chemrev.0c00841
Chem. Rev. XXXX, XXX, XXX−XXX

Scheme 79. Difluoroalkylation and Perfluoroalkylation of Hydrazones

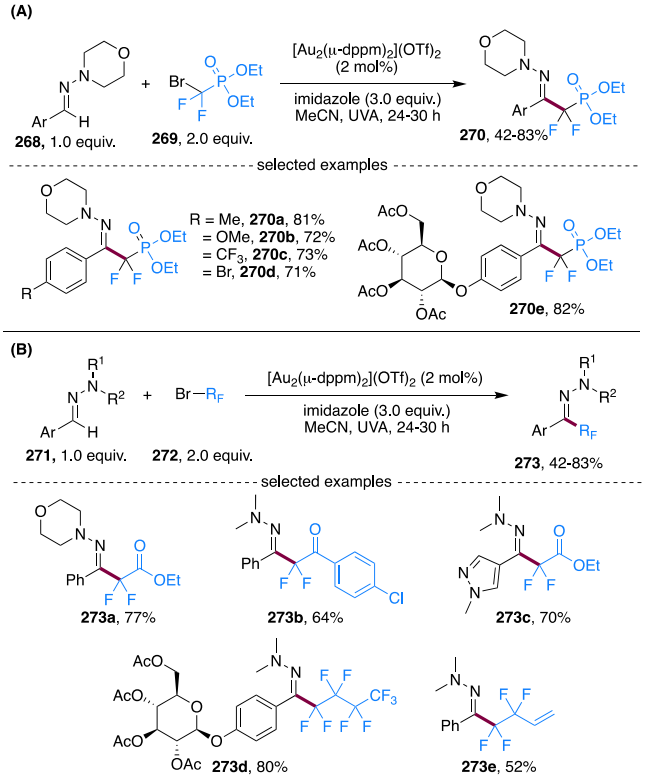

conversions exhibited a broad functional group compatibility and the products were obtained in moderate to high yields.

Further functionalization of the products, such as reduction of the imine using BH_3 in THF (Scheme 80A), hydrolyzation

Scheme 80. Post Functionalization of Obtained Hydrazone Derivatives

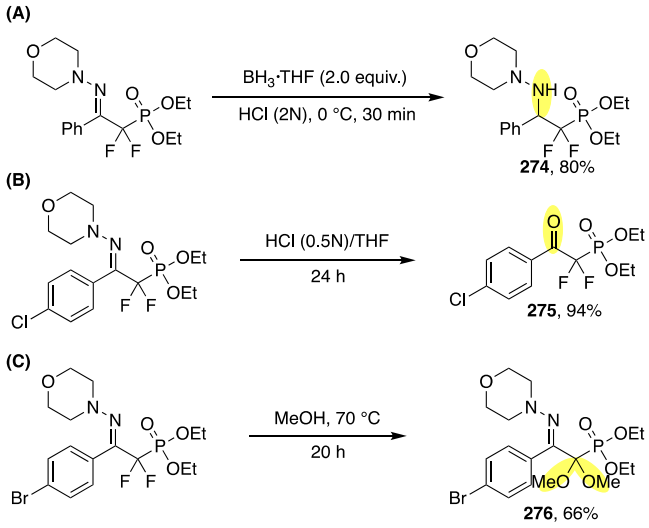

to the corresponding ketone **275** (B) or a direct heating to 70 °C in methanol delivering dimethoxy ketal **276** (C) highlighted the synthetic attractiveness of this method.

As a part of the mechanistic studies, an EPR spin-trapping experiment with DMPO was conducted, and with the aid of a simulation, the DMPO−difluoroalkyl adduct could be distinctly assigned. Moreover, a radical chain mechanism was excluded by determination of the quantum yield (Φ = 0.01) and also by a light on/off experiment, the result of which should be analyzed with caution.[97] A tentative mechanism was suggested, which starts with the usual light excitation of the dinuclear gold(I) catalyst, enabling a SET to fluorinated alkyl bromide **269** under formation of the corresponding alkyl radical **277** (Scheme 81). Next, a radical addition to hydrazone

Scheme 81. Postulated Mechanism for the Light-Mediated Gold-Catalyzed Difluoroalkylation and Perfluoroalkylation of Hydrazones

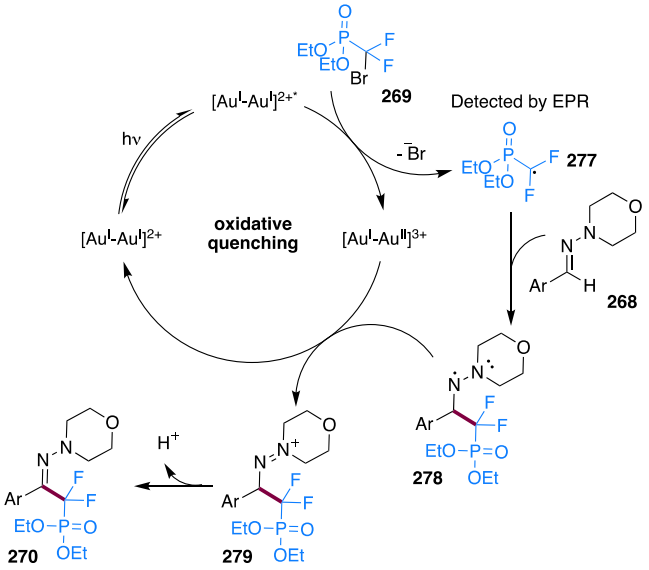

(**268**) afforded a three-electron π-bonding aminyl radical intermediate (**278**). The latter was oxidized by gold species $[Au^{I}–Au^{II}]^{3+}$ and subsequent deprotonation delivered the targeted alkylfluorinated product (**270**).

To understand the reactivity and the likelihood of reductive or oxidative quenching being the major route in the reactions involving the dinuclear gold(I) complex, Barriault and coworkers studied the photophysics and electrochemical properties of several polynuclear gold(I) complexes in 2016.[190] The studies were based on the first published protocol in this field, the intramolecular cyclization of unactivated bromide **238**, where the authors already hypothesized a competing reductive and oxidative quenching in the presence of a tertiary amine base (in that case DIPEA) (Scheme 71).[59] With the aid of phosphorescent measurements, the triplet energy of $[Au_2(\mu\text{-dppm})_2]^{2+}$ was determined, and in combination with the ground-state potentials (obtained through cyclic voltammetry (CV)), the excited state oxidation (E^*_{ox}) and reduction (E^*_{red}) potentials were calculated (Figure 2). As a next step, one can study the thermodynamic feasibility of a reduction or oxidation process. For this, the Gibbs free energy was taken into account, and it showed that a reductive quenching with DIPEA was thermodynamically favored, while an oxidative quenching with substrate **238** was disfavored.

To determine the rate at which the triplet state of $[Au_2(\mu\text{-dppm})_2]^{2+}$ is quenched, time-resolved transient spectroscopy was performed. These experiments revealed similar quenching constants for both **238** and DIPEA (3.1×10^7 M^{-1} s^{-1} for **238** and 2.7×10^7 M^{-1} s^{-1} for DIPEA), however, only 18% of the triplet state were quenched by **238** and 78% were quenched by

https://dx.doi.org/10.1021/acs.chemrev.0c00841
Chem. Rev. XXXX, XXX, XXX−XXX

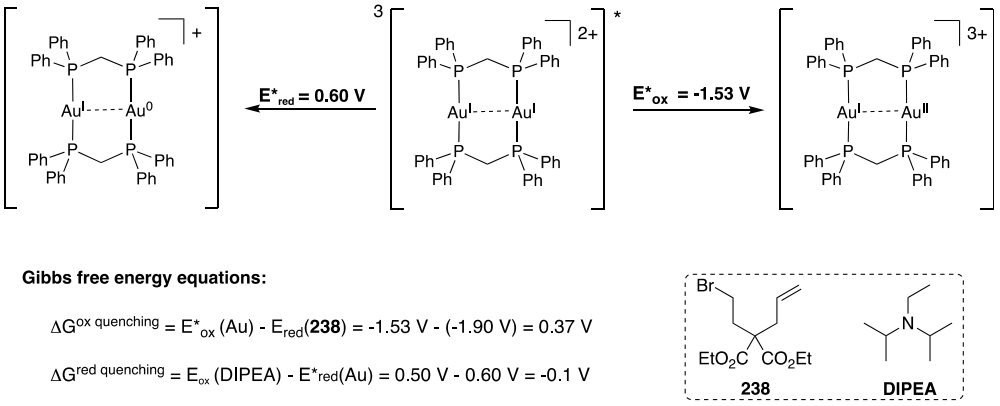

Figure 2. Triplet state reduction and oxidation and the Gibbs free energy equations.

DIPEA. This divergence was attributed to the used excess of DIPEA (5 times), and thus a reductive quenching mechanism as the major route for this specific reaction seemed most likely.

Additionally, the authors dedicated themselves to the slightly contradictory fact that, despite the divergence in redox potentials, the excited $[Au_2(\mu\text{-dppm})_2]^{2+}$ was able to reduce bromoalkanes such as **238**. For this, a chiral alkyl bromide was chosen and the interaction with $[Au_2(\mu\text{-dppm})_2]^{2+}$ was studied by circular dichroism (CD). Interestingly, a new peak was detected, which was assigned to an induction of chirality to achiral dinuclear gold(I) complex due to binding of the chiral alkyl bromide. Thus, the authors suggested a reduction of the carbon−bromo bond through an inner sphere exciplex formation.

In contradiction to this, an operating radical chain process whereby the dinuclear gold(I) catalyst only acted as a radical initiator was disclosed in a computational study by Yu and co-workers.[191]

On the basis of previous findings, Barriault's group further expanded the utility of this dinuclear gold catalyst to a photoinduced intermolecular Minisci-type[192−194] alkylation of heteroarenes with unactivated alkyl bromides.[195] At first, the transformations of heteroarene TFA salt, lepidine-TFA (**280**), were studied. Primary, secondary, and tertiary bromoalkenes worked well to deliver the alkylated chinoline derivatives **281** in moderate to excellent yields (Scheme 82A). To explore the substrate scope with respect to diverse heteroarenes, the authors applied the saturated heterocycle (**282**) with stoichiometric amount of TFA (Scheme 82B). All of the substrates converted smoothly to the C−H activated products in high yields, for example caffeine, was successfully alkylated with bromoadamantyl (**283d**) and bromocyclohexane (**283e**) in 95% and 92% yield. This demonstrated the potential for late-stage functionalization of many substructures found in nature and drug design.

Because of the absence of a tertiary amine base, the mechanism proceeded via an oxidative quenching (Scheme 83). Owing to the proposed ability of an existing inner sphere photoinduced electron transfer (PET), the alkyl bromide was reduced to form an alkyl radical (**284**). The latter, in combination with the protonated heteroarene (**285**, protonated by TFA), produced the aminyl radical intermediate (**286**). Subsequent oxidation of **286** by $[Au_2(\mu\text{-dppm})_2]^{3+}$ completed the catalytic cycle by regenerating the gold catalyst and **287**, which after deprotonation delivered the desired alkylated products.

Scheme 82. Alkylation of (A) Lepidine and (B) Diverse Other Heteroarenes

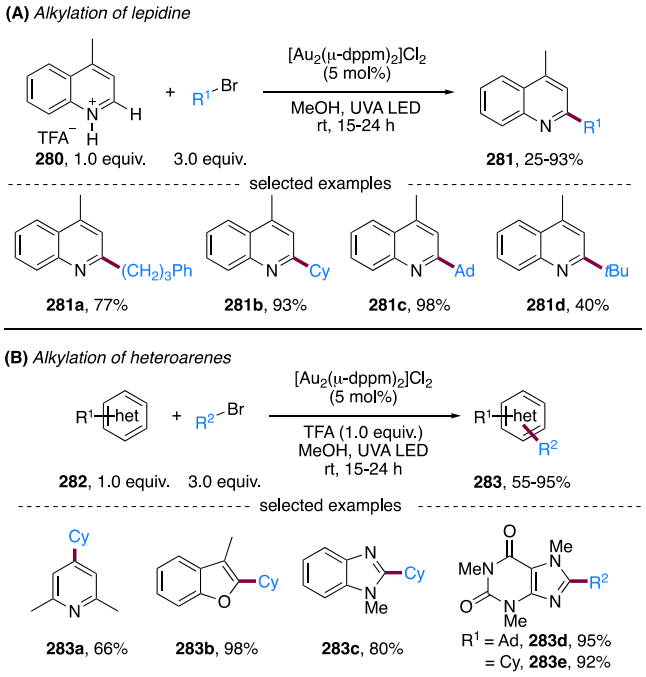

Furthermore, this protocol investigated a three-component (heteroarene (**282**), α-bromoesters (**288**), and simple alkenes (**289**)) tandem reaction based on the radical polarity reversal concept (Scheme 84).[196,197] This idea consisted of the formation of an electrophilic radical from activated α-bromoesters upon reduction by photoexcited gold photocatalyst. Addition of an electrophilic radical to electron-poor heteroarenes was conceptually not feasible, which was also confirmed by control experiments. Thus, the additional alkene (**289**) functioned as an acceptor whereby the electrophilic radical becomes nucleophilic **291** (Scheme 83), enabling the addition to electron-deficient heterocycles (Scheme 83, purple detour). This method showed a good compatibility to give **290** in moderate to very good yields.

So far, bromoalkyls/arenes were successful coupling partners by applying the mild combination of UV-light (or sunlight) and $[Au_2(\mu\text{-dppm})_2]^+$ as catalyst. Therefore, Barriault et al. devoted their efforts to the coupling of vinylic bromides, in particular on the intramolecular arylation of butenolides (**294**) and cyclic enones (**296**) (Scheme 85).[198] After extensive

https://dx.doi.org/10.1021/acs.chemrev.0c00841
Chem. Rev. XXXX, XXX, XXX−XXX

Scheme 83. Mechanism of the Direct Alkylation of Heteroarenes

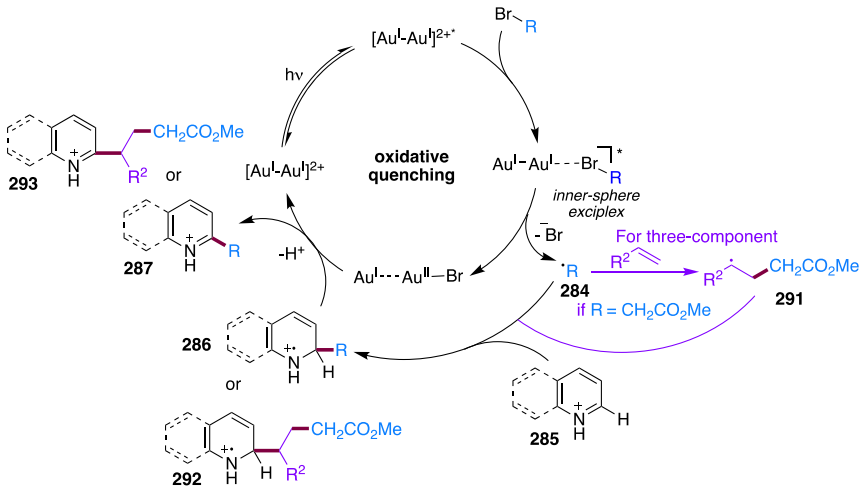

Scheme 84. Three-Component Tandem Radical Alkylation of Heteroarenes

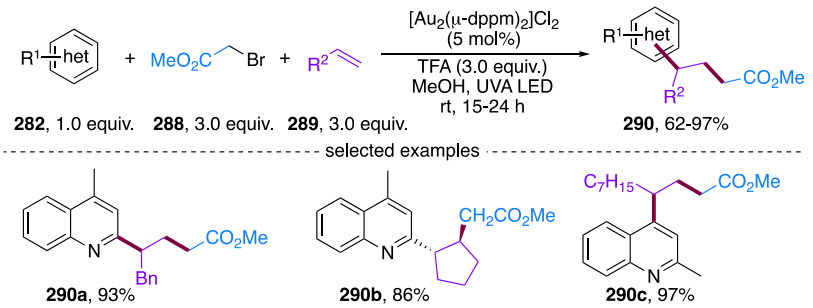

Scheme 85. Dinuclear Gold-Catalyzed Intramolecular Arylation of Butenolides and Cyclic Ketones

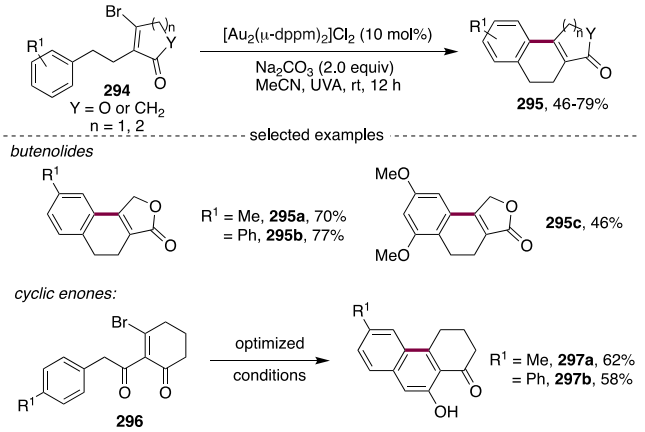

additive screening, the scope of the reaction was studied and delivered the cyclized products (**295**, **297**) in good yields of 62−79%. The only significant aberration occurred by applying an electron-rich arene to afford product **295c** in a yield of 46%.

Considering that most of the previous reports relied on the use of a tertiary amine base as sacrificial electron donor and hydrogen source and thus both mechanistic pathways, oxidative and reductive quenching become feasible. In this case, sodium carbonate worked best as additional base. The value of the redox potential of $CO_3^{\bullet-}/CO_3^{2-}$ (1.5 V),[199] however, was not sufficient enough to turnover the dinuclear gold catalyst in either path (oxidative or reductive). Out of this reason, an oxidative quenching cycle of a type illustrated in Scheme 86 was most likely (sequence of occurring steps were

Scheme 86. Postulated Reaction Mechanism of Intramolecular Arylation of Butenolides and Cyclic Ketones

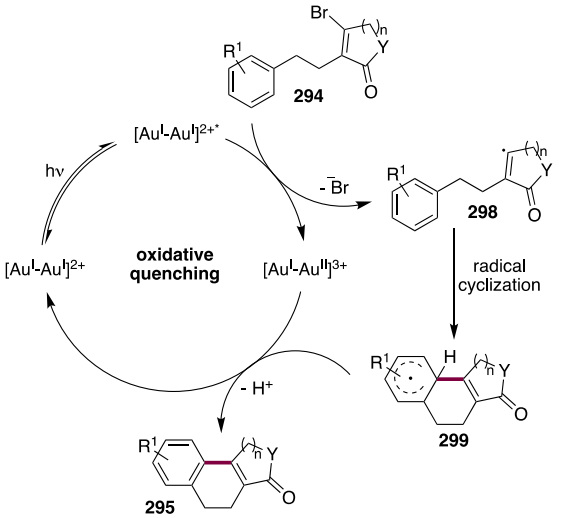

in accordance to the mechanism presented earlier already by Barriault et al.[172] also in the absence of a tertiary amine base). The excited gold photocatalyst reduced the C−Br bond through a SET to generate the vinyl radical (**298**), which cyclized to obtain a tricyclic tertiary radical (**299**). The latter reduced the gold intermediate, and after rearomatization the desired product (**295**) was formed.

https://dx.doi.org/10.1021/acs.chemrev.0c00841
Chem. Rev. XXXX, XXX, XXX−XXX

Scheme 87. Gold-Catalyzed Step in Total Synthesis of (±)-Triptolide

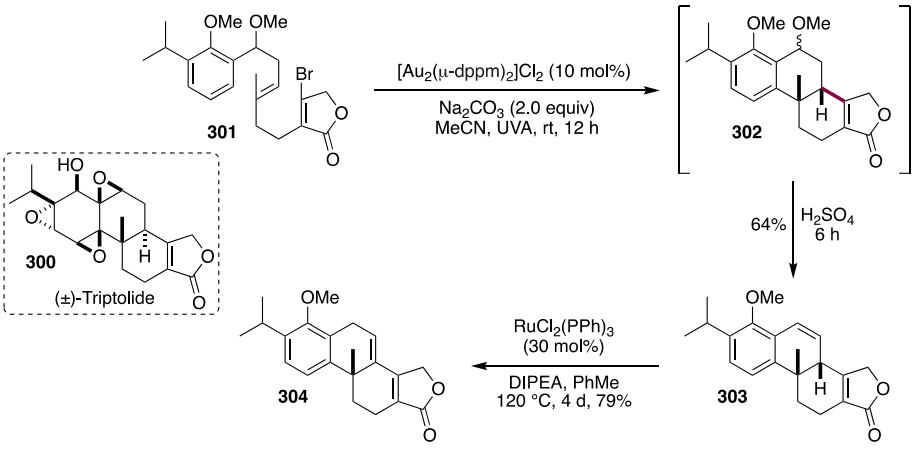

The applicability of this method was demonstrated in the total synthesis of (±)-triptolide (**300**). This naturally occurring diterpene could be isolated from chinese climbing vine *Tripterygium wilfordii*.[200] It shows in vitro and in vivo activity against polycystic kidney disease, pancreatic tumor and exhibits immunosuppressive activities.[201−204] Thus, an easy and straightforward synthesis was envisioned and addressed over the past years.[205−207] Barriault and co-workers aimed to obtain **304** (a key intermediate in the total synthesis of (±)-triptolide) using their intramolecular radical cyclization of the γ-butenolide derivative **301** (Scheme 87). The light-mediated gold-catalyzed radical cyclization afforded **302**, and subsequent treatment with H_2SO_4 gave tetracycle **303**. The relative stereochemistry was *cis* at the ring junction, rather than the desired *trans*, albeit Ru-catalyzed epimerization successfully accessed the desired key intermediate **304**.

An intermolecular photocatalyzed Heck-like coupling of unactivated alkyl bromides by utilizing the dinuclear gold complex was developed by Hashmi and co-workers (Scheme 88).[208] A significant advantage of this method compared to the typical Pd-catalyzed Heck reaction was the tolerance for primary, secondary, and tertiary unactivated alkyl bromides with a β-hydrogen.[209] The success of the reaction was dependent on the choice of the right additives (entries 1−4), whereby the addition of 50 mol % of sodium ascorbate in combination with 1.5 equiv. of $NaHCO_3$ revealed to work out best. Interestingly, the application of other common photocatalysts, $[Ru(bpy)_3]Cl_2$ and $[Ir(ppy)_3]$, completely paralyzed the reaction (entries 5−6). A number of primary, secondary, and tertiary alkyl bromides were compatible, bearing versatile functional groups, namely aldehydes, ketones, esters, nitriles, alcohols, heterocycles, alkynes, ethers, and halogens. All of the 1,1-disubstituted alkenes (**305**) were readily converted, however, a downside of this reaction was the lack of conversion of trisubstituted alkene where only 32% of **306f** could be isolated.

This transformation most likely proceeded via oxidative quenching of excited dinuclear gold(I) photocatalyst to generate an alkyl radical (**307**) by reduction of the alkyl bromide (Scheme 89). This radical was trapped by the alkene derivative (**305**) to give the more stabilized radical **308**. The catalytic cycle was closed by a SET from **308** to the gold intermediate, delivering cationic alkyl species **309** under regeneration of the gold catalyst. Final deprotonation led to the desired alkene (**306**). Notably, the authors suspected that

Scheme 88. Photocatalyzed Heck-Like Coupling of Unactivated Alkyl Bromides

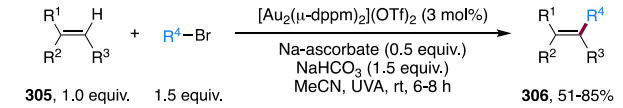

305, 1.0 equiv. 1.5 equiv. **306**, 51-85%

control experiments

For **306a**: $R^1 = R^2 = Ph$, $R^3 = H$, $R^4 = (CH_2)_3CO_2Et$

Entry	Catalyst / base / additive	Yield [%]
1	[Au] / Et_3N / -	36
2	[Au] / Bu_3N / -	37
3	[Au] / $NaHCO_3$ / -	71
4	[Au] / $NaHCO_3$ / Na-ascorbate	91
5	$[Ru(bpy)_3]Cl_2$ / $NaHCO_3$ / Na-ascorbate	-
6	$[Ir(ppy)_3]$ / $NaHCO_3$ / Na-ascorbate	-

selected examples

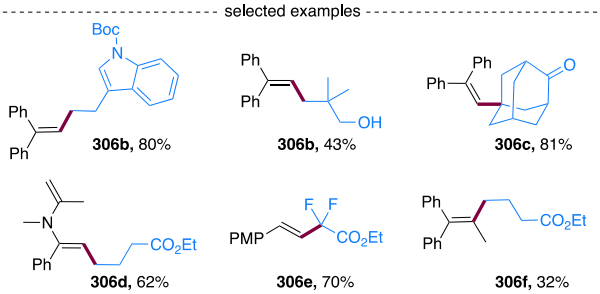

Scheme 89. Speculated Mechanism of Photocatalyzed Heck-Like Coupling

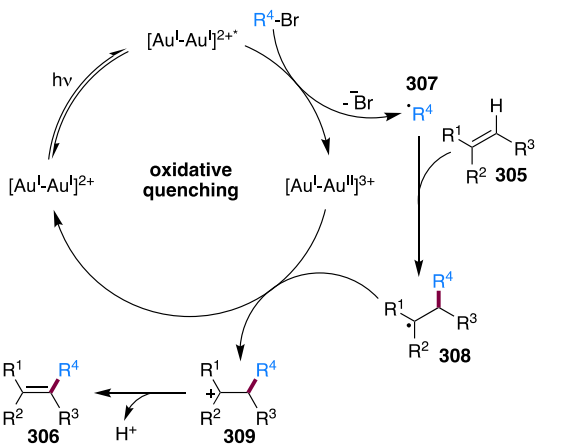

https://dx.doi.org/10.1021/acs.chemrev.0c00841
Chem. Rev. XXXX, XXX, XXX−XXX

the addition of sodium ascorbate avoided the decomposition of the unstable $[Au^{I}–Au^{II}]^{2+}$ intermediate to some extent.

A further study by the group of Barriault aimed at the homocoupling of iodoarenes and bromoalkans by using the tool of photoredox gold catalysis (Scheme 90).[210] In the presence of an organic base, triethylamine (TEA), and an inorganic base, K_2HPO_4, the Ullman-type[211] homocoupling of diverse iodoarens (**310**) was obtained in good yields (Scheme 90A). Notably, in the absence of light or photocatalyst, the reaction did not proceed. Further, by transferring the same conditions to the homocoupling of bromoalkanes (**312**), it was found that the homocoupled product (**313**) was obtained, however, along with a significant amount of dehalogenation to the corresponding alkane. Deuteration of the applied triethylamine and the solvents interestingly resulted in slightly higher yields (89%). The reason for this might be an occurring hydrogen atom transfer (HAT) which proceeded slower with deuterium, allowing more time for free radicals to recombine. Under the conditions of all reagents and solvents deuterated, a small reaction scope was examined and gave **313** in good yields.

As mentioned earlier, in the presence of a tertiary amine base, a reductive quenching mechanism comes into play and might dominate over the oxidative quenching path.[190] Because the relative concentration of free radical intermediates was low, a direct radical–radical recombination became doubtful. Therefore, the authors proposed a reaction mechanism, which was dominated by reductive quenching until a high enough concentration of C-radicals was formed (Scheme 91). At this point, a radical addition to gold(I) to gold(II) became favorable, accepting another radical to reach dialkylated or diarylated gold(III) intermediate **314**. Final reductive elimination would then produce the homocoupled product.

Scheme 90. Homocoupling of (A) iodoarenes and (B) bromoalkanes

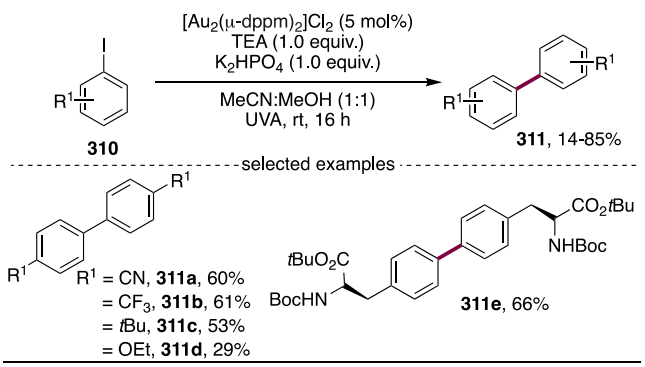

Scheme 91. Postulated Mechanism for the Homocoupling of Iodoarenes and Bromoalkans

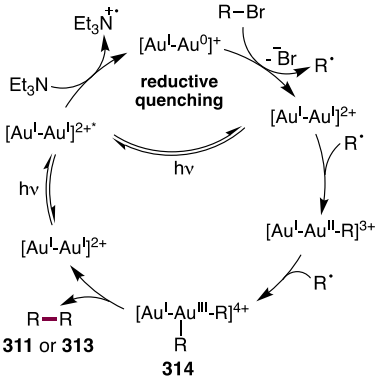

By extending the variety of methodologies by applying the dinuclear gold photocatalyst, the group of Barriault disclosed the alkylative semipinacol rearrangement of TMS-protected α-styrenyl substituted cyclic alcohols (**315**) (Scheme 92).[212] An initial additive screening revealed a full conversion of the silyl-protected α-styrenyl cyclobutanol in the presence of an excess of Na_2CO_3 (3.0 equiv.), yet the desired cyclic ketone (**316a**) could only be isolated in 15% yield (entry 1). Addition of substoichiometric amount of 1,4-diazabicyclo[2.2.2]octane (DABCO) (40 mol %) benefitted the reaction and delivered **316a** in 82% yield (entry 2). Intriguingly, the employment of DABCO as an additive in the intramolecular radical cyclization onto indoles (Scheme 74, entry 3) completely paralyzed the reaction. This further demonstrated the necessity of an additive screening for each novel designed method using the dinuclear gold(I) catalyst and light. A variety of differently functionalized alkyl bromides and TMS-protected α-styrenyl cyclic alcohols were examined. The corresponding cyclic ketones (**316**) were obtained in moderate to very good yields ranging from 27% to 88%. Even though product **316h** was formed from unprotected alcohol, in all other tested cases, the unprotected α-styrenyl alcohols resulted in an unselective product formation. Furthermore, alkyl functionalized alkenes or acyclic α-styrenyl substituted TMS-protected alcohols were incompatible with this method.

Scheme 92. Alkylative Semipinacol Rearrangement of TMS-Protected α-Styrenyl Substituted Cyclic Alcohols

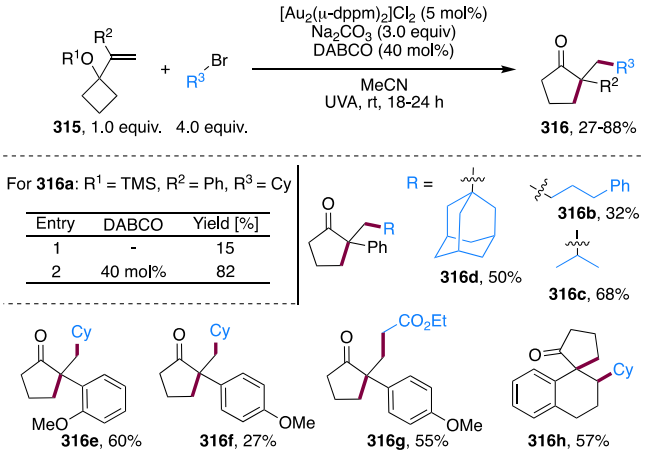

https://dx.doi.org/10.1021/acs.chemrev.0c00841
Chem. Rev. XXXX, XXX, XXX–XXX

On the basis of kinetic studies, the authors proposed that the dinuclear gold catalyst did not only play the role of interacting with the light to reduce the alkyl bromide but also to acted as a Lewis acid to trigger the rearrangement. Thus, the proposed mechanism started by reduction of the alkyl bromide by the light-excited gold photocatalyst under the formation of an alkyl radical (**317**) (Scheme 93). This alkyl radical then added to

Scheme 93. Proposed Reaction Mechanism for the Alkylative Semipinacol Rearrangement of TMS-Protected α-Styrenyl Substituted Cyclic Alcohols

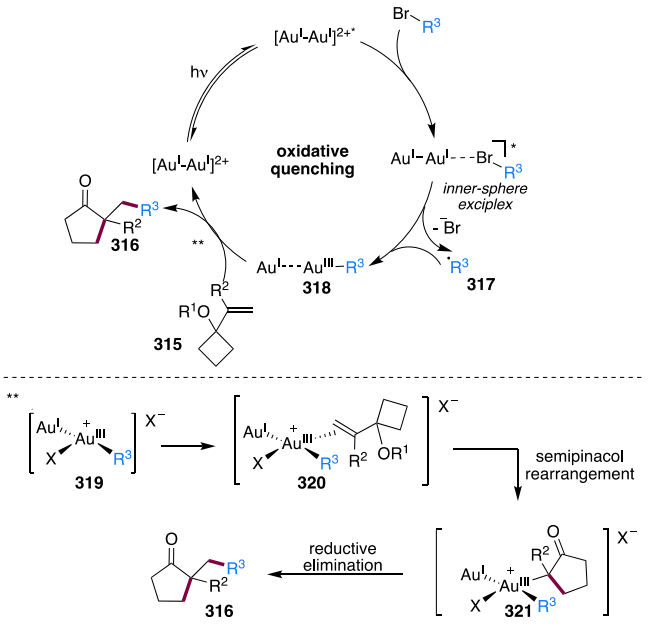

the gold catalyst to form intermediate **318**, and subsequent π-coordination triggered the semipinacol rearrangement to species **321**. Final reductive elimination produced the cyclic ketones (**316**) under regeneration of the gold catalyst. The author hypothesized that DABCO might be a resuscitator of the $[Au^{I}–Au^{II}]^{3+}$ intermediate. On the basis of kinetic studies and quenching experiments, DABCO could also promote a reductive quenching process. Because of the huge difference in applied equivalents, alkyl bromide would undergo a quenching process more frequently.

A further application of the dimeric gold(I) photocatalyst described by Barriault et al. was the diversification of isonitriles.[213] At first, the attention was dedicated to the synthesis of diverse phenanthridines (**323**) under the optimized reaction conditions by applying Na_2CO_3 and a substoichiometric amount of DABCO (Scheme 94). The conversion of primary bromoalkanes delivered the desired products in yields of 33−83% (e.g., **323a**), compounds with secondary (e.g., **323b** and **323c**) or tertiary (e.g., **323d**) alkyl bromides afforded the corresponding products with increased yields of 64% to quantitative. Variation of the substituents on the isonitrile showed that a change in electronic properties on the "right hand ring" (R^2) did not influence the reaction outcome (in comparison, **323e** and **323f**). However, substitutions on the "left hand ring" (R^1) were very sensitive when $R^1 \neq H$ photodegradation was detected. The only exception was a chloro-substituent giving **323h** in 63% yield.

In the same protocol, the authors elegantly applied this method to the synthesis of amides (**325**) from isonitriles (**324**) with a small quantity of water (21 equiv.) (Scheme 95).

Scheme 95. Synthesis of Amides from Isonitriles and Alkyl Bromides

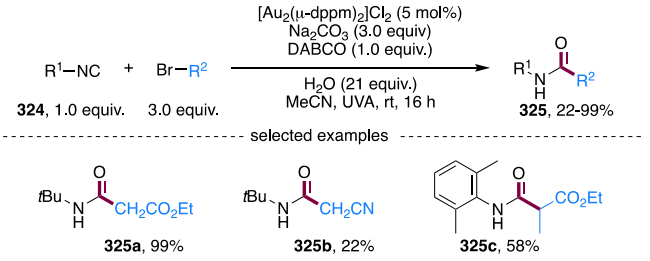

The mechanistic proposal for these transformations was in accordance to the previously described pathways (Scheme 96); a reduction of alkyl bromide to alkyl radical (**326**) through an

Scheme 94. Synthesis of Phenanthridines from Isonitriles and Alkyl Bromides

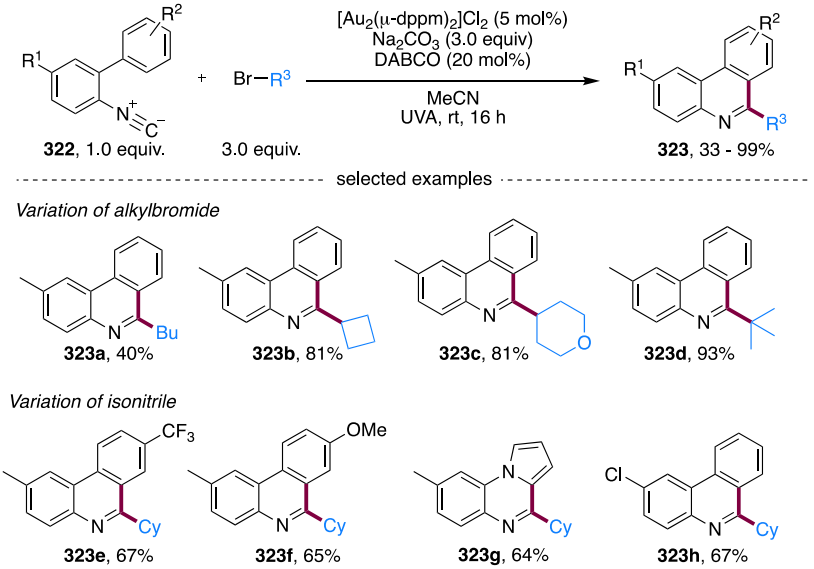

https://dx.doi.org/10.1021/acs.chemrev.0c00841
Chem. Rev. XXXX, XXX, XXX−XXX

Scheme 96. Mechanism of Amide and Phenanthridine Formation from Isonitriles

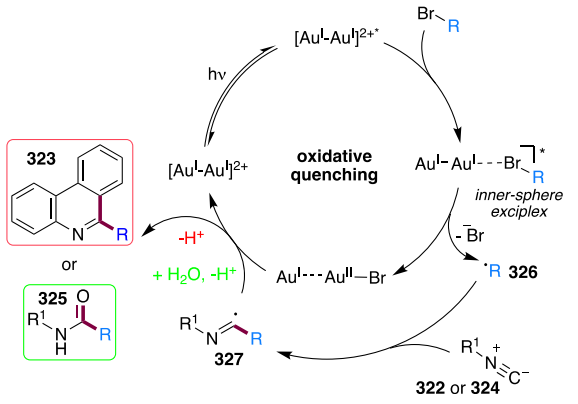

inner-sphere exciplex. In a next step, the radical reacted with isonitriles (**322** or **324**), forming the sp^2-hybridized imidoyl radical **327** (Shono and Saegusa previously showed the feasibility of radical addition to isonitriles to form imidoyl radicals).[214,215] Depending on the isonitrile substrate, two different pathways could be opened up. The formation of a phenanthridine (**323**) resulted from a cyclization of the imidoyl radical to form cyclohexadienyl radical, followed by oxidation by $[Au_2(\mu\text{-dppm})_2]^{3+}$ to regenerate the gold catalyst (red). A second path would be the direct interaction of the imidoyl radical with the gold intermediate to complete the catalytic cycle under formation of the corresponding imidoyl cation (green). The latter was then trapped by water and thus hydrolyzed to form the amide **325**.

The group of Chan developed the regioselective C1-alkynylation of *N*-alkyl-1,2,3,4-tetrahydroisoquinolines (THIQs, **328**) by bromoalkynes (**329**) by employing the dinuclear gold(I) complex and UV-light irradiation (Scheme 97).[216] A series of alkynylated THIQs **330** were obtained in a good functional group tolerance, with yields ranging from 19 to 89%. In general, electron-rich substitutions on both alkyne and THIQs were significantly more compatible than electron-poor. Further, cycloalkylethynyl bromides did not give satisfactory results (**330d**).

To determine whether the reaction pathway proceeded via an oxidative or a reductive quenching pathway, the authors conducted control experiments using a different ratio of both possible quenchers for the excited photocatalyst, THIQ (**328**) or bromoalkyne (**329**). In the optimized reaction, 4.0 equiv. of THIQ were used. By applying equimolar amounts of both gave the product (32%), however, with the recovery of the bromoalkyne (31%). The employment of iodoalkyne instead of bromoalkyne led to a complete conversion, albeit with a low yield of the desired product (11%). On the basis of these results and in combination with the proposed mechanism for the alkynylation of acyclic amines by iodoalkynes (Scheme 77),[176] the authors suggested a reductive quenching pathway to be prominent (Scheme 98). The excited gold(I) catalyst was reduced by THIQ (**328**) to give the nitrogen centered radical cation **331** and $[Au^I—Au^0]^{1+}$. The catalytic cycle was closed by a second SET with bromoalkyne (**329**) to produce an alkynyl radical (**333**). Radical−radical recombination furnished the desired alkynylated product (**330**). The excellent regioselectivity was reasoned by the better radical stability of **332** compared to other optional intermediates such as **334**. To more distinctly determine the occurring pathways, a fluorescence quenching experiment with each of the substrates was conducted and provided the corresponding quenching kinetics.

At this juncture, the dinuclear gold(I) catalyst, $[Au_2(\mu\text{-dppm})_2]^{2+}$, was always excited by UVA light (or sunlight, which also contains the wavelengths of UVA light) and therefore prone to reduce the C−Br bond of alkyl bromides. The group of Hashmi found that a bathochromic red shift of absorption can be achieved on the grounds of an associate formation of the dinuclear gold catalyst and a ligand (Ph_3P or mercaptans).[217] Further, this associate was then assumed to undergo a ligand-to-metal charge transfer (LMCT) whereby a thiyl radical was formed.[218−221] On this basis, the authors developed a C−C coupling by using mercaptans (**337**) to provide electron-deficient alkyl radical precursors which added to styrenes (**336**) under blue LED light irradiation (Scheme

Scheme 97. C1-Slkynylation of THIQ by Bromoalkynes Using the Dinuclear Gold(I) Photocatalyst

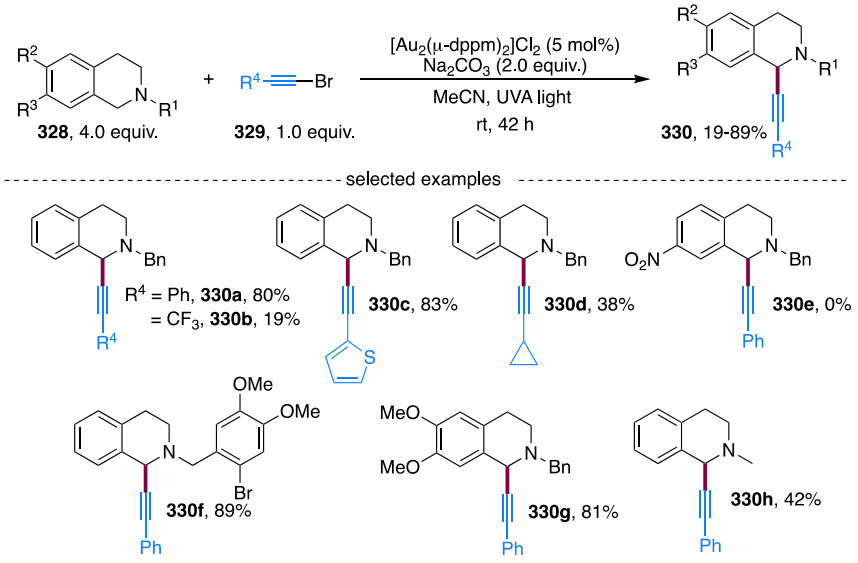

https://dx.doi.org/10.1021/acs.chemrev.0c00841
Chem. Rev. XXXX, XXX, XXX−XXX

Scheme 98. Tentative Reaction Mechanism for the Alkynylation of THIQs

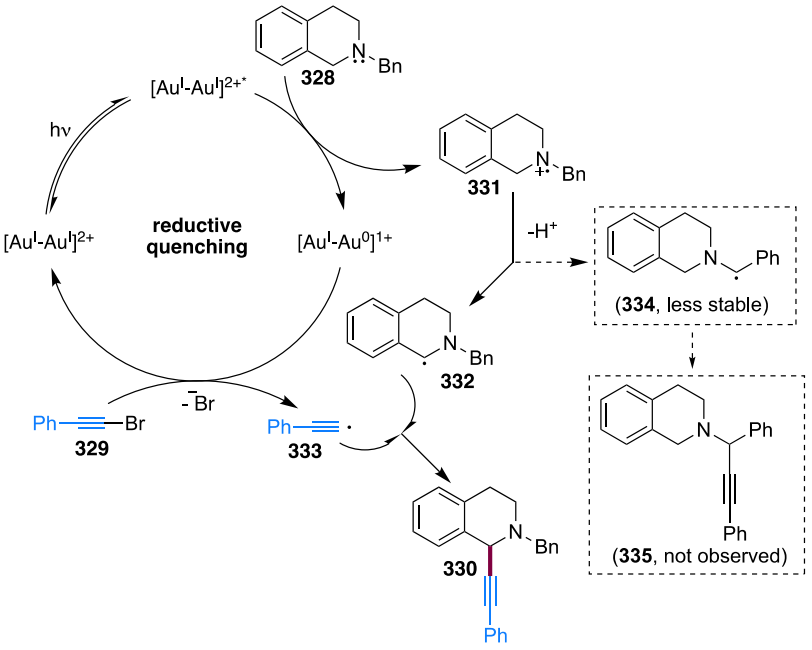

Scheme 99. Selected Examples of the Desulfurizing C−C Coupling of Mercaptans and Styrenes

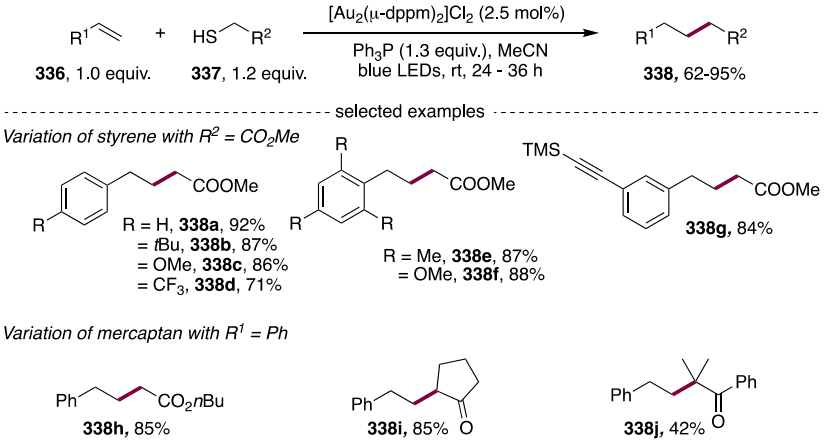

99). The optimal reaction conditions consisted of 2.5 mol % of $[Au_2(\mu\text{-dppm})_2]Cl_2$ and 1.3 equiv. of Ph_3P in MeCN in the presence of blue LEDs. In the absence of either phosphorus, light, or photocatalyst, the reaction did not proceed; also, under thermal conditions (55 °C), no product was obtained. A diverse set of styrenes and mercaptans were evaluated to afford the corresponding desulfurized C−C coupled products in excellent yields of 62−95%. Electron-deficient substituents on the styrene (e.g., **338d**) were tolerated as well as the electron-rich pendants (e.g., **338c**). Further, TMS-protected alkynes (**338g**), as well as *o*-, *m*-, and *p*-substitutions (**338e**, **338f**) were well compatible. With regard to the mercaptans, primary (e.g., **338h**) and secondary mercaptans (e.g., **338i**) were converted in very good yields; a tertiary mercaptan, however, was only obtained in decreased yield (e.g., **338j**).

To demonstrate the versatility of this method, the authors succeeded in modifying a sulfur-containing amino acid exhibiting a free N−H group (**340**, **341**) (Scheme 100A). In addition, polymer **344** was synthesized according to this novel desulfurizing C−C coupling method (Scheme 100B).

As aforementioned, the mechanism was catalyzed by a combination of the dinuclear gold(I) catalyst with mercaptan or a combination of $[Au_2(\mu\text{-dppm})_2]^{2+}$, Ph_3P, and mercaptan (Scheme 101). Upon irradiation with blue LEDs, the associate was excited and a subsequent LMCT delivered radical cation **345**. The latter reacted with Ph_3P to generate *P*-centered radical **346**, which underwent a radical addition to styrene (**336a**) via a β-scission to afford benzyl radical **348**. After hydrogen abstraction from thiol (**337a**), the desired desulfurized product (**338a**) was delivered under formation of a thiol radical (**349**). The reduced gold catalyst was recovered either by reducing radical **348** to its anion (**350**) or by being oxidized by a trace amount of O_2. A quantum yield of 0.20 did not point to a radical chain.

3.2. Energy Transfer Reactions

From a mechanistic point of view, all of the developed methods so far involved a SET with the excited dinuclear gold(I) catalyst to either its reduced or oxidized form. The utility of the dinuclear gold(I) complex in energy transfer reactions was recently reported by Hashmi and co-workers

https://dx.doi.org/10.1021/acs.chemrev.0c00841
Chem. Rev. XXXX, XXX, XXX−XXX

Scheme 100. Application of the Desulfurizing Method to (A) Modification of an Amino Acid and (B) in Polymer Synthesis

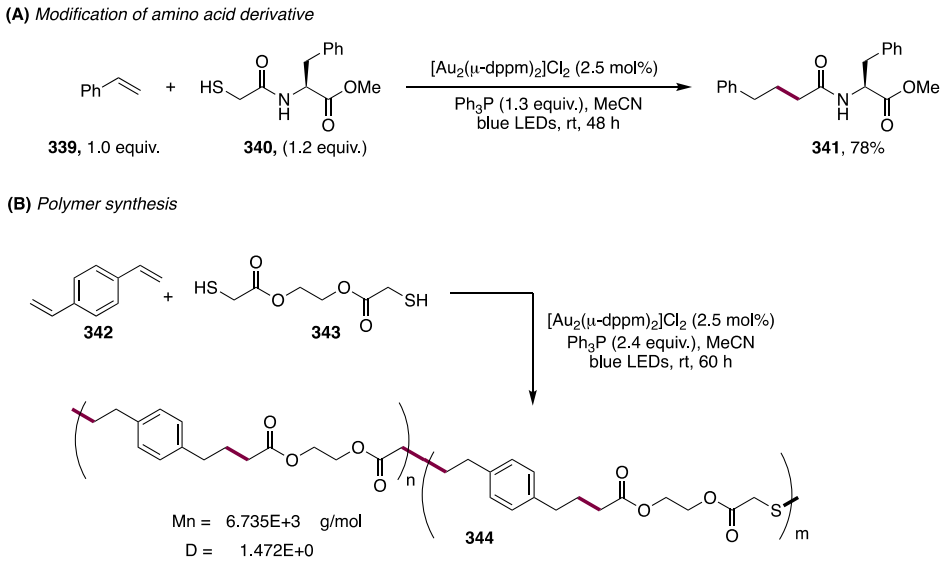

Scheme 101. Proposed Mechanism for the Reductive Desulfurization Reaction

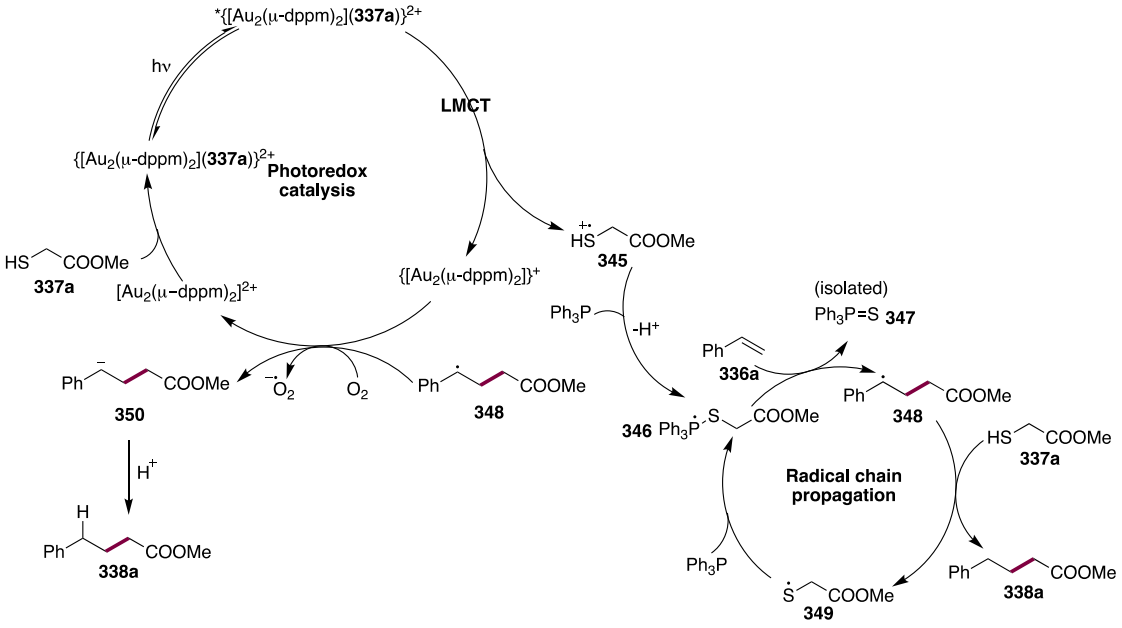

using aryl iodide compounds of type **351** for the synthesis of *gem*-diboronate building blocks **352** (Scheme 102).[222] The reaction merely proceeded by using 1.0 mol % of $[Au_2(\mu\text{-dppm})_2]^{2+}$ and 50 mol % of Na_2CO_3 under light irradiation (entries 1−4). The counteranion of the dinuclear gold(I) also seemed to influence the reaction outcome, while chloride gave 70% of the desired product **352a** and triflate yielded 90% (entry 5). Interestingly, by applying CFL light or UVA light, both had a detrimental effect on the product formation (entries 6−7). A broad reaction scope was demonstrated by chemoselectively accessing various *gem*-diboronate benzofurans, benzothiophene, and indoles in very good yields of 60−90%. Terminal or alkyl-substituted alkynes (R^2), variations in the backbone of the arene (R^1) as well as substitutions in the propargylic moiety (R^3) were all tolerated. A scale up to 1 and 10 g gave **352a** in 89 and 65%, respectively.

These unknown *gem*-diboronate compounds were shown to function as versatile building blocks for further functionalization also in drug and polymer synthesis. Just to name a few examples, **353**−**356** were delivered in moderate to excellent yields under various conditions (Scheme 103). Additionally, compound **357** functioned as a building block for the synthesis of an approved drug, Sertaconazole **360**.

The mechanistic investigations were initiated by UV/vis absorption measurements, indicating that neither the gold(I) catalyst nor the aryl iodide absorbed the light of the employed blue LEDs. Interestingly, by mixing the additional base Na_2CO_3 and $[Au_2(\mu\text{-dppm})_2](OTf)_2$, a new signal in ^{31}P NMR spectroscopy was detected, which was shown to be an aggregate absorbing the light of the blue LEDs, thus acting as the actual photosensitizer in this system. Unfortunately, direct isolation attempts of this associate failed, which should be focused on in the future to further exploit this novel reactivity

https://dx.doi.org/10.1021/acs.chemrev.0c00841
Chem. Rev. XXXX, XXX, XXX−XXX

Scheme 102. Scope of Radical Carbocyclization and *gem*-Diborylation Cascade Reaction

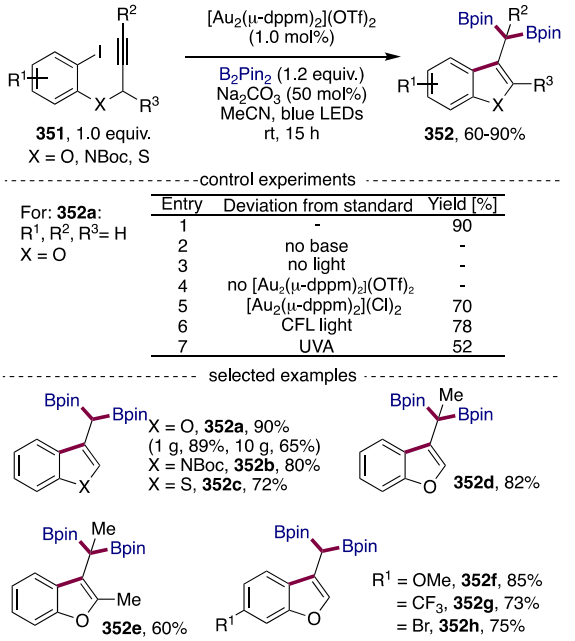

pattern of gold for fruitful transformations. Quantum yield measurements (Φ = 0.35) indicated the absence of a radical chain process. An energy transfer (EnT) reaction[223] was underlined by a direct excitation experiment without the gold photocatalyst and a wavelength of 254 nm. Here, the desired product (**352a**) was obtained in 30% yield.[224] All of the performed studies converged to imply that the combination of the dinuclear gold(I) catalyst and Na_2CO_3 in MeCN formed a novel associate complex (**361**), which was excited by blue LED light irradiation (**361***). As a next step, the energy was transferred on the aryl iodide (**351a**), which led to an excited triplet state (**351a***) under completion of the catalytic cycle (Scheme 104). Subsequently, a homolytic cleavage of the

Scheme 104. Proposed Energy Transfer Mechanism for the Carbocyclization/*gem*-Diborylation of Aryl Iodide Compound 351a

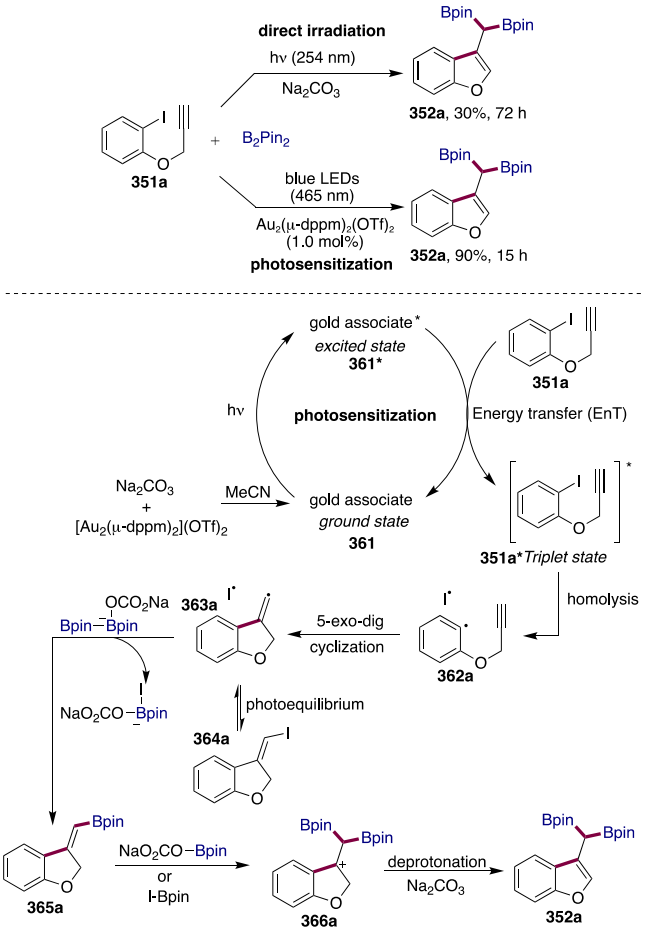

C_{aryl}–I bond occurred providing radical intermediate **362a**, which was followed by a 5-*exo-dig* cyclization affording vinyl

Scheme 103. Further Functionalization of *gem*-Diboronate Compounds

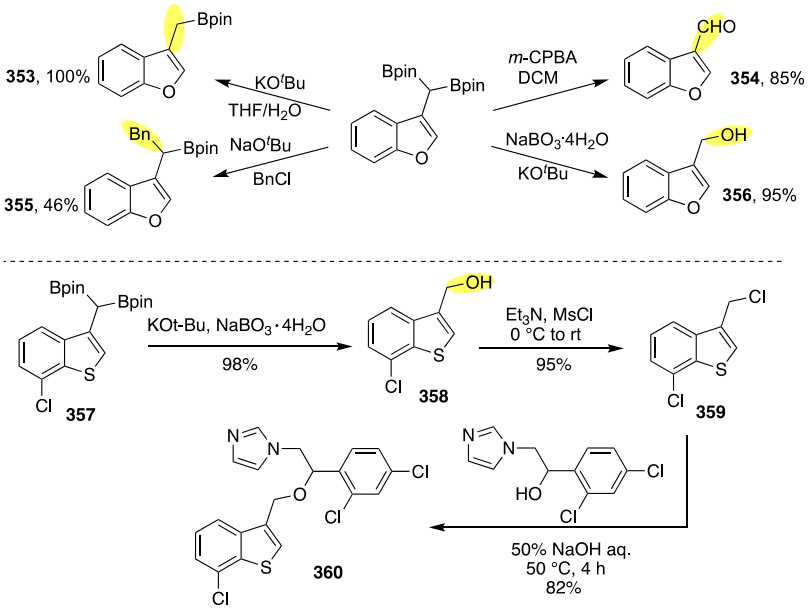

https://dx.doi.org/10.1021/acs.chemrev.0c00841
Chem. Rev. XXXX, XXX, XXX−XXX

Scheme 105. C−H Acetalization of Saturated Heterocycles

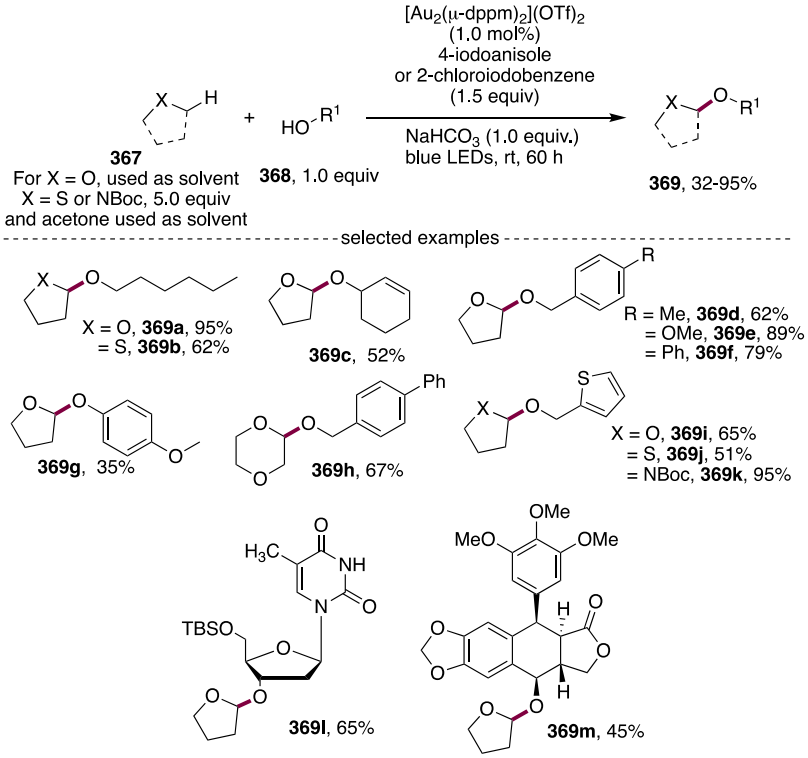

Scheme 106. Postulated Mechanism for the C−H Acetalization of Heterocyclic Ethers

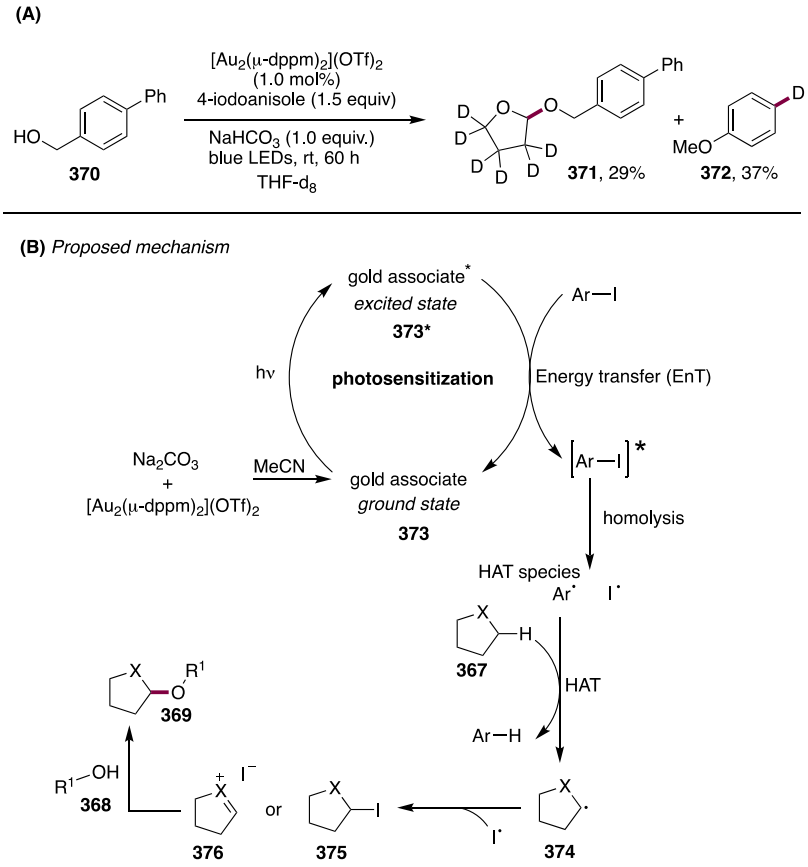

radical **363a** in high regioselectivity. This vinyl radical was proposed to exist in an equilibrium with its recombined vinyl iodide **364a**, which was demonstrated to undergo homolytic cleavage under excitation. The base Na_2CO_3 also acted as an activator to trigger the consecutive borylations forming **366a**. Then final *β*-H elimination delivered the final *gem*-diboronate

https://dx.doi.org/10.1021/acs.chemrev.0c00841
Chem. Rev. XXXX, XXX, XXX−XXX

product (**352a**). It is important to mention that during an energy transfer, the oxidation state of the gold metal center does not change!

After demonstrating the feasibility of an energy transfer reaction by using the dinuclear gold(I) catalyst, the Hashmi group exploited this promising technique further and disclosed a C(sp^3)−H acetalization of saturated heterocycles (**367**) (Scheme 105).[225] Acetals derived from cyclic ethers are highly applicable motifs[226,227] and can be found in several drugs (e.g., epirubicin, streptomycin). Herein, diverse alcohols for the acetalization of ethers were examined and further expanded to thioethers and amides. Primary and secondary alcohols, could be converted in moderate to excellent yields (32−95%). Notably, the less nucleophilic phenol could also be converted (**369g**), albeit in low yield of 35%. For the acetalization of thioethers and amides, a different sacrificial iodoarene, 2-chloroiobenzene, was observed to have a positive influence on the reaction outcome. Additionally, this method was beautifully applied for late-stage functionalization of bioactive molecules, exemplified in Scheme 105. A nucleoside derivative **369l** was obtained in 65% yield and podophyllotoxin **369m** in 45%.

Unlike in the previously described methodology, the reactant itself did not participate directly in the excited-state energy transfer process; instead, sacrificial 4-iodoanisole (or 2-chloroidodobenzene) took this role. An array of mechanistic experiments were performed. Among these, a reaction in deuterated THF, whereby the corresponding product (**371**) was obtained in a low yield, however, more importantly, deuterated anisole (**372**) was isolated in 37% yield (Scheme 106A). This distinctly showed the existence of a hydrogen atom transfer (HAT) reaction from the saturated heterocycle. Further, it was demonstrated that the alcohol was not participating in the radical formation process and a radical chain mechanism was excluded by quantum yield measurements (Φ = 0.14). The postulated mechanism started with the associate formation of $[Au_2(\mu\text{-dppm})_2](OTf)_2$ and $NaHCO_3$, which was excited by blue LED irradiation (Scheme 106B). A subsequent energy transfer from the excited associate (**373***) to aryl iodide triggered a homolytic cleavage to obtain an aryl and iodo radical. The aryl radical was trapped by the α-H of the ether by a HAT process to form radical **374**, which either recombined with the iodo radical (**375**) or was oxidized to an oxocarbenium ion (**376**). The last step was a known literature process,[228−231] the attack of an alcohol to α-halogenated ethers to form the corresponding acetals (**369**).

4. GOLD(III) COMPLEXES AS PHOTOSENSITIZERS

4.1. Homogeneous Applications

In general, luminescent gold(III) complexes are thoroughly studied due to their high applicability in medicine[232−235] and optoelectronic devices[160,236−239] but rarely found in photocatalysis.[240] Compared to gold(I) complexes,[241−243] the luminescence of gold(III) complexes is less favorable because the lower-lying dσ* ($d_{x^2-y^2}$) state could lead to a more effective luminescence quenching.[244] Nevertheless, the incorporation of a strong σ-donating ligand (such as acetylide or NHC) to gold(III) complexes raises the energy of the nonemissive d−d states, which in turn leads to a favored population of the emissive states, thus efficiently solving this problem. The group of Che et al. demonstrated that a *N*-heterocyclic carbene (NHC) ligand successfully increased the luminescence efficiency of a gold(III) complex, gold complex **377** (Figure 3).[245] This gold(III) complex (**377**) exhibits a long-lived (506 μs) and highly emissive triplet excited state in solution with a quantum yield of 0.114 (in comparison: quantum yield of $[Au_2(\mu\text{-dppm})_2]^{2+}$: Φ = 0.23).[56]

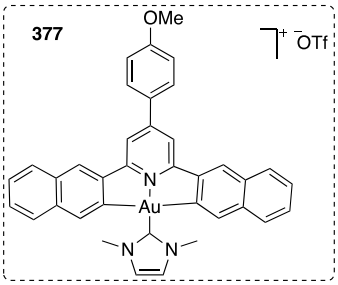

Figure 3. Structure of gold(III) NHC complex used as a photosensitizer.

The fact that such a gold(III) complex featured these characteristics in solution made this complex rather unique and offered a possibility to act as a photosensitizer in homogeneous gold catalysis. Cyclic voltammogram measurements revealed its powerful oxidation potential of 0.75 V vs Cp_2Fe (1.43 vs NHE). To test the photocatalytic ability of **377**, two benchmark reactions were chosen, first the oxidation of secondary amines (**378**) to imines (**379**) and second the oxidative cyanation of tertiary amines (**380**) (Scheme 107).

Scheme 107. (A) Oxidation of Secondary Amines and (B) the Oxidative Cyanation of Tertiary Amines Catalyzed by the Gold(III) Photosensitizer

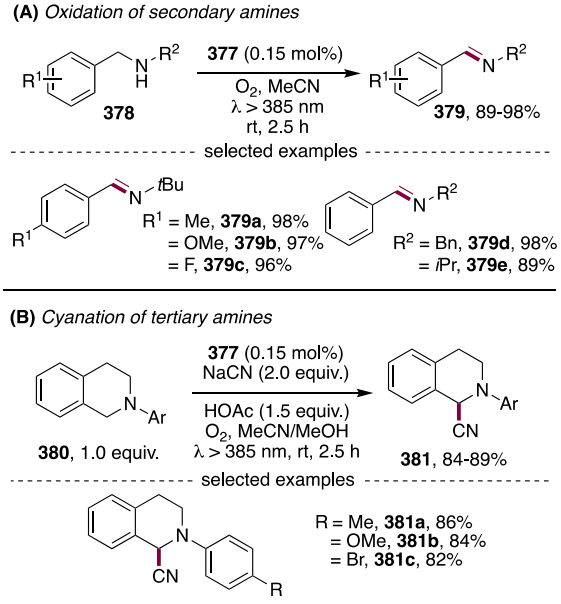

Remarkably, in the presence of oxygen, **377** was found to efficiently catalyze the oxidation with full conversion and delivered the corresponding imines (**379**) with diverse functional groups in yields ranging from 89% to 98% with only 0.15 mol % of the catalyst (Scheme 107A). The authors stated that the oxidation was driven by singlet oxygen, which was produced by harvesting the triplet state of the light-excited gold(III) catalyst. The oxidative cyanation of tertiary amines (**380**) proceeded with the use of sodium cyanate and acetic

https://dx.doi.org/10.1021/acs.chemrev.0c00841
Chem. Rev. XXXX, XXX, XXX−XXX

acid and gave the corresponding products (**381**) with good functional group compatibility (Scheme 107B).

A subsequent work by Zhu and co-workers achieved the aerobic oxidative cross-dehydrogenative coupling of *N*-aryltetrahydroisoquinolines (**383**) with various nucleophiles enabled by a gold(III) photocatalyst (**382**) (Scheme 108A).[246]

Scheme 108. (A) Gold(III) Photocatalyst and (B) the Oxidative Coupling of Ketones

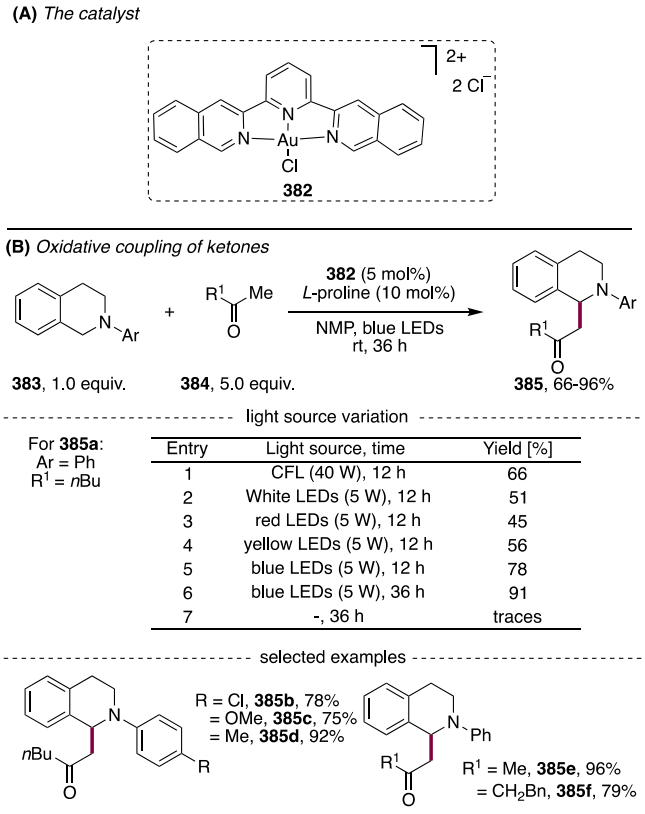

Entry	Light source, time	Yield [%]
1	CFL (40 W), 12 h	66
2	White LEDs (5 W), 12 h	51
3	red LEDs (5 W), 12 h	45
4	yellow LEDs (5 W), 12 h	56
5	blue LEDs (5 W), 12 h	78
6	blue LEDs (5 W), 36 h	91
7	-, 36 h	traces

At first, the oxidative coupling of ketones was studied (Scheme 108B). Interestingly, L-proline was found to have a positive effect on the reaction, however, the reason for this was not mentioned. The process worked in every tested light source, but the remarkable yield of 91% was only obtained with blue LEDs and a reaction time of 36 h (entries 1−6). A control experiment in the absence of light paralyzed the product formation (entry 7). A variety of different ketones, as well as different substituents in the *N*-aryl backbone, were studied and delivered the corresponding products **385** in excellent yields.

This method was also applied for cyclic ketones and malonates in satisfying yields. In addition, the versatility of this protocol was demonstrated by utilizing phosphine oxides and phosphites for an oxidative C−P coupling of amines (**386**) (Scheme 109). A clear mechanistic understanding of this photocatalytic event would benefit the future catalyst and methodology development.

The oxidation of secondary amines to imines was also used by Venkatesan et al. as a benchmark reaction to test the photocatalytic ability of cationic bidentate gold(III) complexes (Scheme 110).[247] Among several other tested gold(III) complexes, complexes **391** and **392** performed best. While for sterically more bulky substituents for R^1 full conversion was detected using **391** (entries 1 and 3), gold(III) complex **392** only converted the secondary amines with 72% and 53%,

Scheme 109. Oxidative C−P Coupling of Amines and Phosphine Oxides and Phosphites

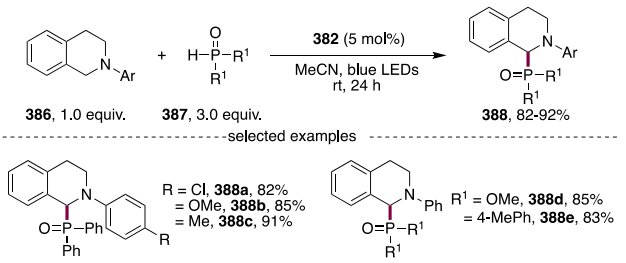

Scheme 110. Oxidation of Secondary Amines to Imines by Venkatesan et al.

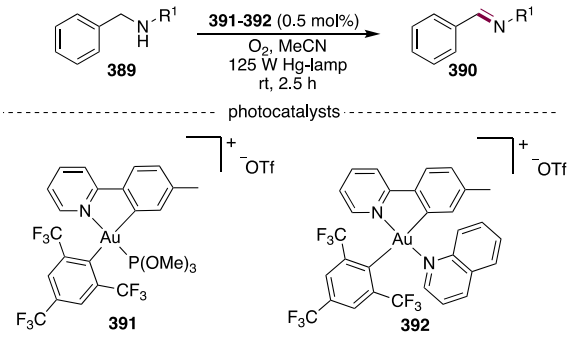

Entry	Catalyst	R^1	Conversion [%]
1	**391**	*t*Bu	100
2	**392**	*t*Bu	72
3	**391**	Bn	100
4	**392**	Bn	53
5	**391**	*i*Pr	12
6	**392**	*i*Pr	8
7	**391**	Me	2
8	**392**	Me	-

respectively (entries 2 and 4). Isopropyl or methyl substituents did not give satisfactory results (entries 4−8), which was attributed to the radical stability. However, the gold(III) NHC complex **377**, developed by the group of Che, delivered also the sterically less hindered imines in excellent yield (compare **379e**, Scheme 107, using *i*Pr).

4.2. Heterogeneous Applications

Metal−organic framework (MOF) composited with luminescent gold(III) complexes were also applied as heterogeneous photosensitizers. The research group of Che tested the photocatalytic activity of four different luminescent gold(III) complexes in different types of MOFs.[248] One of the most common test reactions in this realm is the oxidation of secondary amines to imines and thus will be further discussed herein based on best performing gold(III) complex **395** (Scheme 111). The considered metal organic framework mainly consisted of a cadmium salt, 3,3′,3′′-((1,3,5-triazine-2,4,6-triyl)tris(azanediyl) and DMF, for simplification called MOF1. For the oxidation of **393**, the encapsulated gold(III) complex **395** in MOF1 (**395**@MOF1) (1.70 wt % **395**), a turnover number of 692 could be achieved, while the free gold(III) complex in solution (homogeneously) did not exceed a turnover number of 390. By using MOF1 without gold, only traces of the imine could be detected. The **395**@MOF1 also exhibited a longer photoactivity with only small variations after 10 h compared to a significant decrease after 2 h of the free gold(III) catalyst. Interestingly, a substrate size-selectivity

https://dx.doi.org/10.1021/acs.chemrev.0c00841
Chem. Rev. XXXX, XXX, XXX−XXX

Scheme 111. Comparison of 395@MOF1 and Free Gold(III) Complex as Photosensitizer

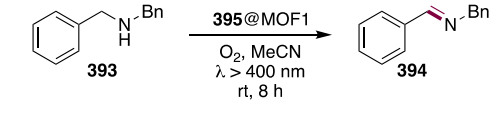

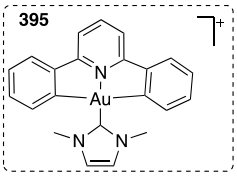

Entry	Catalyst	Turnover #
1	free **395**	390
2	**395**@MOF1	693

experiment of **395**@MOF1 and free **395** showed that for the free **395** catalyst, the reaction proceeded without selectivity (1:1). However, the more bulky substrates were not converted by the MOF. This clearly showed that the reaction mainly occurred in the channels of the MOF framework. Further, ICP measurements revealed nearly the same content of gold in the **395**@MOF1 sample before and after photocatalysis.

Even higher turnover numbers for this benchmark reaction were reached by Su and co-workers by using the same luminescent gold(III) complex (**395**, Scheme 111), however, a different host structure.[249] To test the photocatalytic activity, the authors also chose the oxidation of secondary amines to imines. In this case, the best performing MOF was based on $InCl_3$ and 1,3,5-tris(4-carboxy-phenyl)benzene (called ZJU-28) (Scheme 112). The results were compared with the free

Scheme 112. Photocatalytic Oxidation of Secondary Amine to Imine with Different Heterogeneous and Homogeneous Photosensitizers

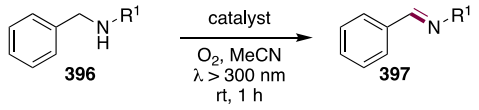

R^1 = *t*Bu		R^1 = Bn	
Catalyst	Turnover #	Catalyst	Turnover #
free **395**	453	free **395**	322
395@MOF2	75	**395**@MOF2	31
395@ZJU-28	1548	**395**@ZJU-28	1122

homogeneous catalyst **395** and another gold(III) encapsulated MOF consisting of a cadmium salt and 2,4,6-tris(2,5-dicarboxyl-phenylamino)-1,3,5-triazine (MOF2). Notably, the homogeneous gold(III) catalyst (**395**) performed better than the **395**@MOF2. The **395**@ZJU-28 metal−organic framework overall achieved the best turnover numbers of over a 1000. To compare the results provided by Su even better with the previous findings of Che, the attention has to be drawn to the benzyl substituent. One can distinctly quote from the tables that the **395**@ZJU-28 MOF overall gave the best results. This was a great enhancement in the photocatalytic activity of MOFs composited with luminescent gold(III) complexes.

The reason for the significant difference in photocatalytic activity of both MOFs might be due to the different host structures and thus exhibiting varying pore sizes. With larger pore sizes, more sterically hindered substrates can, literally speaking, enter the channel to the reactive gold(III) sites. This was further highlighted by a size-selective experiment (Scheme 113). By applying equal amounts of substrate **398** and **399**, the

Scheme 113. Size-Selective Oxidation of 398 and 399

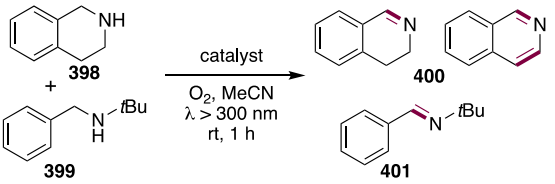

Catalyst	Yield ratio of **400**:**401**
free **395**	≈ 1:1
395@MOF2	≈ 38:1
395@ZJU-28	≈ 1.9:1

three observed catalysts delivered the expected results. While **395**@ZJU-28 gave the two products **400** and **401** in a ratio of 1.9:1, the other heterogeneous photocatalyst **395**@MOF2 with comparably smaller pore sizes demonstrated a high selectivity toward product **400**. Knowing this, the different luminescent gold(III) complexes could be encapsulated in MOFs with appropriate pore size to achieve the desired reactions selectively. Important to note, the heterogeneous photocatalyst **395**@ZJU-28 did not only catalyze the oxidation of secondary amines better than other heterogeneous catalysts but also than the free gold(III) catalyst in solution, homogeneously.

5. SUMMARY AND OUTLOOK

Combining homogeneous gold catalysis and light opens up fascinating possibilities for organic synthesis. All of these elegant methods have one thing in common, achieving the difficult valence change of gold under very mild conditions by avoiding the use of strong external oxidants. One segment of this research field is dominated by the use of mononuclear gold(I) catalysts in combination with a photosensitizer. Remarkably, these transformations could also successfully be catalyzed by the sole use of a gold catalyst or, in a few cases, by applying diazonium salts or diazonium derivatives which themselves absorb light. The second segment includes light-absorbing dinuclear gold(I) photocatalyst in combination with UVA light, a versatile method to generate radical intermediates from unactivated alkyl, vinyl, and aryl bromides. Here either oxidative quenching or reductive quenching represent mechanistic possibilities, different from the dominance of oxidative quenching in the case of the mononuclear gold(I) catalysts. First remarkable examples also indicated the feasibility of an energy transfer reaction (EnT), rather than an electron transfer. This was achieved by the in situ formation of an aggregate of a gold complex and a coordinating ligand or base, which acted as the novel photosensitizer. The third segment covers rare examples of the application of luminescent gold(III) complexes in photocatalysis, homogeneously or heterogeneously encapsulated in metalorganic frameworks.

Despite the significant number of exceptional applications in the rapidly growing field of gold photocatalysis presented in this review, some limitations and scientific problems remained and should be approached in the future:

(1) The in-depth mechanistic study of the reaction involving mononuclear gold(I) complexes (especially in the absence of a photosensitizer) and aryldiazonium salts. This would help to gain a better understanding of the distinct role of gold in these transformations and could help to design fluorescent mono- and poly-LAu(I)-X

https://dx.doi.org/10.1021/acs.chemrev.0c00841
Chem. Rev. XXXX, XXX, XXX−XXX

complexes. Subsequently, the strongest limitation of mononuclear gold(I)-mediated photoreactions, the restriction to the use of aryldiazonium salts for the vast majority should be addressed. To broaden the spectrum of reagents, one aim should be the use of cheap and commercially abundant aryl halides, which would open a new window of opportunity in gold photocatalysis.

(2) The isolation or characterization of the gold aggregate enabling the possibility of an EnT, should be in the focus of future studies. This would help the development of new gold-based photocatalysts leading to new promising synthetic applications.

(3) Even though luminescent gold(III) complexes have been thoroughly studied, their application in photocatalysis was massively neglected. The few known examples could provide the basis for the synthesis and discovery of a new generation of fluorescent gold(III) photocatalysts. Their photocatalytic application to H_2-production, CO_2-reduction, and novel organic transformations could be envisioned.

(4) Since the luminescence properties of Ph_3PAuCl was first disclosed in 1970,[241] a growing number of mono-, di-, and polynuclear luminescent Au(I) complexes with different ligands have been reported. The closed-shell $5d^{10}$ electronic configuration of gold(I) is unique to involve aurophilic attraction between two gold centers, favoring the luminescence properties. This increases the attractiveness of these gold complexes in the family of luminescent metal complexes. Accordingly, the future exploration of these well-defined gold complexes in photocatalysis would be a nice addition to existing photochemical reactions.

(5) One can dream of the design of chiral gold photocatalysts for enantioselective transformations, in which the gold complex plays a dual role, π-activator and photosensitizer.

AUTHOR INFORMATION

Corresponding Author

Jin Xie − *State Key Laboratory of Coordination Chemistry, Jiangsu Key Laboratory of Advanced Organic Materials, Chemistry and Biomedicine Innovation Center (ChemBIC), School of Chemistry and Chemical Engineering, Nanjing University, Nanjing 210023, China;* orcid.org/0000-0003-2600-6139; Email: xie@nju.edu.cn

Authors

Sina Witzel − *Organisch-Chemisches Institut, Heidelberg University, 69120 Heidelberg, Germany*

A. Stephen K. Hashmi − *Organisch-Chemisches Institut, Heidelberg University, 69120 Heidelberg, Germany; Chemistry Department, Faculty of Science, King Abdulaziz University, Jeddah 21589, Saudi Arabia;* orcid.org/0000-0002-6720-8602

Complete contact information is available at: https://pubs.acs.org/10.1021/acs.chemrev.0c00841

Notes

The authors declare no competing financial interest.

Biographies

Sina Witzel studied chemistry at Heidelberg University, where she received her Bachelor degree in 2014. During her Master studies, she joined the group of Prof. R. Sarpong at the University of California at Berkeley as a research scholar. Her Master thesis was absolved with Prof. A. S. K. Hashmi in cooperation with the pharmaceutical company AbbVie. Since 2017, she is working with Prof. A. S. K. Hashmi as a Ph.D. student in the field of photoinduced gold-catalyzed cross-coupling reactions. In 2018, she completed a research stay with Prof. M. Tilset at the University of Oslo.

A. Stephen K. Hashmi studied chemistry at LMU Munich, where he obtained his diploma and Ph.D. with Prof. G. Szeimies in the field of nickel- and iron-catalyzed cross coupling of strained organic compounds. His postdoctorate with Prof. B. M. Trost at Stanford University covered transition metal-catalyzed enyne metathesis. After his habilitation on enantiomerically pure organopalladium compounds and palladium-catalyzed conversions of allenes with Prof. J. Mulzer at the FU Berlin, the JWG-University Frankfurt, and the University of Vienna, in 1998, he was awarded a Heisenberg fellowship of the DFG for a proposal on gold-catalyzed reactions for organic synthesis, a topic which still is a major focus of the group. The next stations were the University of Tasmania 1999, Marburg University 1999−2000, and in 2001, he was appointed Professor for Organic Chemistry at Stuttgart University, and since 2007 he is Full Professor for Organic Chemistry at Heidelberg University. In 2013−2019, he served as Vice Rector for Research and Transfer of Heidelberg University.

Jin Xie at Nanjing University was born in Chongqing, China, in 1985. He received his Bachelor degree from Northeast Forestry University in 2008, and a Ph.D. degree in 2013 from Nanjing University working under the direction of Prof. Chengjian Zhu. From 2014 until 2017, he was working as an advanced research associate in the group of Prof. A. S. K. Hashmi at Heidelberg University. In 2017, he came back to Nanjing University to start his independent career. His lab current research interest lies in radical chemistry and organometallic chemistry.

ACKNOWLEDGMENTS

S.W. acknowledges the financial support by the Landesgraduiertenförderung of the state of Baden-Württemberg. A.S.K.H. is grateful for support by the Deutsche Forschungsgemeinschaft (DFG, priority program SPP 2102). J.X. thanks the Fundamental Research Funds for the Central Universities (020514380214), the National Natural Science Foundation of China (21971108 and 21702098), and the Natural Science Foundation of Jiangsu Province (BK20190006), "Innovation & Entrepreneurship Talents Plan" of Jiangsu Province, and "Jiangsu Six Peak Talent Project" for financial support.

REFERENCES

(1) Dyker, G. An Eldorado for Homogeneous Catalysis? *Angew. Chem., Int. Ed.* **2000**, *39*, 4237−4239.
(2) Hashmi, A. S. K. Homogeneous Gold Catalysts and Alkynes: A Successful Liaison. *Gold Bull.* **2003**, *36*, 3−9.
(3) Hashmi, A. S. K. Homogeneous Catalysis by Gold. *Gold Bull.* **2004**, *37*, 51−65.
(4) Hashmi, A. S. K.; Hutchings, G. J. Gold Catalysis. *Angew. Chem., Int. Ed.* **2006**, *45*, 7896−7936.
(5) Fürstner, A.; Davies, P. W. Catalytic Carbophilic Activation: Catalysis by Platinum and Gold π-Acids. *Angew. Chem., Int. Ed.* **2007**, *46*, 3410−3449.
(6) Gorin, D. J.; Toste, F. D. Relativistic Effects in Homogeneous Gold Catalysis. *Nature* **2007**, *446*, 395−403.

(7) Hashmi, A. S. K. Gold-Catalyzed Organic Reactions. *Chem. Rev.* **2007**, *107*, 3180−3211.
(8) Arcadi, A. Alternative Synthetic Methods through New Developments in Catalysis by Gold. *Chem. Rev.* **2008**, *108*, 3266−3325.
(9) Hashmi, A. S. K.; Rudolph, M. Gold Catalysis in Total Synthesis. *Chem. Soc. Rev.* **2008**, *37*, 1766−1775.
(10) Jiménez-Núñez, E.; Echavarren, A. M. Gold-Catalyzed Cycloisomerizations of Enynes: A Mechanistic Perspective. *Chem. Rev.* **2008**, *108*, 3326−3350.
(11) Bandini, M. Gold-Catalyzed Decorations of Arenes and Heteroarenes with C-C Multiple Bonds. *Chem. Soc. Rev.* **2011**, *40*, 1358−1367.
(12) Corma, A.; Leyva-Pérez, A.; Sabater, M. J. Gold-Catalyzed Carbon-Heteroatom Bond-Forming Reactions. *Chem. Rev.* **2011**, *111*, 1657−1712.
(13) Hashmi, A. S. K. Gold-Catalyzed Organic Reactions. In *Inventing Reactions*; Gooßen, L. J., Ed.; Springer: Berlin, Heidelberg, 2013; pp 143−164.
(14) Braun, I.; Asiri, A. M.; Hashmi, A. S. K. Gold Catalysis 2.0. *ACS Catal.* **2013**, *3*, 1902−1907.
(15) Yang, W.; Hashmi, A. S. K. Mechanistic Insights into the Gold Chemistry of Allenes. *Chem. Soc. Rev.* **2014**, *43*, 2941−2955.
(16) Xie, J.; Pan, C.; Abdukader, A.; Zhu, C. Gold-Catalyzed C(sp^3)-H Bond Functionalization. *Chem. Soc. Rev.* **2014**, *43*, 5245−5256.
(17) Hashmi, A. S. K. Dual Gold Catalysis. *Acc. Chem. Res.* **2014**, *47*, 864−876.
(18) Zhang, L. A Non-Diazo Approach to α-Oxo Gold Carbenes via Gold-Catalyzed Alkyne Oxidation. *Acc. Chem. Res.* **2014**, *47*, 877−888.
(19) Zheng, Z.; Wang, Z.; Wang, Y.; Zhang, L. Au-Catalysed Oxidative Cyclisation. *Chem. Soc. Rev.* **2016**, *45*, 4448−4458.
(20) Pflästerer, D.; Hashmi, A. S. K. Gold Catalysis in Total Synthesis - Recent Achievements. *Chem. Soc. Rev.* **2016**, *45*, 1331−1367.
(21) Bratsch, S. G. Standard Electrode Potentials and Temperature Coefficients in Water at 298.15 K. *J. Phys. Chem. Ref. Data* **1989**, *18*, 1−21.
(22) Wang, W.; Jasinski, J.; Hammond, G. B.; Xu, B. Fluorine-Enabled Cationic Gold Catalysis: Functionalized Hydration of Alkynes. *Angew. Chem., Int. Ed.* **2010**, *49*, 7247−7252.
(23) Garcia, P.; Malacria, M.; Aubert, C.; Gandon, V.; Fensterbank, L. Gold-Catalyzed Cross-Couplings: New Opportunities for C-C Bond Formation. *ChemCatChem* **2010**, *2*, 493−497.
(24) Hopkinson, M. N.; Gee, A. D.; Gouverneur, V. Au^{I}/Au^{III} Catalysis: An Alternative Approach for C-C Oxidative Coupling. *Chem. - Eur. J.* **2011**, *17*, 8248−8262.
(25) Peng, Y.; Cui, L.; Zhang, G.; Zhang, L. Gold-Catalyzed Homogeneous Oxidative C-O Bond Formation: Efficient Synthesis of 1-Benzoxyvinyl Ketones. *J. Am. Chem. Soc.* **2009**, *131*, 5062−5063.
(26) Zhang, G.; Cui, L.; Wang, Y.; Zhang, L. Homogeneous Gold-Catalyzed Oxidative Carboheterofunctionalization of Alkenes. *J. Am. Chem. Soc.* **2010**, *132*, 1474−1475.
(27) Miró, J.; del Pozo, C. Fluorine and Gold: A Fruitful Partnership. *Chem. Rev.* **2016**, *116*, 11924−11966.
(28) Hashmi, A. S. K.; Ramamurthi, T. D.; Rominger, F. Synthesis, Structure and Reactivity of Organogold Compounds of Relevance to Homogeneous Gold Catalysis. *J. Organomet. Chem.* **2009**, *694*, 592−597.
(29) Trost, B. M. The Atom Economy-a Search for Synthetic Efficiency. *Science* **1991**, *254*, 1471.
(30) Trost, B. M. Atom Economy-A Challenge for Organic Synthesis: Homogeneous Catalysis Leads the Way. *Angew. Chem., Int. Ed. Engl.* **1995**, *34*, 259−281.
(31) Sheldon, R. A. Atom Efficiency and Catalysis in Organic Synthesis. *Pure Appl. Chem.* **2000**, *72*, 1233−1246.
(32) Roth, H. D. The Beginnings of Organic Photochemistry. *Angew. Chem., Int. Ed. Engl.* **1989**, *28*, 1193−1207.
(33) Ciamician, G. The Photochemistry of the Future. *Science* **1912**, *36*, 385−394.
(34) Prier, C. K.; Rankic, D. A.; MacMillan, D. W. C. Visible Light Photoredox Catalysis with Transition Metal Complexes: Applications in Organic Synthesis. *Chem. Rev.* **2013**, *113*, 5322−5363.
(35) Xie, J.; Jin, H.; Xu, P.; Zhu, C. When C-H Bond Functionalization Meets Visible-Light Photoredox Catalysis. *Tetrahedron Lett.* **2014**, *55*, 36−48.
(36) Zeitler, K. Photoredox Catalysis with Visible Light. *Angew. Chem., Int. Ed.* **2009**, *48*, 9785−9789.
(37) Skubi, K. L.; Blum, T. R.; Yoon, T. P. Dual Catalysis Strategies in Photochemical Synthesis. *Chem. Rev.* **2016**, *116*, 10035−10074.
(38) Teegardin, K.; Day, J. I.; Chan, J.; Weaver, J. Advances in Photocatalysis: A Microreview of Visible Light Mediated Ruthenium and Iridium Catalyzed Organic Transformations. *Org. Process Res. Dev.* **2016**, *20*, 1156−1163.
(39) Marzo, L.; Pagire, S. K.; Reiser, O.; König, B. Visible-Light Photocatalysis: Does It Make a Difference in Organic Synthesis? *Angew. Chem., Int. Ed.* **2018**, *57*, 10034−10072.
(40) Shon, J.-H.; Teets, T. S. Photocatalysis with Transition Metal Based Photosensitizers. *Comments Inorg. Chem.* **2020**, *40*, 53−85.
(41) Glaser, F.; Wenger, O. S. Recent Progress in the Development of Transition-Metal Based Photoredox Catalysts. *Coord. Chem. Rev.* **2020**, *405*, 213129.
(42) Romero, N. A.; Nicewicz, D. A. Organic Photoredox Catalysis. *Chem. Rev.* **2016**, *116*, 10075−10166.
(43) Wang, C.-S.; Dixneuf, P. H.; Soulé, J.-F. Photoredox Catalysis for Building C-C Bonds from C(sp^2)-H Bonds. *Chem. Rev.* **2018**, *118*, 7532−7585.
(44) Narayanam, J. M. R.; Stephenson, C. R. J. Visible Light Photoredox Catalysis: Applications in Organic Synthesis. *Chem. Soc. Rev.* **2011**, *40*, 102−113.
(45) Tucker, J. W.; Stephenson, C. R. J. Shining Light on Photoredox Catalysis: Theory and Synthetic Applications. *J. Org. Chem.* **2012**, *77*, 1617−1622.
(46) McAtee, R. C.; McClain, E. J.; Stephenson, C. R. J. Illuminating Photoredox Catalysis. *Trends in Chemistry* **2019**, *1*, 111−125.
(47) Martin, M. M.; Lindqvist, L. The pH Dependence of Fluorescein Fluorescence. *J. Lumin.* **1975**, *10*, 381−390.
(48) Shen, T.; Zhao, Z.-G.; Yu, Q.; Xu, H.-J. Photosensitized Reduction of Benzil by Heteroatom-Containing Anthracene Dyes. *J. Photochem. Photobiol., A* **1989**, *47*, 203−212.
(49) Angnes, R. A.; Li, Z.; Correia, C. R. D.; Hammond, G. B. Recent Synthetic Additions to the Visible Light Photoredox Catalysis Toolbox. *Org. Biomol. Chem.* **2015**, *13*, 9152−9167.
(50) Hopkinson, M. N.; Tlahuext-Aca, A.; Glorius, F. Merging Visible Light Photoredox and Gold Catalysis. *Acc. Chem. Res.* **2016**, *49*, 2261−2272.
(51) McCallum, T.; Rohe, S.; Barriault, L. Thieme Chemistry Journals Awardees − Where Are They Now? What's Golden: Recent Advances in Organic Transformations Using Photoredox Gold Catalysis. *Synlett* **2017**, *28*, 289−305.
(52) Zhang, M.; Zhu, C.; Ye, L.-W. Recent Advances in Dual Visible Light Photoredox and Gold-Catalyzed Reactions. *Synthesis* **2017**, *49*, 1150−1157.
(53) Zidan, M.; Rohe, S.; McCallum, T.; Barriault, L. Recent Advances in Mono and Binuclear Gold Photoredox Catalysis. *Catal. Sci. Technol.* **2018**, *8*, 6019−6028.
(54) Akram, M. O.; Banerjee, S.; Saswade, S. S.; Bedi, V.; Patil, N. T. Oxidant-free Oxidative Gold Catalysis: The New Paradigm in Cross-Coupling Reactions. *Chem. Commun.* **2018**, *54*, 11069−11083.
(55) Medina-Mercado, I.; Porcel, S. Insights into the Mechanism of Gold(I) Oxidation with Aryldiazonium Salts. *Chem. - Eur. J.* **2020**, *26*, 16206.
(56) Che, C.-M.; Kwong, H.-L.; Yam, V. W.-W.; Cho, K.-C. Spectroscopic Properties and Redox Chemistry of the Phosphorescent Excited State of $[Au_2(dppm)_2]^{2+}$[dppm = bis(diphenylphosphino)-methane]. *J. Chem. Soc., Chem. Commun.* **1989**, 885−886.

https://dx.doi.org/10.1021/acs.chemrev.0c00841
Chem. Rev. XXXX, XXX, XXX−XXX

(57) Li, D.; Che, C.-M.; Kwong, H.-L.; Yam, V. W.-W. Photo-induced C-C Bond Formation From Alkyl Halides Catalysed by Luminescent Dinuclear Gold(I) and Copper(I) Complexes. *J. Chem. Soc., Dalton Trans.* **1992**, 3325−3329.
(58) Schmidbaur, H.; Wohlleben, A.; Wagner, F.; Orama, O.; Huttner, G. Gold-Komplexe von Diphosphinomethanen, I. Synthese und Kristallstruktur zweikerniger Gold (I)-Verbindungen. *Chem. Ber.* **1977**, *110*, 1748−1754.
(59) Revol, G.; McCallum, T.; Morin, M.; Gagosz, F.; Barriault, L. Photoredox Transformations with Dimeric Gold Complexes. *Angew. Chem., Int. Ed.* **2013**, *52*, 13342−13345.
(60) Huang, L.; Rudolph, M.; Rominger, F.; Hashmi, A. S. K. Photosensitizer-Free Visible-Light-Mediated Gold-Catalyzed 1,2-Difunctionalization of Alkynes. *Angew. Chem., Int. Ed.* **2016**, *55*, 4808−4813.
(61) Nugent, W. A. Black Swan Events" in Organic Synthesis. *Angew. Chem., Int. Ed.* **2012**, *51*, 8936−8949.
(62) Fu, W.-F.; Chan, K.-C.; Miskowski, V. M.; Che, C.-M. The Intrinsic 3[dσ*pσ] Emission of Binuclear Gold(I) Complexes with Two Bridging Diphosphane Ligands Lies in the Near UV; Emissions in the Visible Region Are Due to Exciplexes. *Angew. Chem., Int. Ed.* **1999**, *38*, 2783−2785.
(63) Ma, C.; Chan, C. T.-L.; To, W.-P.; Kwok, W.-M.; Che, C.-M. Deciphering Photoluminescence Dynamics and Reactivity of the Luminescent Metal−Metal-Bonded Excited State of a Binuclear Gold(I) Phosphine Complex Containing Open Coordination Sites. *Chem. - Eur. J.* **2015**, *21*, 13888−13893.
(64) Schmidbaur, H.; Raubenheimer, H. G. Excimer and Exciplex Formation in Gold(I) Complexes Preconditioned by Aurophilic Interactions. *Angew. Chem., Int. Ed.* **2020**, *59*, 14748−14771.
(65) Fry, A. J.; Krieger, R. L. Electrolyte Effects upon the Polarographic Reduction of Alkyl Halides in Dimethyl Sulfoxide. *J. Org. Chem.* **1976**, *41*, 54−57.
(66) Rondinini, S.; Mussini, P. R.; Muttini, P.; Sello, G. Silver as a Powerful Electrocatalyst for Organic Halide Reduction: The Critical Role of Molecular Structure. *Electrochim. Acta* **2001**, *46*, 3245−3258.
(67) Koike, T.; Akita, M. Visible-light Radical Reaction Designed by Ru- and Ir-based Photoredox Catalysis. *Inorg. Chem. Front.* **2014**, *1*, 562−576.
(68) Sahoo, B.; Hopkinson, M. N.; Glorius, F. Combining Gold and Photoredox Catalysis: Visible Light-Mediated Oxy- and Amino-arylation of Alkenes. *J. Am. Chem. Soc.* **2013**, *135*, 5505−5508.
(69) Hopkinson, M. N.; Sahoo, B.; Glorius, F. Dual Photoredox and Gold Catalysis: Intermolecular Multicomponent Oxyarylation of Alkenes. *Adv. Synth. Catal.* **2014**, *356*, 2794−2800.
(70) Shu, X.-Z.; Zhang, M.; He, Y.; Frei, H.; Toste, F. D. Dual Visible Light Photoredox and Gold-Catalyzed Arylative Ring Expansion. *J. Am. Chem. Soc.* **2014**, *136*, 5844−5847.
(71) Patil, D. V.; Yun, H.; Shin, S. Catalytic Cross-Coupling of Vinyl Golds with Diazonium Salts under Photoredox and Thermal Conditions. *Adv. Synth. Catal.* **2015**, *357*, 2622−2628.
(72) Zhang, Q.; Zhang, Z.-Q.; Fu, Y.; Yu, H.-Z. Mechanism of the Visible Light-Mediated Gold-Catalyzed Oxyarylation Reaction of Alkenes. *ACS Catal.* **2016**, *6*, 798−808.
(73) Um, J.; Yun, H.; Shin, S. Cross-Coupling of Meyer-Schuster Intermediates under Dual Gold-Photoredox Catalysis. *Org. Lett.* **2016**, *18*, 484−487.
(74) Tlahuext-Aca, A.; Hopkinson, M. N.; Garza-Sanchez, R. A.; Glorius, F. Alkyne Difunctionalization by Dual Gold/Photoredox Catalysis. *Chem. - Eur. J.* **2016**, *22*, 5909−5913.
(75) Alcaide, B.; Almendros, P.; Busto, E.; Luna, A. Domino Meyer−Schuster/Arylation Reaction of Alkynols or Alkynyl Hydroperoxides with Diazonium Salts Promoted by Visible Light under Dual Gold and Ruthenium Catalysis. *Adv. Synth. Catal.* **2016**, *358*, 1526−1533.
(76) Xia, Z.; Khaled, O.; Mouriès-Mansuy, V.; Ollivier, C.; Fensterbank, L. Dual Photoredox/Gold Catalysis Arylative Cyclization of *o*-Alkynylphenols with Aryldiazonium Salts: A Flexible Synthesis of Benzofurans. *J. Org. Chem.* **2016**, *81*, 7182−7190.
(77) Qu, C.; Zhang, S.; Du, H.; Zhu, C. Cascade Photoredox/Gold Catalysis: Access to Multisubstituted Indoles via Aminoarylation of Alkynes. *Chem. Commun.* **2016**, *52*, 14400−14403.
(78) Alcaide, B.; Almendros, P.; Aparicio, B.; Lázaro-Milla, C.; Luna, A.; Faza, O. N. Gold-Photoredox-Cocatalyzed Tandem Oxycyclization/Coupling Sequence of Allenols and Diazonium Salts with Visible Light Mediation. *Adv. Synth. Catal.* **2017**, *359*, 2789−2800.
(79) Bansode, A. H.; Shaikh, S. R.; Gonnade, R. G.; Patil, N. T. Intramolecular *ipso*-Arylative Cyclization of Aryl-Alkynoates and *N*-Arylpropiolamides with Aryldiazonium Salts through Merged Gold/Visible Light Photoredox Catalysis. *Chem. Commun.* **2017**, *53*, 9081−9084.
(80) Mayans, J. G.; Suppo, J.-S.; Echavarren, A. M. Photoredox-Assisted Gold-Catalyzed Arylative Alkoxycyclization of 1,6-Enynes. *Org. Lett.* **2020**, *22*, 3045−3049.
(81) Nieto-Oberhuber, C.; Muñoz, M. P.; Buñuel, E.; Nevado, C.; Cárdenas, D. J.; Echavarren, A. M. Cationic Gold(I) Complexes: Highly Alkynophilic Catalysts for the *exo*- and *endo*-Cyclization of Enynes. *Angew. Chem., Int. Ed.* **2004**, *43*, 2402−2406.
(82) Nieto-Oberhuber, C.; López, S.; Echavarren, A. M. Intramolecular [4 + 2] Cycloadditions of 1,3-Enynes or Arylalkynes with Alkenes with Highly Reactive Cationic Phosphine Au(I) Complexes. *J. Am. Chem. Soc.* **2005**, *127*, 6178−6179.
(83) He, Y.; Wu, H.; Toste, F. D. A Dual Catalytic Strategy for Carbon−Phosphorus Cross-Coupling via Gold and Photoredox Catalysis. *Chem. Sci.* **2015**, *6*, 1194−1198.
(84) Kim, S.; Rojas-Martin, J.; Toste, F. D. Visible Light-Mediated Gold-Catalysed Carbon(sp^2)−Carbon(sp) Cross-Coupling. *Chem. Sci.* **2016**, *7*, 85−88.
(85) Schießl, J.; Schulmeister, J.; Doppiu, A.; Wörner, E.; Rudolph, M.; Karch, R.; Hashmi, A. S. K. An Industrial Perspective on Counter Anions in Gold Catalysis: On Alternative Counter Anions. *Adv. Synth. Catal.* **2018**, *360*, 3949−3959.
(86) Schießl, J.; Schulmeister, J.; Doppiu, A.; Wörner, E.; Rudolph, M.; Karch, R.; Hashmi, A. S. K. An Industrial Perspective on Counter Anions in Gold Catalysis: Underestimated with Respect to "Ligand Effects. *Adv. Synth. Catal.* **2018**, *360*, 2493−2502.
(87) Jia, M.; Bandini, M. Counterion Effects in Homogeneous Gold Catalysis. *ACS Catal.* **2015**, *5*, 1638−1652.
(88) Zhdanko, A.; Maier, M. E. Explanation of Counterion Effects in Gold(I)-Catalyzed Hydroalkoxylation of Alkynes. *ACS Catal.* **2014**, *4*, 2770−2775.
(89) Tlahuext-Aca, A.; Hopkinson, M. N.; Sahoo, B.; Glorius, F. Dual Gold/Photoredox-Catalyzed C(sp)-H Arylation of Terminal Alkynes with Diazonium Salts. *Chem. Sci.* **2016**, *7*, 89−93.
(90) Cai, R.; Lu, M.; Aguilera, E. Y.; Xi, Y.; Akhmedov, N. G.; Petersen, J. L.; Chen, H.; Shi, X. Ligand-Assisted Gold-Catalyzed Cross-Coupling with Aryldiazonium Salts: Redox Gold Catalysis without an External Oxidant. *Angew. Chem., Int. Ed.* **2015**, *54*, 8772−8776.
(91) Cornilleau, T.; Hermange, P.; Fouquet, E. Gold-Catalysed Cross-Coupling Between Aryldiazonium Salts and Arylboronic Acids: Probing the Usefulness of Photoredox Conditions. *Chem. Commun.* **2016**, *52*, 10040−10043.
(92) Gauchot, V.; Lee, A.-L. Dual Gold Photoredox C(sp^2)-C(sp^2) Cross Couplings- Development and Mechanistic Studies. *Chem. Commun.* **2016**, *52*, 10163−10166.
(93) Tabey, A.; Berlande, M.; Hermange, P.; Fouquet, E. Mechanistic and Asymmetric Investigations of the Au-Catalysed Cross-Coupling between Aryldiazonium Salts and Arylboronic Acids using (P,N) Gold Complexes. *Chem. Commun.* **2018**, *54*, 12867−12870.
(94) Liu, L.-P.; Xu, B.; Mashuta, M. S.; Hammond, G. B. Synthesis and Structural Characterization of Stable Organogold(I) Compounds. Evidence for the Mechanism of Gold-Catalyzed Cyclizations. *J. Am. Chem. Soc.* **2008**, *130*, 17642−17643.
(95) Partyka, D. V.; Zeller, M.; Hunter, A. D.; Gray, T. G. Relativistic Functional Groups: Aryl Carbon-Gold Bond Formation

https://dx.doi.org/10.1021/acs.chemrev.0c00841
Chem. Rev. XXXX, XXX, XXX−XXX

by Selective Transmetalation of Boronic Acids. *Angew. Chem., Int. Ed.* **2006**, *45*, 8188−8191.
(96) Akram, M. O.; Mali, P. S.; Patil, N. T. Cross-Coupling Reactions of Aryldiazonium Salts with Allylsilanes under Merged Gold/Visible-Light Photoredox Catalysis. *Org. Lett.* **2017**, *19*, 3075−3078.
(97) McCallum, T.; Pitre, S. P.; Morin, M.; Scaiano, J. C.; Barriault, L. The Photochemical Alkylation and Reduction of Heteroarenes. *Chem. Sci.* **2017**, *8*, 7412−7418.
(98) Chakrabarty, I.; Akram, M. O.; Biswas, S.; Patil, N. T. Visible Light Mediated Desilylative $C(sp^2)$-$C(sp^2)$ Cross-Coupling Reactions of Arylsilanes with Aryldiazonium Salts under Au(i)/Au(iii) Catalysis. *Chem. Commun.* **2018**, *54*, 7223−7226.
(99) Alcaide, B.; Almendros, P.; Busto, E.; Lázaro-Milla, C. Photoinduced Gold-Catalyzed Domino C(sp) Arylation/Oxyarylation of TMS-Terminated Alkynols with Arenediazonium Salts. *J. Org. Chem.* **2017**, *82*, 2177−2186.
(100) Alcaide, B.; Almendros, P.; Busto, E.; Herrera, F.; Lázaro-Milla, C.; Luna, A. Photopromoted Entry to Benzothiophenes, Benzoselenophenes, 3H-Indoles, Isocoumarins, Benzosultams, and (Thio)flavones by Gold-Catalyzed Arylative Heterocyclization of Alkynes. *Adv. Synth. Catal.* **2017**, *359*, 2640−2652.
(101) Wetzel, A.; Gagosz, F. Gold-Catalyzed Transformation of 2-Alkynyl Arylazides: Efficient Access to the Valuable Pseudoindoxyl and Indolyl Frameworks. *Angew. Chem., Int. Ed.* **2011**, *50*, 7354−7358.
(102) Lu, B.; Luo, Y.; Liu, L.; Ye, L.; Wang, Y.; Zhang, L. Umpolung Reactivity of Indole Through Gold Catalysis. *Angew. Chem., Int. Ed.* **2011**, *50*, 8358−8362.
(103) Song, X.-R.; Qiu, Y.-F.; Liu, X.-Y.; Liang, Y.-M. Recent Advances in the Tandem Reaction of Azides with Alkynes or Alkynols. *Org. Biomol. Chem.* **2016**, *14*, 11317−11331.
(104) Huang, D.; Yan, G. Recent Advances in Reactions of Azides. *Adv. Synth. Catal.* **2017**, *359*, 1600−1619.
(105) Wang, Z.-S.; Tan, T.-D.; Wang, C.-M.; Yuan, D.-Q.; Zhang, T.; Zhu, P.; Zhu, C.; Zhou, J.-M.; Ye, L.-W. Dual Gold/Photoredox-Catalyzed Bis-Arylative Cyclization of Chiral Homopropargyl Sulfonamides with Diazonium Salts: Rapid Access to Enantioenriched 2,3-Dihydropyrroles. *Chem. Commun.* **2017**, *53*, 6848−6851.
(106) Li, H.; Shan, C.; Tung, C.-H.; Xu, Z. Dual Gold and Photoredox Catalysis: Visible Light-Mediated Intermolecular Atom Transfer Thiosulfonylation of Alkenes. *Chem. Sci.* **2017**, *8*, 2610−2615.
(107) Manteau, B.; Pazenok, S.; Vors, J.-P.; Leroux, F. R. New Trends in the Chemistry of α-Fluorinated Ethers, Thioethers, Amines and Phosphines. *J. Fluorine Chem.* **2010**, *131*, 140−158.
(108) Leroux, F.; Jeschke, P.; Schlosser, M. α-Fluorinated Ethers, Thioethers, and Amines: Anomerically Biased Species. *Chem. Rev.* **2005**, *105*, 827−856.
(109) Yu, X.-H.; Qing, F.-L. Indirect Trifluoromethylthiolation Methods. In *Emerging Fluorinated Motifs*; Ma, J.-A., Cahard, D., Eds.; Wiley Online Library, 2020; pp 289−307.
(110) Trost, B. M.; Kalnmals, C. A. Sulfones as Chemical Chameleons: Versatile Synthetic Equivalents of Small-Molecule Synthons. *Chem. - Eur. J.* **2019**, *25*, 11193−11213.
(111) Nájera, C.; Yus, M. Desulfonylation Reactions: Recent Developments. *Tetrahedron* **1999**, *55*, 10547−10658.
(112) Julia, M.; Paris, J.-M. Syntheses a l'Aide de Sulfones v(+)-Methode de Synthese Generale de Doubles Liaisons. *Tetrahedron Lett.* **1973**, *14*, 4833−4836.
(113) Xia, Z.; Corcé, V.; Zhao, F.; Przybylski, C.; Espagne, A.; Jullien, L.; Le Saux, T.; Gimbert, Y.; Dossmann, H.; Mouriès-Mansuy, V.; Ollivier, C.; Fensterbank, L. Photosensitized Oxidative Addition to Gold(I) Enables Alkynylative Cyclization of *o*-Alkylnylphenols with Iodoalkynes. *Nat. Chem.* **2019**, *11*, 797−805.
(114) Serra, J.; Parella, T.; Ribas, X. Au(III)-Aryl Intermediates in Oxidant-free C−N and C−O Cross-Coupling Catalysis. *Chem. Sci.* **2017**, *8*, 946−952.
(115) Harper, M. J.; Arthur, C. J.; Crosby, J.; Emmett, E. J.; Falconer, R. L.; Fensham-Smith, A. J.; Gates, P. J.; Leman, T.; McGrady, J. E.; Bower, J. F.; Russell, C. A. Oxidative Addition, Transmetalation, and Reductive Elimination at a 2,2-Bipyridyl-Ligated Gold Center. *J. Am. Chem. Soc.* **2018**, *140*, 4440−4445.
(116) Zeineddine, A.; Estévez, L.; Mallet-Ladeira, S.; Miqueu, K.; Amgoune, A.; Bourissou, D. Rational Development of Catalytic Au(I)/Au(III) Arylation Involving Mild Oxidative Addition of Aryl Halides. *Nat. Commun.* **2017**, *8*, 565.
(117) Joost, M.; Zeineddine, A.; Estévez, L.; Mallet-Ladeira, S.; Miqueu, K.; Amgoune, A.; Bourissou, D. Facile Oxidative Addition of Aryl Iodides to Gold(I) by Ligand Design: Bending Turns on Reactivity. *J. Am. Chem. Soc.* **2014**, *136*, 14654−14657.
(118) Dumele, O.; Wu, D.; Trapp, N.; Goroff, N.; Diederich, F. Halogen Bonding of (Iodoethynyl)benzene Derivatives in Solution. *Org. Lett.* **2014**, *16*, 4722−4725.
(119) Fukuda, Y.; Utimoto, K. Effective Transformation of Unactivated Alkynes into Ketones or Acetals with a Gold(III) Catalyst. *J. Org. Chem.* **1991**, *56*, 3729−3731.
(120) Casado, R.; Contel, M.; Laguna, M.; Romero, P.; Sanz, S. Organometallic Gold(III) Compounds as Catalysts for the Addition of Water and Methanol to Terminal Alkynes. *J. Am. Chem. Soc.* **2003**, *125*, 11925−11935.
(121) Lein, M.; Rudolph, M.; Hashmi, S. K.; Schwerdtfeger, P. Homogeneous Gold Catalysis: Mechanism and Relativistic Effects of the Addition of Water to Propyne. *Organometallics* **2010**, *29*, 2206−2210.
(122) Huang, L.; Rominger, F.; Rudolph, M.; Hashmi, A. S. K. A General Access to Organogold(III) Complexes by Oxidative Addition of Diazonium Salts. *Chem. Commun.* **2016**, *52*, 6435−6438.
(123) Liu, Y.; Yang, Y.; Zhu, R.; Liu, C.; Zhang, D. The Dual Role of Gold(I) Complexes in Photosensitizer-Free Visible-Light-Mediated Gold-Catalyzed 1,2-Difunctionalization of Alkynes: A DFT Study. *Chem. - Eur. J.* **2018**, *24*, 14119−14126.
(124) Witzel, S.; Xie, J.; Rudolph, M.; Hashmi, A. S. K. Photosensitizer-Free, Gold-Catalyzed C−C Cross-Coupling of Boronic Acids and Diazonium Salts Enabled by Visible Light. *Adv. Synth. Catal.* **2017**, *359*, 1522−1528.
(125) Xie, J.; Sekine, K.; Witzel, S.; Krämer, P.; Rudolph, M.; Rominger, F.; Hashmi, A. S. K. Light-Induced Gold-Catalyzed Hiyama Arylation: A Coupling Access to Biarylboronates. *Angew. Chem., Int. Ed.* **2018**, *57*, 16648−16653.
(126) Witzel, S.; Sekine, K.; Rudolph, M.; Hashmi, A. S. K. New Transmetalation Reagents for the Gold-Catalyzed Visible Light-Enabled $C(sp$ or $sp^2)$-$C(sp^2)$ Cross-Coupling with Aryldiazonium Salts in the Absence of a Photosensitizer. *Chem. Commun.* **2018**, *54*, 13802−13804.
(127) Taschinski, S.; Döpp, R.; Ackermann, M.; Rominger, F.; de Vries, F.; Menger, M. F. S. J.; Rudolph, M.; Hashmi, A. S. K.; Klein, J. E. M. N. Light-Induced Mechanistic Divergence in Gold(I) Catalysis: Revisiting the Reactivity of Diazonium Salts. *Angew. Chem., Int. Ed.* **2019**, *58*, 16988−16993.
(128) Tang, H.-J.; Zhang, X.; Zhang, Y.-F.; Feng, C. Visible-Light-Assisted Gold-Catalyzed Fluoroarylation of Allenoates. *Angew. Chem., Int. Ed.* **2020**, *59*, 5242−5247.
(129) Okoromoba, O. E.; Han, J.; Hammond, G. B.; Xu, B. Designer HF-Based Fluorination Reagent: Highly Regioselective Synthesis of Fluoroalkenes and *gem*-Difluoromethylene Compounds from Alkynes. *J. Am. Chem. Soc.* **2014**, *136*, 14381−14384.
(130) Zeng, X.; Liu, S.; Shi, Z.; Liu, G.; Xu, B. Synthesis of α-Fluoroketones by Insertion of HF into a Gold Carbene. *Angew. Chem., Int. Ed.* **2016**, *55*, 10032−10036.
(131) O'Connor, T. J.; Toste, F. D. Gold-Catalyzed Hydrofluorination of Electron-Deficient Alkynes: Stereoselective Synthesis of β-Fluoro Michael Acceptors. *ACS Catal.* **2018**, *8*, 5947−5951.
(132) Wolstenhulme, J. R.; Rosenqvist, J.; Lozano, O.; Ilupeju, J.; Wurz, N.; Engle, K. M.; Pidgeon, G. W.; Moore, P. R.; Sandford, G.; Gouverneur, V. Asymmetric Electrophilic Fluorocyclization with Carbon Nucleophiles. *Angew. Chem., Int. Ed.* **2013**, *52*, 9796−9800.

https://dx.doi.org/10.1021/acs.chemrev.0c00841
Chem. Rev. XXXX, XXX, XXX−XXX

(133) Braun, M.-G.; Katcher, M. H.; Doyle, A. G. Carbofluorination via a Palladium-Catalyzed Cascade Reaction. *Chem. Sci.* **2013**, *4*, 1216−1220.
(134) Barnette, W. E. *N*-Fluoro-*N*-Alkylsulfonamides: Useful Reagents for the Fluorination of Carbanions. *J. Am. Chem. Soc.* **1984**, *106*, 452−454.
(135) Umemoto, T.; Fukami, S.; Tomizawa, G.; Harasawa, K.; Kawada, K.; Tomita, K. Power- and Structure-Variable Fluorinating Agents. The *N*-Fluoropyridinium Salt System. *J. Am. Chem. Soc.* **1990**, *112*, 8563−8575.
(136) Nyffeler, P. T.; Durón, S. G.; Burkart, M. D.; Vincent, S. P.; Wong, C.-H. Selectfluor: Mechanistic Insight and Applications. *Angew. Chem., Int. Ed.* **2005**, *44*, 192−212.
(137) Sherborne, G. J.; Gevondian, A. G.; Funes-Ardoiz, I.; Dahiya, A.; Fricke, C.; Schoenebeck, F. Modular and Selective Arylation of Aryl Germanes (C-$GeEt_3$) over C-Bpin, C-SiR3 and Halogens Enabled by Light-Activated Gold Catalysis. *Angew. Chem., Int. Ed.* **2020**, *59*, 15543−15548.
(138) Deng, J.-R.; Chan, W.-C.; Chun-Him Lai, N.; Yang, B.; Tsang, C.-S.; Chi-Bun Ko, B.; Lai-Fung Chan, S.; Wong, M.-K. Photosensitizer-Free Visible Light-Mediated Gold-Catalysed *cis*-Difunctionalization of Silyl-Substituted Alkynes. *Chem. Sci.* **2017**, *8*, 7537−7544.
(139) Liu, Y.; Yang, Y.; Zhu, R.; Liu, C.; Zhang, D. DFT Study on Photosensitizer-Free Visible-Light-Mediated Au-Catalyzed cis-Difunctionalization of Alkynes: Mechanism and Selectivities as Compared to Rh Catalysis. *J. Org. Chem.* **2019**, *84*, 16171−16182.
(140) Granzhan, A.; Ihmels, H. Playing Around with the Size and Shape of Quinolizinium -Derivatives: Versatile Ligands for Duplex, Triplex, Quadruplex and Abasic Site-Containing DNA. *Synlett* **2016**, *27*, 1775−1793.
(141) Sucunza, D.; Cuadro, A. M.; Alvarez-Builla, J.; Vaquero, J. J. Recent Advances in the Synthesis of Azonia Aromatic Heterocycles. *J. Org. Chem.* **2016**, *81*, 10126−10135.
(142) Granzhan, A.; Ihmels, H.; Viola, G. 9-Donor-Substituted Acridizinium Salts: Versatile Environment-Sensitive Fluorophores for the Detection of Biomacromolecules. *J. Am. Chem. Soc.* **2007**, *129*, 1254−1267.
(143) Sauer, C.; Liu, Y.; De Nisi, A.; Protti, S.; Fagnoni, M.; Bandini, M. Photocatalyst-free, Visible Light Driven, Gold Promoted Suzuki Synthesis of (Hetero)biaryls. *ChemCatChem* **2017**, *9*, 4456−4459.
(144) Crespi, S.; Protti, S.; Fagnoni, M. Wavelength Selective Generation of Aryl Radicals and Aryl Cations for Metal-Free Photoarylations. *J. Org. Chem.* **2016**, *81*, 9612−9619.
(145) Malacarne, M.; Protti, S.; Fagnoni, M. A Visible-Light-Driven, Metal-free Route to Aromatic Amides via Radical Arylation of Isonitriles. *Adv. Synth. Catal.* **2017**, *359*, 3826−3830.
(146) Winston, M. S.; Wolf, W. J.; Toste, F. D. Photoinitiated Oxidative Addition of CF_3I to Gold(I) and Facile Aryl-CF_3 Reductive Elimination. *J. Am. Chem. Soc.* **2014**, *136*, 7777−7782.
(147) Tamaki, A.; Kochi, J. K. Catalytic Mechanism Involving Oxidative Addition in the Coupling of Alkylgold(I) with Alkyl Halides. *J. Organomet. Chem.* **1972**, *40*, C81−C84.
(148) Johnson, A.; Puddephatt, R. J. Oxidative Addition Reactions of Methylgold(I) Compounds. *Inorg. Nucl. Chem. Lett.* **1973**, *9*, 1175−1177.
(149) Tamaki, A.; Magennis, S. A.; Kochi, J. K. Rearrangement and Decomposition of Trialkylgold(III) Complexes. *J. Am. Chem. Soc.* **1973**, *95*, 6487−6488.
(150) Tamaki, A.; Kochi, J. K. Oxidative Addition in the Coupling of Alkylgold(I) with Alkyl Halides. *J. Organomet. Chem.* **1974**, *64*, 411−425.
(151) Shiotani, A.; Schmidbaur, H. Organogold-Chemie IX. Versuche zur Oxydativen Addition an Organogold-Komplexen. *J. Organomet. Chem.* **1972**, *37*, C24−C26.
(152) Johnson, A.; Puddephatt, R. J. Oxidative Addition Reactions of Methyl Iodide with Some Methylgold(I) Compounds. *J. Organomet. Chem.* **1975**, *85*, 115−121.
(153) Johnson, A.; Puddephatt, R. J. Reactions of Trifluoromethyl Iodide with Methylgold(I) Complexes. Preparation of Trifluoromethyl-Gold(I) and -Gold(III) Complexes. *J. Chem. Soc., Dalton Trans.* **1976**, 1360−1363.
(154) Tlahuext-Aca, A.; Hopkinson, M. N.; Daniliuc, C. G.; Glorius, F. Oxidative Addition to Gold(I) by Photoredox Catalysis: Straightforward Access to Diverse (C,N)-Cyclometalated Gold(III) Complexes. *Chem. - Eur. J.* **2016**, *22*, 11587−11592.
(155) Kim, S.; Toste, F. D. Mechanism of Photoredox-Initiated C-C and C-N Bond Formation by Arylation of IPrAu(I)−CF_3 and IPrAu(I)−Succinimide. *J. Am. Chem. Soc.* **2019**, *141*, 4308−4315.
(156) Eppel, D.; Rudolph, M.; Rominger, F.; Hashmi, A. S. K. Mercury-Free Synthesis of Pincer [ĈN̂C]AuIII Complexes by an Oxidative Addition/CH Activation Cascade. *ChemSusChem* **2020**, *13*, 1986−1990.
(157) To, W.-P.; Zhou, D.; Tong, G. S. M.; Cheng, G.; Yang, C.; Che, C.-M. Highly Luminescent Pincer Gold(III) Aryl Emitters: Thermally Activated Delayed Fluorescence and Solution-Processed OLEDs. *Angew. Chem., Int. Ed.* **2017**, *56*, 14036−14041.
(158) Constable, E. C.; Leese, T. A. Cycloaurated Derivatives of 2-Phenylpyridine. *J. Organomet. Chem.* **1989**, *363*, 419−424.
(159) Au, V. K.-M.; Wong, K. M.-C.; Zhu, N.; Yam, V. W.-W. Luminescent Cyclometalated N-Heterocyclic Carbene-Containing Organogold(III) Complexes: Synthesis, Characterization, Electrochemistry, and Photophysical Studies. *J. Am. Chem. Soc.* **2009**, *131*, 9076−9085.
(160) Kumar, R.; Nevado, C. Cyclometalated Gold(III) Complexes: Synthesis, Reactivity, and Physicochemical Properties. *Angew. Chem., Int. Ed.* **2017**, *56*, 1994−2015.
(161) Quiclet-Sire, B.; Zard, S. Z. Fun With Radicals: Some New Perspectives for Organic Synthesis. *Pure Appl. Chem.* **2010**, *83*, 519−551.
(162) Baguley, P. A.; Walton, J. C. Flight from the Tyranny of Tin: The Quest for Practical Radical Sources Free from Metal Encumbrances. *Angew. Chem., Int. Ed.* **1998**, *37*, 3072−3082.
(163) Studer, A.; Amrein, S. Tin Hydride Substitutes in Reductive Radical Chain Reactions. *Synthesis* **2002**, *2002*, 835−849.
(164) McCallum, T.; Slavko, E.; Morin, M.; Barriault, L. Light-Mediated Deoxygenation of Alcohols with a Dimeric Gold Catalyst. *Eur. J. Org. Chem.* **2015**, *2015*, 81−85.
(165) Appel, R. Tertiary Phosphane/Tetrachloromethane, a Versatile Reagent for Chlorination, Dehydration, and P-N Linkage. *Angew. Chem., Int. Ed. Engl.* **1975**, *14*, 801−811.
(166) Dai, C.; Narayanam, J. M. R.; Stephenson, C. R. J. Visible-Light-Mediated Conversion of Alcohols to Halides. *Nat. Chem.* **2011**, *3*, 140−145.
(167) Barton, D. H.; McCombie, S. W. A New Method for the Deoxygenation of Secondary Alcohols. *J. Chem. Soc., Perkin Trans. 1* **1975**, 1574−1585.
(168) Barton, D. H.; Jang, D. O.; Jaszberenyi, J. C. The Invention of Radical Reactions. Part 32. Radical Deoxygenations, Dehalogenations, and Deaminations with Dialkyl Phosphites and Hypophosphorous Acid as Hydrogen Sources. *J. Org. Chem.* **1993**, *58*, 6838−6842.
(169) Ueng, S.-H.; Fensterbank, L.; Lacôte, E.; Malacria, M.; Curran, D. P. Radical Deoxygenation of Xanthates and Related Functional Groups with New Minimalist *N*-Heterocyclic Carbene Boranes. *Org. Lett.* **2010**, *12*, 3002−3005.
(170) Zhang, L.; Koreeda, M. Radical Deoxygenation of Hydroxyl Groups via Phosphites. *J. Am. Chem. Soc.* **2004**, *126*, 13190−13191.
(171) Nishina, Y.; Ohtani, B.; Kikushima, K. Bromination of Hydrocarbons with CBr_4, Initiated by Light-Emitting Diode Irradiation. *Beilstein J. Org. Chem.* **2013**, *9*, 1663−1667.
(172) Kaldas, S. J.; Cannillo, A.; McCallum, T.; Barriault, L. Indole Functionalization via Photoredox Gold Catalysis. *Org. Lett.* **2015**, *17*, 2864−2866.
(173) Artis, D. R.; Cho, I.-S.; Jaime-Figueroa, S.; Muchowski, J. M. Oxidative Radical Cyclization of (l-Iodoalkyl)indoles and Pyrroles. Synthesis of (−)-Monomorine and Three Diastereomers. *J. Org. Chem.* **1994**, *59*, 2456−2466.

https://dx.doi.org/10.1021/acs.chemrev.0c00841
Chem. Rev. XXXX, XXX, XXX−XXX

(174) Magolan, J.; Kerr, M. A. Expanding the Scope of $Mn(OAc)_3$-Mediated Cyclizations: Synthesis of the Tetracyclic Core of Tronocarpine. *Org. Lett.* **2006**, *8*, 4561−4564.
(175) Miloserdov, F. M.; Kirillova, M. S.; Muratore, M. E.; Echavarren, A. M. Unified Total Synthesis of Pyrroloazocine Indole Alkaloids Sheds Light on Their Biosynthetic Relationship. *J. Am. Chem. Soc.* **2018**, *140*, 5393−5400.
(176) Xie, J.; Shi, S.; Zhang, T.; Mehrkens, N.; Rudolph, M.; Hashmi, A. S. K. A Highly Efficient Gold-Catalyzed Photoredox (-$C(sp^3)$-H Alkynylation of Tertiary Aliphatic Amines with Sunlight. *Angew. Chem., Int. Ed.* **2015**, *54*, 6046−6050.
(177) McNally, A.; Prier, C. K.; MacMillan, D. W. C. Discovery of an α-Amino C-H Arylation Reaction Using the Strategy of Accelerated Serendipity. *Science* **2011**, *334*, 1114−1117.
(178) Fischer, H. The Persistent Radical Effect: A Principle for Selective Radical Reactions and Living Radical Polymerizations. *Chem. Rev.* **2001**, *101*, 3581−3610.
(179) Xie, J.; Jin, H.; Hashmi, A. S. K. The Recent Achievements of Redox-Neutral Radical C-C Cross-Coupling Enabled by Visible-Light. *Chem. Soc. Rev.* **2017**, *46*, 5193−5203.
(180) Leifert, D.; Studer, A. The Persistent Radical Effect in Organic Synthesis. *Angew. Chem., Int. Ed.* **2020**, *59*, 74−108.
(181) Nzulu, F.; Telitel, S.; Stoffelbach, F.; Graff, B.; Morlet-Savary, F.; Lalevée, J.; Fensterbank, L.; Goddard, J.-P.; Ollivier, C. A Dinuclear Gold(i) Complex as a Novel Photoredox Catalyst for Light-Induced Atom Transfer Radical Polymerization. *Polym. Chem.* **2015**, *6*, 4605−4611.
(182) Ma, W.; Chen, D.; Wang, L.; Ma, Y.; Zhao, C.; Yang, W. Visible Light-Controlled Radical Polymerization of Propargyl Methacrylate Activated by a Photoredox Catalyst fac-[Ir(ppy)3]. *J. Macromol. Sci., Part A: Pure Appl.Chem.* **2015**, *52*, 761−769.
(183) Xie, J.; Zhang, T.; Chen, F.; Mehrkens, N.; Rominger, F.; Rudolph, M.; Hashmi, A. S. K. Gold-Catalyzed Highly Selective Photoredox $C(sp^2)$-H Difluoroalkylation and Perfluoroalkylation of Hydrazones. *Angew. Chem., Int. Ed.* **2016**, *55*, 2934−2938.
(184) Job, A.; Janeck, C. F.; Bettray, W.; Peters, R.; Enders, D. The SAMP-/RAMP-Hydrazone Methodology in Asymmetric Synthesis. *Tetrahedron* **2002**, *58*, 2253−2329.
(185) Sugiura, M.; Kobayashi, S. *N*-Acylhydrazones as Versatile Electrophiles for the Synthesis of Nitrogen-Containing Compounds. *Angew. Chem., Int. Ed.* **2005**, *44*, 5176−5186.
(186) Lazny, R.; Nodzewska, A. *N,N*-Dialkylhydrazones in Organic Synthesis. From Simple *N,N*-Dimethylhydrazones to Supported Chiral Auxiliaries. *Chem. Rev.* **2010**, *110*, 1386−1434.
(187) Xu, P.; Li, W.; Xie, J.; Zhu, C. Exploration of C-H Transformations of Aldehyde Hydrazones: Radical Strategies and Beyond. *Acc. Chem. Res.* **2018**, *51*, 484−495.
(188) Müller, K.; Faeh, C.; Diederich, F. Fluorine in Pharmaceuticals: Looking Beyond Intuition. *Science* **2007**, *317*, 1881−1886.
(189) Purser, S.; Moore, P. R.; Swallow, S.; Gouverneur, V. Fluorine in Medicinal Chemistry. *Chem. Soc. Rev.* **2008**, *37*, 320−330.
(190) McTiernan, C.; Morin, M.; McCallum, T.; Scaiano, J.; Barriault, L. Polynuclear Gold (I) Complexes in Photoredox Catalysis: Understanding Their Reactivity through Characterization and Kinetic Analysis. *Catal. Sci. Technol.* **2016**, *6*, 201−207.
(191) Yu, H.; Zhang, X.; Zhang, S. Mechanism of Photocatalytic Cyclization of Bromoalkenes with a Dimeric Gold Complex. *Organometallics* **2018**, *37*, 1725−1733.
(192) Minisci, F.; Bernardi, R.; Bertini, F.; Galli, R.; Perchinummo, M. Nucleophilic character of alkyl radicals-VI: A New Convenient Selective Alkylation of Heteroaromatic Bases. *Tetrahedron* **1971**, *27*, 3575−3579.
(193) Minisci, F.; Citterio, A.; Giordano, C. Electron-Transfer Processes: Peroxydisulfate, a Useful and Versatile Reagent in Organic Chemistry. *Acc. Chem. Res.* **1983**, *16*, 27−32.
(194) Fontana, F.; Minisci, F.; Nogueira Barbosa, M. C.; Vismara, E. Homolytic Acylation of Protonated Pyridines and Pyrazines with n-Keto Acids: The Problem of Monoacylation. *J. Org. Chem.* **1991**, *56*, 2866−2869.
(195) McCallum, T.; Barriault, L. Direct Alkylation of Heteroarenes with Unactivated Bromoalkanes Using Photoredox Gold Catalysis. *Chem. Sci.* **2016**, *7*, 4754−4758.
(196) Roberts, B. P. Polarity-Reversal Catalysis of Hydrogen-Atom Abstraction Reactions: Concepts and Applications in Organic Chemistry. *Chem. Soc. Rev.* **1999**, *28*, 25−35.
(197) Xu, W.; Ma, J.; Yuan, X.-A.; Dai, J.; Xie, J.; Zhu, C. Synergistic Catalysis for the Umpolung Trifluoromethylthiolation of Tertiary Ethers. *Angew. Chem., Int. Ed.* **2018**, *57*, 10357−10361.
(198) Cannillo, A.; Schwantje, T. R.; Bégin, M.; Barabé, F.; Barriault, L. Gold-Catalyzed Photoredox $C(sp^2)$ Cyclization: Formal Synthesis of (±)-Triptolide. *Org. Lett.* **2016**, *18*, 2592−2595.
(199) Huie, R. E.; Clifton, C. L.; Neta, P. Electron Transfer Reaction Rates and Equilibria of the Carbonate and Sulfate Radical Anions. *Radiat. Phys. Chem.* **1991**, *38*, 477−481.
(200) Kupchan, S. M.; Court, W. A.; Dailey, R. G., Jr; Gilmore, C. J.; Bryan, R. F. Tumor Inhibitors. LXXIV. Triptolide and Tripdiolide, Novel Antileukemic Diterpenoid Triepoxides from Tripterygium Wilfordii. *J. Am. Chem. Soc.* **1972**, *94*, 7194−7195.
(201) Yang, Y.; Liu, Z.-h.; Tolosa, E.; Yang, J.-W.; Li, L.-S. Triptolide Induces Apoptotic Death of T lymphocyte. *Immunopharmacology* **1998**, *40*, 139−149.
(202) Leuenroth, S. J.; Okuhara, D.; Shotwell, J. D.; Markowitz, G. S.; Yu, Z.; Somlo, S.; Crews, C. M. Triptolide is a Traditional Chinese Medicine-Derived Inhibitor of Polycystic Kidney Disease. *Proc. Natl. Acad. Sci. U. S. A.* **2007**, *104*, 4389−4394.
(203) Phillips, P. A.; Dudeja, V.; McCarroll, J. A.; Borja-Cacho, D.; Dawra, R. K.; Grizzle, W. E.; Vickers, S. M.; Saluja, A. K. Triptolide Induces Pancreatic Cancer Cell Death via Inhibition of Heat Shock Protein 70. *Cancer Res.* **2007**, *67*, 9407−9416.
(204) Chugh, R.; Sangwan, V.; Patil, S. P.; Dudeja, V.; Dawra, R. K.; Banerjee, S.; Schumacher, R. J.; Blazar, B. R.; Georg, G. I.; Vickers, S. M.; et al. A Preclinical Evaluation of Minnelide as a Therapeutic Agent Against Pancreatic Cancer. *Sci. Transl. Med.* **2012**, *4*, 156ra139.
(205) Buckanin, R. S.; Chen, S. J.; Frieze, D. M.; Sher, F. T.; Berchtold, G. A. Total Synthesis of Triptolide and Triptonide. *J. Am. Chem. Soc.* **1980**, *102*, 1200−1201.
(206) Lai, C. K.; Buckanin, R. S.; Chen, S. J.; Zimmerman, D. F.; Sher, F. T.; Berchtold, G. A. Total synthesis of Racemic Triptolide and Triptonide. *J. Org. Chem.* **1982**, *47*, 2364−2369.
(207) Miller, N. A.; Willis, A. C.; Sherburn, M. S. Formal Total Synthesis of Triptolide. *Chem. Commun.* **2008**, 1226−1228.
(208) Xie, J.; Li, J.; Weingand, V.; Rudolph, M.; Hashmi, A. S. K. Intermolecular Photocatalyzed Heck-like Coupling of Unactivated Alkyl Bromides by a Dinuclear Gold Complex. *Chem. - Eur. J.* **2016**, *22*, 12646−12650.
(209) Oestreich, M. *The Mizoroki−Heck Reaction*; Wiley, 2009.
(210) Tran, H.; McCallum, T.; Morin, M.; Barriault, L. Homocoupling of Iodoarenes and Bromoalkanes Using Photoredox Gold Catalysis: A Light Enabled Au(III) Reductive Elimination. *Org. Lett.* **2016**, *18*, 4308−4311.
(211) Ullmann, F.; Bielecki, J. Über Synthesen in der Biphenylreihe. *Ber. Dtsch. Chem. Ges.* **1901**, *34*, 2174−2185.
(212) Zidan, M.; McCallum, T.; Thai-Savard, L.; Barriault, L. Photoredox Meets Gold Lewis Acid Catalysis in the Alkylative Semipinacol Rearrangement: a Photocatalyst with a Dark Side. *Org. Chem. Front.* **2017**, *4*, 2092−2096.
(213) Rohe, S.; McCallum, T.; Morris, A. O.; Barriault, L. Transformations of Isonitriles with Bromoalkanes Using Photoredox Gold Catalysis. *J. Org. Chem.* **2018**, *83*, 10015−10024.
(214) Shono, T.; Kimura, M.; Ito, Y.; Nishida, K.; Oda, R. Studies of Isocyanide. II. The Reaction of Isocyanide with Some Radical Sources. *Bull. Chem. Soc. Jpn.* **1964**, *37*, 635−637.
(215) Ito, Y.; Inubushi, Y.; Saegusa, T. 1-(*N*-Alkyliminoformyl)azole - a Reagent of *trans*-Formimidoylation. *Tetrahedron Lett.* **1974**, *15*, 1283−1286.
(216) Zhao, Y.; Jin, J.; Chan, P. W. H. Gold Catalyzed Photoredox C1-Alkynylation of *N*-Alkyl-1,2,3,4-tetrahydroisoquinolines by 1-

https://dx.doi.org/10.1021/acs.chemrev.0c00841
Chem. Rev. XXXX, XXX, XXX−XXX

Bromoalkynes with UVA LED Light. *Adv. Synth. Catal.* **2019**, *361*, 1313−1321.
(217) Zhang, L.; Si, X.; Yang, Y.; Witzel, S.; Sekine, K.; Rudolph, M.; Rominger, F.; Hashmi, A. S. K. Reductive C-C Coupling by Desulfurizing Gold-Catalyzed Photoreactions. *ACS Catal.* **2019**, *9*, 6118−6123.
(218) Gimeno, M. C.; Laguna, A. Three- and Four-Coordinate Gold(I) Complexes. *Chem. Rev.* **1997**, *97*, 511−522.
(219) Vogler, A.; Kunkely, H. Photoreactivity of Gold Complexes. *Coord. Chem. Rev.* **2001**, *219*−*221*, 489−507.
(220) Tiekink, E. R. T.; Kang, J.-G. Luminescence Properties of Phosphinegold(I) Halides and Thiolates. *Coord. Chem. Rev.* **2009**, *253*, 1627−1648.
(221) Ferle, A.; Pizzuti, L.; Inglez, S. D.; Caires, A. R. L.; Lang, E. S.; Back, D. F.; Flores, A. F. C.; Júnior, A. M.; Deflon, V. M.; Casagrande, G. A. The First Gold(I) Complexes Based on Thiocarbamoyl-Pyrazoline Ligands: Synthesis, Structural Characterization and Photophysical Properties. *Polyhedron* **2013**, *63*, 9−14.
(222) Zhang, L.; Si, X.; Rominger, F.; Hashmi, A. S. K. Visible-Light-Induced Radical Carbo-Cyclization/gem-Diborylation through Triplet Energy Transfer between a Gold Catalyst and Aryl Iodides. *J. Am. Chem. Soc.* **2020**, *142*, 10485−10493.
(223) Strieth-Kalthoff, F.; James, M. J.; Teders, M.; Pitzer, L.; Glorius, F. Energy Transfer Catalysis Mediated by Visible Light: Principles, Applications, Directions. *Chem. Soc. Rev.* **2018**, *47*, 7190−7202.
(224) Qiu, G.; Li, Y.; Wu, J. Recent Developments for the Photoinduced Ar-X Bond Dissociation Reaction. *Org. Chem. Front.* **2016**, *3*, 1011−1027.
(225) Si, X.; Zhang, L.; Wu, Z.; Rudolph, M.; Asiri, A. M.; Hashmi, A. S. K. Visible Light-Induced α-C(sp^3)-H Acetalization of Saturated Heterocycles Catalyzed by a Dimeric Gold Complex. *Org. Lett.* **2020**, *22*, 5844−5849.
(226) Jiang, M.; Tang, D.; Zhao, X.; Li, Q.; Zhuang, Y.; Wei, X.; Li, X.; Liu, Y.; Wu, X.-Y.; Shao, Z.; et al. Design and Synthesis of New Acid Cleavable Linkers for DNA Sequencing by Synthesis. *Nucleosides, Nucleotides Nucleic Acids* **2014**, *33*, 774−785.
(227) Johnson, J. W.; Gretes, M.; Goodfellow, V. J.; Marrone, L.; Heynen, M. L.; Strynadka, N. C. J.; Dmitrienko, G. I. Cyclobutanone Analogues of β-Lactams Revisited: Insights into Conformational Requirements for Inhibition of Serine- and Metallo-β-Lactamases. *J. Am. Chem. Soc.* **2010**, *132*, 2558−2560.
(228) Durán-Peña, M. J.; Botubol-Ares, J. M.; Hanson, J. R.; Hernández-Galán, R.; Collado, I. G. Unexpected Mild Protection of Alcohols as 2-O-THF and 2-O-THP Ethers Catalysed by Cp_2TiCl Reveal an Intriguing Role of the Solvent in the Single-Electron Transfer Reaction. *Eur. J. Org. Chem.* **2015**, *2015*, 6333−6340.
(229) Baati, R.; Valleix, A.; Mioskowski, C.; Barma, D. K.; Falck, J. R. A Convenient Synthesis of 2-Tetrahydrofuranyl Ethers. *Org. Lett.* **2000**, *2*, 485−487.
(230) Beniazza, R.; Abadie, B.; Remisse, L.; Jardel, D.; Lastécouères, D.; Vincent, J.-M. Light-Promoted Metal-Free Cross Dehydrogenative Couplings on Ethers Mediated by NFSI: Reactivity and Mechanistic Studies. *Chem. Commun.* **2017**, *53*, 12708−12711.
(231) French, A. N.; Cole, J.; Wirth, T. Tetrahydrofuranylation of Alcohols Using Hypervalent Iodine Reagents. *Synlett* **2004**, *2004*, 2291−2294.
(232) Bertrand, B.; Williams, M. R. M.; Bochmann, M. Gold(III) Complexes for Antitumor Applications: An Overview. *Chem. - Eur. J.* **2018**, *24*, 11840−11851.
(233) Sun, R. W.-Y.; Che, C.-M. The Anti-Cancer Properties of Gold(III) Compounds with Dianionic Porphyrin and Tetradentate Ligands. *Coord. Chem. Rev.* **2009**, *253*, 1682−1691.
(234) Zou, T.; Lum, C. T.; Lok, C.-N.; Zhang, J.-J.; Che, C.-M. Chemical Biology of Anticancer Gold(iii) and Gold(i) Complexes. *Chem. Soc. Rev.* **2015**, *44*, 8786−8801.
(235) Fung, S. K.; Zou, T.; Cao, B.; Lee, P.-Y.; Fung, Y. M. E.; Hu, D.; Lok, C.-N.; Che, C.-M. Cyclometalated Gold(III) Complexes Containing *N*-Heterocyclic Carbene Ligands Engage Multiple Anti-Cancer Molecular Targets. *Angew. Chem., Int. Ed.* **2017**, *56*, 3892−3896.
(236) Yam, V. W.-W.; Cheng, E. C.-C. Highlights on the Recent Advances in Gold Chemistry-a Photophysical Perspective. *Chem. Soc. Rev.* **2008**, *37*, 1806−1813.
(237) To, W.-P.; Chan, K. T.; Tong, G. S. M.; Ma, C.; Kwok, W.-M.; Guan, X.; Low, K.-H.; Che, C.-M. Strongly Luminescent Gold(III) Complexes with Long-Lived Excited States: High Emission Quantum Yields, Energy Up-Conversion, and Nonlinear Optical Properties. *Angew. Chem., Int. Ed.* **2013**, *52*, 6648−6652.
(238) Visbal, R.; Gimeno, M. C. *N*-Heterocyclic Carbene Metal Complexes: Photoluminescence and Applications. *Chem. Soc. Rev.* **2014**, *43*, 3551−3574.
(239) Beucher, H.; Kumar, S.; Merino, E.; Hu, W.-H.; Stemmler, G.; Cuesta-Galisteo, S.; González, J. A.; Jagielski, J.; Shih, C.-J.; Nevado, C. Highly Efficient Green Solution Processable Organic Light-Emitting Diodes Based on a Phosphorescent K3-(N̂ĈC)Gold(III)-Alkynyl Complex. *Chem. Mater.* **2020**, *32*, 1605−1611.
(240) Chan, C.-W.; Wong, W.-T.; Che, C.-M. Gold(III) Photooxidants. Photophysical, Photochemical Properties, and Crystal Structure of a Luminescent Cyclometalated Gold(III) Complex of 2,9-Diphenyl-1,10-Phenanthroline. *Inorg. Chem.* **1994**, *33*, 1266−1272.
(241) Ziolo, R. F.; Lipton, S.; Dori, Z. The Photoluminescence of Phosphine Complexes of d ^{10} Metals. *J. Chem. Soc. D* **1970**, 1124−1125.
(242) Gade, L. H. Hyt was of Gold, and Shon so Bryghte···": Luminescent Gold(I) Compounds. *Angew. Chem., Int. Ed. Engl.* **1997**, *36*, 1171−1173.
(243) He, X.; Yam, V. W.-W. Luminescent Gold(I) Complexes for Chemosensing. *Coord. Chem. Rev.* **2011**, *255*, 2111−2123.
(244) Bronner, C.; Wenger, O. S. Luminescent Cyclometalated Gold(III) Complexes. *Dalton Trans.* **2011**, *40*, 12409−12420.
(245) To, W.-P.; Tong, G. S.-M.; Lu, W.; Ma, C.; Liu, J.; Chow, A. L.-F.; Che, C.-M. Luminescent Organogold(III) Complexes with Long-Lived Triplet Excited States for Light-Induced Oxidative C-H Bond Functionalization and Hydrogen Production. *Angew. Chem., Int. Ed.* **2012**, *51*, 2654−2657.
(246) Xue, Q.; Xie, J.; Jin, H.; Cheng, Y.; Zhu, C. Highly Efficient Visible-Light-Induced Aerobic Oxidative C-C, C-P Coupling from C-H Bonds Catalyzed by a Gold(III)-Complex. *Org. Biomol. Chem.* **2013**, *11*, 1606−1609.
(247) Zehnder, T. N.; Blacque, O.; Venkatesan, K. Luminescent Monocyclometalated Cationic Gold(III) Complexes: Synthesis, Photophysical Characterization and Catalytic Investigations. *Dalton Transactions* **2014**, *43*, 11959−11972.
(248) Sun, C.-Y.; To, W.-P.; Wang, X.-L.; Chan, K.-T.; Su, Z.-M.; Che, C.-M. Metal−Organic Framework Composites with Luminescent Gold(III) Complexes. Strongly Emissive and Long-Lived Excited States in Open Air and Photo-Catalysis. *Chem. Sci.* **2015**, *6*, 7105−7111.
(249) Han, Q.; Wang, Y.-L.; Sun, M.; Sun, C.-Y.; Zhu, S.-S.; Wang, X.-L.; Su, Z.-M. Metal-Organic Frameworks with Organogold(III) Complexes for Photocatalytic Amine Oxidation with Enhanced Efficiency and Selectivity. *Chem. - Eur. J.* **2018**, *24*, 15089−15095.

https://dx.doi.org/10.1021/acs.chemrev.0c00841
Chem. Rev. XXXX, XXX, XXX−XXX